ISTANBUL TECHNICAL UNIVERSITY ★ GRADUATE SCHOOL

SIMULATION OF WATER RESOURCE RECOVERY FACILITIES WITH AN OPEN SOURCE SOFTWARE

M.Sc. THESIS

Doğa BİNAY

Department of Environmental Engineering

Environmental Biotechnology Programme

FEBRUARY 2022

ISTANBUL TECHNICAL UNIVERSITY ★ GRADUATE SCHOOL

SIMULATION OF WATER RESOURCE RECOVERY FACILITIES WITH AN OPEN SOURCE SOFTWARE

M.Sc. THESIS

Doğa BİNAY
(501181808)

Department of Environmental Engineering

Environmental Biotechnology Programme

Thesis Advisor: Assoc. Prof. Dr. Özlem KARAHAN ÖZGÜN

FEBRUARY 2022

ISTANBUL TEKNİK ÜNİVERSİTESİ ★ LİSANSÜSTÜ EĞİTİM ENSTİTÜSÜ

SU KAYNAĞI GERİ KAZANIM TESİSLERİNİN AÇIK KAYNAK YAZILIM İLE SİMÜLASYONU

YÜKSEK LİSANS TEZİ

Doğa BİNAY
(501181808)

Çevre Mühendisliği Anabilim Dalı

Çevre Biyoteknolojisi Programı

Tez Danışmanı: Doç. Dr. Özlem KARAHAN ÖZGÜN

ŞUBAT 2022

Doğa Binay, a M.Sc student of İTU Graduate School student ID 501181808, successfully defended the thesis entitled "SIMULATION OF WATER RESOURCE RECOVERY FACILITIES WITH AN OPEN SOURCE SOFTWARE", which he prepared after fulfilling the requirements specified in the associated legislations, before the jury whose signatures are below.

Thesis Advisor :	**Assoc. Prof. Dr. Özlem Karahan Özgün** Istanbul Technical University	.....
Jury Members :	**Prof. Dr. Hüseyin Erdem Görgün** Istanbul Technical University	.....
	Prof. Dr. Gülsüm Yılmaz Istanbul University Cerrahpaşa	.....

Date of Submission : 14 January 2022
Date of Defense : 11 February 2022

FOREWORD

I owe my supervisor Assoc. Prof. Dr. Özlem KARAHAN ÖZGÜN a debt of gratitude for supporting me through my roughest times that could end up turning me into to a purposeless and a desperate person by inspiring me with her love for the profession, unhesitantly and consistently helping me out about any kind of problem I have faced, answering all my questions on wastewater treatment modelling and on any other aspect of environmental biotechnology whether the answers are obvious and the questions are relatable or not and lastly but most importantly, by being the most great-hearted person I have ever known whom I consider as a second mother of mine. Thanks to her I could be able to complete my thesis studies and become the passionate person I am today.

I will always be grateful to Dr. Onur Yılmaz ÖZCAN for wholeheartedly supporting me literally anytime I have asked for his assistance and his guidance through my master thesis studies and the Fit4Reuse project. I will always admire his passion for becoming the better version of himself, his curiosity for learning new things and his perseverance on the objectives he is willing to achieve. I have been learning so much from observing his approach towards the problems we encounter and working with him has been a privilege.

Finally, I would like to thank the most loving and caring parents in the world for sacrificing so much for me in every sense I can think of and never hesitating to support me morally and materially. I know that you were so proud of me when I got accepted to this programme and I will do my best to be worthy of your efforts, dad.

January 2022

Doğa BİNAY
Environmental Engineer

TABLE OF CONTENTS

Page

ABBREVIATIONS

ASM1 **:** Activated Sludge Model No.1
ASM2 **:** Activated Sludge Model No.2
ASM2d **:** Activated Sludge Model No.2d
ASM3 **:** Activated Sludge Model No.3
BDF **:** Backward Differentiation Formula
BOD **:** Biochemical Oxygen Demand
CAS **:** Conventional Activated Sludge
COD **:** Chemical Oxygen Demand
CSTR **:** Continuously Stirred Tank Reactor
CSV **:** Comma Separated Values
EBPR **:** Enhanced Biological Phosphorus Removal
GUI **:** Graphical User Interface
HRT **:** Hydraulic Retention Time
IWA **:** International Water Association
IAWQ **:** International Association on Water Quality
IWSA **:** International Water Supply Association
MLE **:** Modified Ludzack-Ettinger
ODE **:** Ordinary Differential Equations
OOP **:** Object Oriented Programming
pCOD **:** Particulate COD
RMSE **:** Root Means Square Error
SRT **:** Sludge Retention Time
TN **:** Total Nitrogen
TKN **:** Total Kjeldahl Nitrogen
UCT **:** University of Cape Town
WRRF **:** Water Resource Recovery Facility
WWTP **:** Wastewater Treatment Plant
XML **:** Extensible Markup Language

SYMBOLS

an : Suffix for anoxic reactor

ae : Suffix for aerobic reactor

b_A : Endogenous decay coefficient for autotrophic biomass (d^{-1})

b_H : Endogenous decay coefficient for heterotrophic biomass (d^{-1})

dt : Iteration time interval

f_{EX} : Particulate inert COD fraction of biomass

f_{ES} : Soluble inert COD fraction of biomass

f_{SH} : Rapidly hydrolyzable fraction of the influent COD

f_{SI} : Soluble inert fraction of the influent COD

f_{SND} : Soluble biodegradable organic nitrogen fraction of the total biodegradable organic nitrogen

f_{SP} : Soluble inert organic product fraction of soluble inert metabolic products

f_{SS} : Readily biodegradable fraction of the influent COD

f_{XH} : Heterotrophic biomass fraction of the influent COD

f_{XA} : Autotrophic biomass fraction of the influent COD

f_{XI} : Particulate inert fraction of the influent COD

f_{XND} : Particulate biodegradable organic nitrogen fraction of the total biodegradable organic nitrogen

f_{XP} : Particulate inert organic product fraction of soluble inert metabolic products

f_{XS} : Slowly biodegradable fraction of the influent COD

i_{XB} : Nitrogen content of the active sludge (g N /g cell COD)

i_{XP} : Nitrogen content of the endogenous sludge (g N /g COD)

k_{hS} : Maximum specific hydrolysis rate of S_H (d^{-1})

k_{hX} : Maximum specific hydrolysis rate of Xs (d^{-1})

kLa : Overall oxygen transfer coefficient (d^{-1})

$K_{NH,H}$: NH_4-N half-saturation constant for heterotrophic growth (g NH_4-N/m^3)

$K_{NH,A}$: NH_4-N half-saturation constant for autotrophic growth (g NH_4-N/m^3)

K_{NO} : Half-saturation constant for NO_3-N (g NO_3-N/m^3)

$K_{O,A}$: Oxygen half-saturation coefficient for autotrophic growth (g O^2/m^3)

$K_{O,H}$: Oxygen half-saturation coefficient for heterotrophic growth (gO^2/m^3)

K_S : Oxygen half-saturation constant for the carbon source (g COD/m^3)

K_{XS} : Hydrolyze half-saturation constant for S_H (g S_H /g cell COD)

K_{XX} : Hydrolyze half-saturation constant for Xs (g X_S /g cell COD)

Q : Flowrate (m^3/day)

$Q_{internal}$: Internal recycle flowrate (m^3/day)

Q_{sludge} : Sludge recycle flowrate (m^3/day)

$Q_{influent}$: Influent flowrate (m^3/day)

$Q_{reactor}$: Reactor flowrate (m^3/day)

$R_{internal}$: Internal recycle ratio

R_{sludge} : Sludge recycle ratio

S_{ALK} : Alkalinity concentration (molar)

S_H : Rapidly hydrolyzable COD (g COD/m^3)

S_I : Soluble inert COD (g COD/m^3)

S_{ND} : Soluble biodegradable organic nitrogen concentration (g COD/m^3)

S_{NH} : Ammonia nitrogen concentration (g COD/m^3)

S_{NO} : Nitrate nitrogen concentration (g COD/m^3)

S_O : Dissolved oxygen concentration (g O^2/m^3)

S_{Osat} : Dissolved oxygen saturation concentration (g O^2/m^3)

S_S : Readily biodegradable COD (g COD/m^3)

S_P : Soluble inert organic product concentration (g COD/m^3)

X_A : Autotrophic biomass concentration (g COD/m^3)

X_H : Heterotrophic biomass concentration (g COD/m^3)

X_I : Particulate inert COD (g COD/m^3)

X_{ND} : Particulate biodegradable organic nitrogen concentration (g COD/m^3)

X_P : Particulate inert organic product concentration (g COD/m^3)

X_S : Slowly hydrolyzable COD (g COD/m^3)

$V_{Aerobic}$: Volume of the aerobic reactor (m^3)

V_{Anoxic} : Volume of the anoxic reactor (m^3)

Y_A : Autotrophic growth yield coefficient (g cell COD/g COD)

Y_H : Heterotrophic growth yield coefficient (g cell COD/g COD)

Y_{HD} : Yield coefficient of the denitrifiers (g cell COD/g NH_4-N COD)

$\mu_{A,max}$: Maximum specific growth rate of autotrophic biomass (d^{-1})

$\mu_{H,max}$: Maximum specific growth rate of heterotrophic biomass (d^{-1})

η_{decay} : Correction factor for b_H under anoxic conditions

η_{growth} : Correction factor for μ_{maxH} under anoxic conditions

θ_X : Sludge retention time (d^{-1})

LIST OF TABLES

Page

LIST OF FIGURES

Page

SIMULATION OF WATER RESOURCE RECOVERY FACILITIES WITH AN OPEN SOURCE SOFTWARE
SUMMARY

Digitalization is in an uprising trend for more than a decade on many aspects of wastewater treatment processes and these days we are coming across with the term more than ever. Simulation softwares are virtual platforms, a projection of a particular configuration created by the users that can process the data provided with the help of consistent mathematical model implementations.

By doing this, environmental engineers are able to control and optimize the operational parameters and use if for finding the most cost-efficient treatment configuration while upgrading an existing facility process scheme or even before constructing it. In other words, engineers can prevent excessive construction and operational costs along with excessive energy consumptions.

The motivations of this thesis study is to emphasize the need for popularizing creating functionable softwares with user friendly interfaces, creating specific softwares for divergent configurations and usage of modelling in academy as it is so benefitial for the students to familiarize with the fundamentals of modeling during their undergraduate lectures in terms of the convenience it provides for operational and kinetic parameters.

An open-source software able to perform simulations of water resource recovery facilities with Modified Ludzack-Ettinger configuration has been developed within the scope of this study.

Python programming language has been chosen for the development of the software due to its easy to learn syntax and its open-source libraries that contain powerful packages such as NumPy, SciPy, PySide2, Matplotlib and Pandas.

The data handling of inputs and outputs have been achieved with the help of useful built-in functions of NumPy and Pandas, whereas the graphical user interface of the software have been created with PySide2. SciPy.integrate's solve_ivp function has been used for performing computations of ordinary differential equations with the backward differentiation formula (BDF) method which is a multi-step variable-order implicit method used in solving stiff problems.

Lastly for the development phase, figure canvas class of Matplotlib package has been integrated to the interface for visualizing the results of performed simulations.

A biochemical process model, consisting of 10 processes and 2 operational parameters defined for 15 state variables, have been created for the specific configuration that includes hydrolization processes of rapidly hydrolyzable COD, slowly hydrolyzable COD, soluble organic nitrogen and particulate organic nitrogen along with the growth and decay processes of heterotrophic and autotrophic biomasses.

Activated Sludge Model No. 1 (ASM1) has been taken as a base model for the creation of software model meanwhile endogenous respiration process definitions for two different heterotrophic organism species were adopted from the Activated Sludge Model No. 3 (ASM3).

Modifications have been made to the hybrid process model as the ammonification of soluble organic nitrogen process from Activated Sludge Model No. 1 and the storage mechanism of Activated Sludge Model No. 3 were removed from the process model in this thesis study.

Once the process model was created, mass balance equations of each state variable were implemented in the software. Configuration reactors were considered as Continuously Stirred Tank Reactors (CSTR) and therefore were assumed as ideal reactors. The reactant concentrations were considered to be distributed homogenously through the reactors meaning that the reactant concentrations within the reactor are assumed to be equal to the effluent concentrations of the reactors.

Rate of accumulation in the reactors were computed for each state variable for defining the mass balance equations of the specific configuration. Cofefficients and stoichiometric parameters defined on process model matrix were multiplied by the process rates of each component for calculating the rate of accumulation in the reactors.

Operational processes like constant feed of dissolved oxygen and sludge disposal process for the particulate matter that are going to be wasted were included in the matrix.

Computation of sludge disposal was achieved by a sludge retention time input parameter and correction factors for the process rates of denitrifiers were also included to kinetic parameters alongside the coefficients of heterotrophic and autotrophic growth and decay processes. Lastly, hydrolysis rates and coefficients were appended to the model.

Calibration and validation of the process model have been achieved by using the data set of an existing WRRF. First 220 days of the data set of 363 days were used for the calibration and last 143 days were used for the validation of the parameter coefficients. Root Mean Square Error (RMSE) and Janus Coefficient methods have been selected for evaluating the precision of model simulation outputs. The most precise predictions in the calibration were achieved for the NH4-N and the NO3-N parameters with Root Mean Square Error values of 1,73 and 2,01, respectively while in the validation phase, the most precise predictions were achieved for the NH4-N and the TKN parameters with Root Mean Square Error values of 0,65 and 0,78, respectively. The least precise predictions were computed for the COD and pCOD parameters on both of the calibration and validation processes with Root Mean Square Error values of 14,41 and 14,14, respectively for the calibration and 5,82 and 7,93, respectively for the validation processes.

The verification of the developed software was achieved by implementing the Modified-Ludzack Ettinger model in AQUASIM, an acknowledged simulation software used in environmental science, and comparing the results obtained from AQUASIM and the developed software created in this thesis study.

Several simulations were done using the same operational parameters, kinetic and stoichiometric coefficients in each software while changing the parameters and coefficients each time a simulation was performed. Similarly, simulation outputs of each software were compared with simulations having different step sizes like 10^{-1}, 10^{-2} and 10^{-3}. On all of the simulations mentioned, it was seen that the outputs of the developed software matched the outputs of AQUASIM software.

In conclusion, a useful tool to predict the performances of nitrogen removal process schemes for different water quality and treatment requirements was created in this thesis study. Considering a decent automation integration is achieved to the software, the developed software will increase the control of facility operators over the operation of the systems. The need for specific case studies on the modeled configuration will reduce with the efficient use of the software and younger generations of environmental engineers will be provided a better mean of comprehension for the operational, kinetic and stoichiometric parameters and their impacts on the processes.

SU KAYNAĞI GERİ KAZANIM TESİSLERİNİN AÇIK KAYNAK YAZILIM İLE SİMÜLASYONU
ÖZET

Dijitalizasyon, özellikle geçtiğimiz on yıldan fazla bir süre zarfından itibaren atıksu arıtımı konusunda oldukça yaygınlaşmakta olan ve günümüzde artık her alanda daha sık karşılaştığımız bir kavrama dönüşmüştür. Özellikle teknolojik alanlardaki gelişmeler de göz önüne alındığında, atıksu arıtımı simülasyonlarının ve bu simülasyonların gerçek hayattaki sorunlara getirebileceği çözümlerle ilgili yazılımların sayısı gün geçtikçe artmaktadır.

Bu simülasyon programları sayesinde kullanıcılar, spesifik konfigürasyonların sanal bir ortamdaki yansımasını oluşturarak, elde edilen analiz sonuçlarını işleme özelliğine sahip yazılımlar vasıtasıyla ve tutarlı matematiksel modellerin yardımıyla farklı senaryoları test edebilmektedirler.

Atıksu arıtımı konusu üzerine geliştirilen yazılımlar sayesinde günümüzde çevre mühendisleri ve bu alanda çalışmakta olan, atıksu arıtma tesislerinin proses ve işletmesinde görev alan tüm bireyler tesis işletimi ve kontrolünde değer taşıyan parametrelerin optimizasyonunu sağlayabilmektedir.

Öte yandan mevcut olan tesislerin modifikasyonu veya dizayn aşamasındaki tesislerin tasarımında kullanılan yazılımlar sayesinde, belirlenen standart deşarj limitlerini sağlayan en düşük maliyetli konfigürasyon tasarımı seçeneklerini de değerlendirebilmektedirler.

Atıksu arıtımı konusunda ve gittikçe yaygınlaşmakta olan su kaynaklarının geri kazanımı üzerine artan çalışmalar da göz önüne alındığında, bu tez çalışmasının amacı ülkemizde de bu türde kullanıcı dostu arayüze sahip, fonksiyonel ve spesifik bir alana yoğunlaşarak dünyaca kabul gören bir biyolojik azot giderimi konfigürasyonunun simülasyonlarının yapılabileceği kullanışlı bir yazılım geliştirmektir.

Geliştirilen yazılımı oluşturmaktaki bir diğer motivasyon ise, lisans ve yüksek lisans derecelerinde eğitim gören öğrencilerin modelleme ile tanışmalarını kolaylaştırmak ve modellemenin temel elementlerinin öğrencilerin atıksu arıtımı proseslerinde kullanılan kinetik parametreler ve işletme koşullarının kavranması sürecinde sağladığı faydalardan yararlanabilmeleridir.

Bu tez kapsamında Modified Ludzack-Ettinger konfigürasyonuna sahip su geri kazanım tesislerinin farklı senaryolar için simülasyonlarının mümkün olduğu bir açık kaynak yazılımı geliştirilmiştir.

Programın geliştirilmesinde, sözdiziminin kolayca anlaşılabilir olması ve NumPy, SciPy, PySide2, Matplotlib ve Pandas gibi birçok önemli açık kaynak kütüphaneyi ve modülü içerisinde bulunduran Python programlama dili kullanılmıştır.

Simülasyon sırasında kullanılan girdiler ve simülasyon sonrasında kaydedilen ve görselleştirilen çıktıların işlenmesinin gerçekleştirilebilmesi için, içerisinde kullanışlı hazır fonksiyonları barındıran NumPy ve Pandas modülleri kullanılmıştır.

Kullanıcı arayüzünün geliştirilmesi esnasında Qt Framework'un bünyesinde bulunan ve içerisinde çeşitli görsel araç barındıran PySide2 paketi tercih edilmiştir.

Kütle denklemlerini içeren adi diferansiyel denklemlerin çözümü için SciPy.integrate modülünün solve_ivp fonksiyonu kaynak koduna entegre edilmiştir.

Adi diferansiyel denklemlerin çözümü sırasında çok adımlı bir örtük türevleme metodu olan BDF (backward differentiation formula) metodu kullanılmıştır. Fonksiyonun içerisinde Radau, Runge Kutta ve LSODA gibi farklı çözüm metodları da bulunmasına rağmen bu metodun tercih edilmesinin sebebi, yazılımın ve yazılıma entegre edilen proses modelinin verifikasyonunun yapılacağı AQUASIM programında da BDF metodunun uygulanmasıdır.

Yazılımın geliştirilmesi aşamasında son olarak Matplotlib paketinin figür kanvas sınıfı arayüze entegre edilerek yürütülen simülasyonların sonuçlarının grafiksel olarak arayüz içerisindeki sonuçlar kısmına yansıtılması sağlanmıştır. Elde edilen çıktıların görselleştirilmesi için NumPy fonksiyonlarıyla kaynak kodu içerisinde depolanan çıktıların figür kanvas sınıfına iletilmesi sağlanmıştır. Programda kullanılan tüm paketlerin birbirleriyle olan etkileşimlerinin verimini arttırmak ve yazılım hızının arttırılması amacıyla optimum fonksiyon algoritmaları tasarlanmıştır.

Belirtilen konfigürasyon içerisinde gerçekleşen biyokimyasal reaksiyonları ve operasyonel parametreleri içeren bir proses modeli tanımlanmıştır. Oluşturulan proses modeli 15 durum değişkeni için tanımlanan 10 proses ve 2 işletim parametresini barındırmaktadır. Bu proseslerden bazıları heterotrofik ve ototrofik biyokütlerinin çoğalma ve içsel solunum hızlarını ifade etmekte iken substrat ve azot gideriminde son derece önemli olan hidroliz hızları ve tanımlanan tüm reaksiyon denklemlerinde kullanılan hız katsayıları, kinetik ve stokiyometrik katsayılar ve işletim parametreleri de modelin içerisine dahil edilmiştir.

Biyokimyasal proses modelinin hazırlanma sürecinde reaksiyon hızları, prosesler ve durum değişkenleri için Aktif Çamur Modeli No.1 (ASM1) referans alınmıştır. Aktif Çamur Modeli No. 1'e ilaveten anoksik ortamlarda elektron alıcısı olarak oksijen (O_2) yerine nitrat (NO_3) kullanabilen heterotrofik bakteriler ile aerobik ortamlarda çoğalan heterotrofik bakterilerin içsel solunum proses tanımları Aktif Çamur Modeli No.3 (ASM3)'ten benimsenmiştir. Bu sayede Aktif Çamur Modeli No. 1 (ASM1)'in aksine iki türün çoğalma ve içsel solunum hızları ayrı tutulmuştur.

Oluşturulan hibrit modelde Aktif Çamur Modeli No.1'e özgü çözünmüş organik azotların amonifikasyonu da çıkarılmıştır. Modelde Aktif Çamur Modeli No.3'te tanımlanan depolama mekanizması da benimsenmemiştir.

Proses modelinin tamamlanmasının ardırdan her durum değişkenine özgü kütle denklemleri oluşturulmuş, aerobik ve anoksik reaktörlerin tanımları yapılmıştır. Kütle denklemlerinin oluşturulmasında aerobik hat çıkışına bağlı içsel geri devir hattı ve çöktürme verimine bağlı olarak çamur geri devir hattından anoksik reaktöre devir edilecek parametre konsantrasyonları da göz önünde bulundurulmuştur. Yazılımda oluşturulan reaktörler, sürekli karıştırmalı reaktörler (CSTR) olarak tanımlanmıştır ve ideal reaktör özellikleri taşıdıkları varsayılmıştır. Bu sebeple reaktör içerisinde bulunan durum değişkenleri konsantrasyonlarının reaktör boyunca homojen bir dağılım gösterdikleri ve reaktörlerin çıkış hattında bulunan parametre konsantrasyonlarının da reaktörlerin içerisindeki konsantrasyonlara eşit oldukları varsayılmıştır.

Yine kütle denklemlerinin oluşturulması sırasında her durum değişkenine özgü akümülasyon hızının hesaplanması ile sağlanmıştır. Reaktörlerdeki birikim miktarının hesaplanması esnasında ise proses modeli için hazırlanan matris formatı kullanılmıştır. Bu formata göre her parametrenin bulunduğu sütundaki stokiyometrik katsayılar, o katsayıları içeren satırdaki proseslerin reaksiyon hızlarıyla çarpılmıştır. Kümülatif olarak her durum değişkeni için bulunduğu sütundaki tüm stokiyometrik katsayıların

reaksiyon hızları ile çarpılarak toplanması yoluyla elde edilen birikim miktarları, ilgili durum değişkenlerinin kütle denklemlerine eklenmiştir.

Biyokimyasal proseslerin haricinde, model matrisinde bulunan havalandırma ve çamur atımı işlemleri için de aynı uygulama tekrar edilmiştir. Havalandırma ve çamur atımı işlemlerinin sadece aerobik reaktörde kullanılmalarına dikkat edilmiş, atılan çamur miktarı iki reaktörün toplam hacmine oranlanarak tüm sistemin çamur atım gereksinimi aerobik reaktör üzerinden sağlanmıştır.

Çamur atımı işlemi için kullanıcılar tarafından arayüz yardımı ile alınan çamur yaşı parametresi kullanılmıştır. Aerobik reaktör çıkışından sonra gelen içsel geri devir hattının debisi giriş, içsel geri devir hattı ve çamur geri devir hattı debilerinin toplamına eşit olan reaktör debisinden çıkarılmış ve çöktürme tankına giriş debisi ile çamur geri devir hattı debisi toplamının ulaşması sağlanmıştır. Bu noktada kullanıcılardan alınan çöktürme verimi katsayısı sayesinde partiküler ve çözünür madde konsantrasyonlarının anoksik reaktöre ve çıkış suyu hattına iletilmeleri sağlanmıştır.

Yazılımın kalibrasyon ve validasyonu mevcut bir atıksu arıtma tesisine ait olan 363 günlük giriş suyu ve çıkış suyu verileri kullanılarak yapılmıştır. Kalibrasyon sırasında 363 günlük verinin ilk 220 günü kullanılarak gerekli katsayıların güncellenmesi sağlanmış, kalan 143 günlük veri ise kalibre edilen katsayılar ile yapılan simülasyonlar sayesinde validasyon işleminde kullanılmıştır. Simülasyon sonrası elde edilen çıkış suyu değerlerinde toplam azot (TN), toplam kjeldahl azotu (TKN), nitrat azotu (NO_3-N), amonyak azotu (NH_4-N), biyokimsayal oksijen ihtiyacı (BOD), kimyasal oksijen ihtiyacı (COD) ve partiküler kimyasal oksijen ihtiyacı (pCOD) değerleri, tesise ait analiz sonuçlarıyla karşılaştırılmıştır. Kalibrasyon ve validasyon işlemlerinin matematiksel olarak değerlendirilmesi, Kök Ortalama Kare Hatası (RMSE) metodu ve Janus katsayısı hesabı ile sağlanmıştır. Kök Ortalama Kare Hatası (RMSE) metoduna göre karşılaştırılan parametrelerden elde edilen değer sıfır (0) değerine yaklaştıkça modelin bu parametreler için kesinliği de o seviyede artmaktadır. Validasyon ve kalibrasyonda elde edilen Kök Ortalama Kare Hatası sonuçlarının oranlanması ile elde edilen Janus katsayısı ise, sonuç bir (1) değerine yaklaştıkça ilgili parametrenin kalibrasyon ve validasyon aşamalarında daha tutarlı bir dağılım sergilediğini göstermektedir. Buna göre kalibrasyon işlemi sonrasında analiz sonuçları ile en tutarlı davranışı gösteren parametreler sırasıyla 1,73 ve 2,01 Kök Ortalama Kare Hatası değerlerine sahip olan amonyak azotu (NH_4-N) ve nitrat azotu (NO_3-N) değerleri olurken, validasyon işlemi sonrasında analiz sonuçları ile en tutarlı davranışı gösteren parametreler sırasıyla 0,65 ve 0,78 Kök Ortalama Kare Hatası değerlerine sahip olan amonyak azotu (NH_4-N) ve toplam kjeldahl azotu (TKN) değerleri olmuştur. Janus katsayıları göz önüne alındığında ise kalibrasyon ve validasyon aşamalarında en tutarlı dağılımı sergileyen parametrelerin sırasıyla 0,75 ve 0,73 değerlerine sahip olan nitrat azotu (NO_3-N) ve toplam azot (TN) değerleri olduğu belirlenmiştir.

Tez kapsamında geliştirilen yazılımın doğrulanması için çevre biliminde tanınmış bir simülasyon programı olan AQUASIM kullanılmıştır. Yazılımda kullanılan modifiye edilmiş Ludzack Ettinger konfigürasyonu birebir şekilde AQUASIM'de tasarlanarak aynı katsayı değerleri ve işletme koşulları ile yürütülen simülasyonlar sonucu geliştirilen yazılımda elde edilen sonuçlar ile AQUASIM'de elde edilen sonuçların birbiriyle uyuştuğu gözlemlenmiştir.

Yapılan çalışmalar ve elde edilen sonuçlar doğrultusunda kullanışlı, kullanıcı dostu bir arayüze sahip olan, entegre edilen konfigürasyonda azot giderim simülasyonlarında

hassas sonuçlar elde edebilen ve otomasyon sistemi ile modifiye edilmesi durumunda atıksu arıtma tesislerinde işletme kontrolünü ve verimliliğini arttırabilecek bir yazılım elde edilmiştir.

1. INTRODUCTION

1.1 Purpose of Thesis

The dramatical increase in world population over the last decades and the rising rates of industrialization around the world has led the environmental science community to a pursuit of accelaration in wastewater treatment enhancements. The improvement of wastewater treatment technologies such as Conventional Activated Sludge (CAS) configuration yielded new concepts and the possibility of further wastewater treatment options. Recently, a transition to Resource Recovery notion is popular around the European countries which aims the removal of nutrients in wastewater, such as nitrogen and phosphorus, by means of advanced wastewater treatment technologies in addition to carbon removal. In order to integrate with and become a part of this conceptual conversion phase, comprehension of Water Resource Recovery Facilitiy (WRRF) dynamics and biochemical processes that occur in these environments is crucial. Modelling is considered as one of the key instruments that assists the environmental science community with having a better grasp of nutrient removal configurations and matters that comes within. In consideration of the given information, the purpose of this thesis study is to create a specialized open-source software provided with a graphical user interface focusing on nitrogen removal process in WRRFs. The structure of software model enables further enhancements and integrations for possible different solutions. This software also aims to create a simulation tool where undergraduate and graduate environmental engineers/scientists will be able to conceive the significance of modifications in operational parameters and develop their knowledge in biological nitrogen removal with the help of included Modified Ludzack-Ettinger model in a more feasible way. It should be taken into consideration that most of the existing simulation platforms possess a lot of divergent functions and therefore, are not suitable for students to master specific subjects. Consequently, building specialized simulation platforms on particular aspects of wastewater treatment technologies should become prevalent in the near future.

1.2 Scope of Thesis

Building an educational simulation platform for the environmental science students of next generations which will enable them to have a better understanding of the carbon and nutrient removal configurations is in the scope of this thesis study. Integrating the included model with time seris input has been achieved while at the same time providing the users with the option of evaluating changes in operational parameters with constant input values has been succeeded. Validation and calibration of the particular software was conducted in regard of real data taken from an existing Wastewater Treatment Plant (WWTP) and further verification of the software was carried out by comparison of outputs with a simulation software recognized in the field of wastewater treatmeant modelling.

2. LITERATURE

2.1 Conventional Activated Sludge Configuration

Carbon removal process in wastewater treatment is accomplished through complicated biochemical chain reactions performed by specific microorganisms under certain conditions. The most common system designed for biological carbon removal in wastewater engineering is the conventional activated sludge (CAS) configuration. CAS systems consist of an aeration tank, a settling tank and a recycle flow pipeline where huge amount of the biomass in the effluent flow is fed back to the aeration tank to sustain organic matter utilization and the excess amount of sludge is disposed in a daily routine from waste disposal pipeline as it can be seen in Figure 2.1. Biodegradation of organic carbon in the influent wastewater occurs due to growth and maintenance activities of heterotrophic bacteria. These heterotrophic bacteria requires sufficient amounts of dissolved oxygen concentration in aerobic reactor for the utilization of organic material by oxidation reactions. As the dissolved oxygen concentration in influent wastewater is neglected, constant feed of dissolved oxygen is essential for the heterotrophic bacteria to prevail. Autotrophic bacteria also increases oxygen demand in the aeration tank as nitrification of ammonia to nitrate nitrogen requires oxygen. In addition to ammonia, treatment of phosphorus in small quantities is also achieved due to biomass growth as the biomass requires nutrients for the growth process.

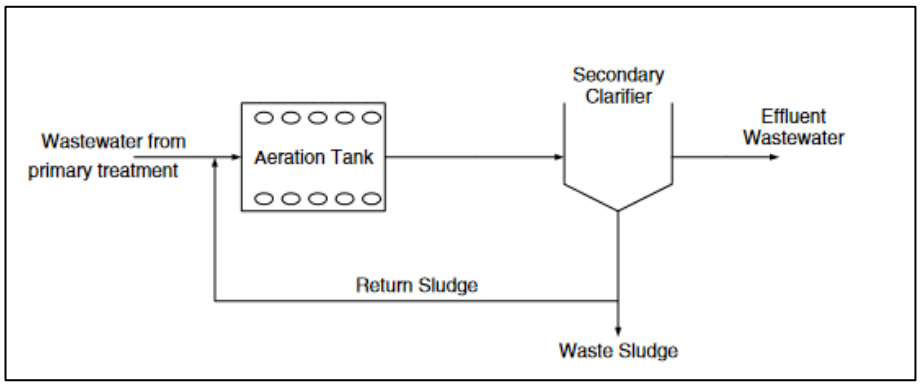

Figure 2.1 : CAS configuration flow and recycle flow diagram (Coskuner & Jassim, 2008).

Although the CAS configuration has been a common choice of method for carbon removal in wastewater through the years, with the innovations in wastewater treatment technologies and the global conceptual evolution on the prospect of resource sustainability, environmental science and technology is obliged to implement advanced wastewater treatment systems designed for nutrient removal.

2.2 Biological Nutrient Removal in Resource Recovery Facilities

The emerging developments in wastewater engineering and technological advancements in the field have given wastewater experts an opportunity to increase their precision in predicting possible future scenarios. Governments have noticed the significance of sustainable development policy since resources were limited and the demand in resources were on the rise (Yang et al., 2020). A schematic expression of wastewater treatment phases, technologies, and utilizations of effluents has been given in Figure 2.2.

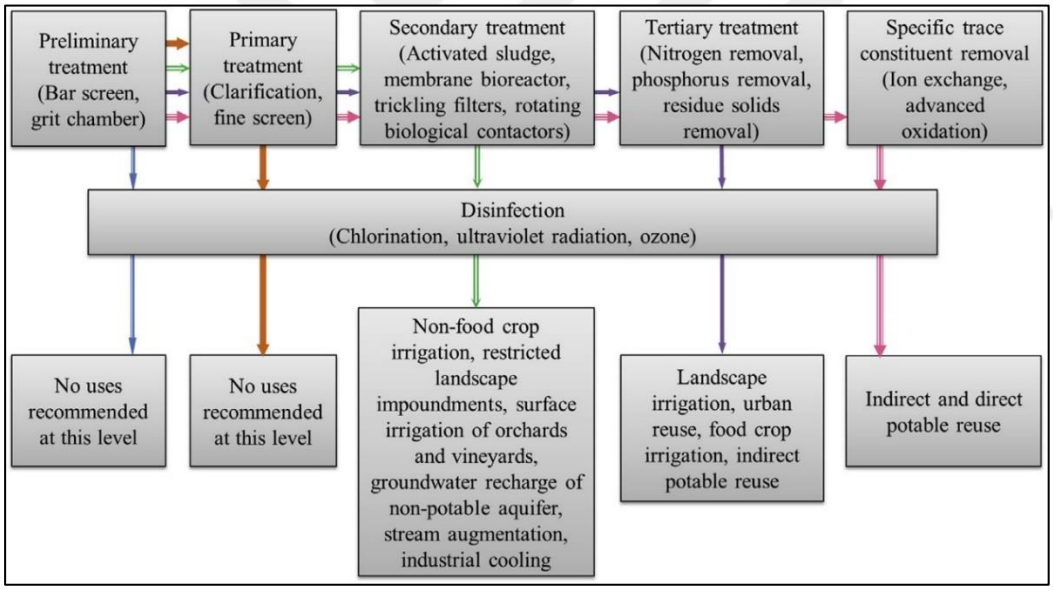

Figure 2.2 : Wastewater treatment phases, technologies, and utilizations of effluents (Mo & Zhang, 2013).

It should be noted that a more comprehensive course of action has been published by the European Union Parliament covering the directives for water reuse criterias. As a result, awareness in terms such as resource management and sustainability have raised and modifications in wastewater treatment for resource recovery have expanded. At the present time, development in energy efficiency and resource recovery are the main approaches in improving sustainability of WWTPs (Mo & Zhang, 2013).

Recovering resources existing in wastewater has a paramount importance in wastewater treatment plants during the transmutation process of renewable energy, water intended to be used in other applications and biofertilizer from those resources (Chrispim, Scholz & Nolasco, 2020). Concisely, resource recovery targets the complete utilization of different outputs from each wastewater treatment process intending to convert them into practical products as it can be seen in Figure 2.3. It also aims to prevent the wastage of organic carbon, metals, and global nutrients substantial in wastewater for achieving industrial sustainability (Puyol & Batstone, 2017).

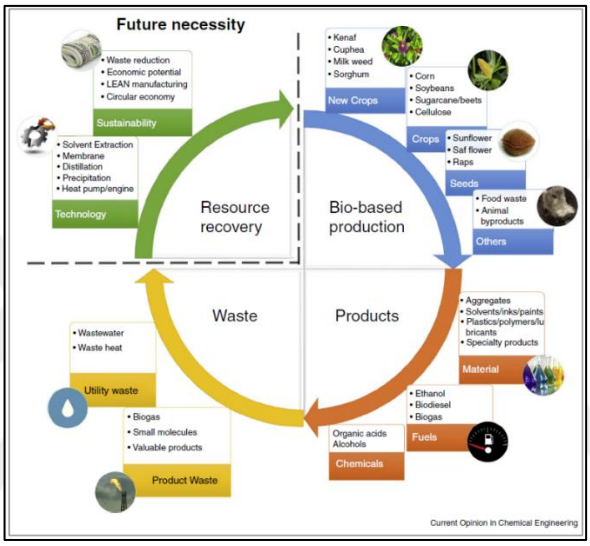

Figure 2.3 : Bio-based production processes including resource recovery (Puyol & Batstone, 2017).

The two major nutrients present in wastewater are nitrogen and phosphorus. It is vital to have a deep understanding of biochemical reactions, system dynamics, and balance equations in the removal processes of each nutrient. Therefore, creating a viable framework of biological nutrient removal processes prior to the enhancements like life cycle assesment and resource recovery tools to the simulation platform is crucial in terms of accuracy in software integration. Particularly for nitrogen, nitrification and denitrification processes must be conceived along with current modifications designed based on the relevance of each process. Enhancement of stated tools must be achieved only after the model framework is created and the conversion reactions of vital parameters are comprehended as the carbon and nitrogen contents of wastewater morphs into carbon dioxide, biomass, and nitrogen gas due to bacterial activities in the course of activated sludge treatment (Ansari et al., 2017).

2.2.1 Biological nitrogen removal processes

2.2.1.1 Nitrification

Nitrification process is the first phase of a two-step nitrification-denitrification cycle used in the biological removal of nitrogen from wastewater. It takes place in an aerobic environment where the chemotrophic bacteria are capable of yielding nitrogen oxides by oxidizing existing ammonia nitrogen (NH_4^+) in the reactor. The oxidation process of ammonia nitrogen itself is a two-step chain of reactions consisting of the conversion of ammonia nitrogen (NH_4^+) into nitrite (NO_2^-) and the conversion of nitrite (NO2-) into nitrate (NO_3^-) as it can be seen in Equations 2.1 and 2.2, respectively.

$$NH_4^+ + 1{,}5O_2 \rightarrow NO_2^- + 2H^+ + H_2O \quad (2.1)$$

$$NO_2^- + 0{,}5O_2 \rightarrow NO_3^- \quad (2.2)$$

The conversion reaction of ammonia nitrogen into nitrite is accomplished by Nitrosomonas species, whereas latter is achieved by Nitrobacter species. Each bacteria species yields the products with the help of their ability to use nitrogen forms as electron donor, while utilizing carbondioxide (CO_2) as electron donor and the oxygen (O_2) as electron acceptor. Hence, maintaining sufficient amount of dissolved oxygen concentration in the aerobic reactor is crucial and a drop below critical dissolved oxygen concentrations in the reactor might end up adversely affecting the reaction or even cease the growth of particular bacteria. Even though aeration of aerobic reactor is of great importance in regard of system sustainability and in an aerobic reactor the oxygen concentration should not fall under 0.5 mg/L according to (Bozek, Navratil & Kellner, 2005), operational parameters such as temperature, pH, hydraulic retention time (HRT), and sludge retention time (SRT) are also vital for the autotrophic bacteria to prevail. The effects of these parameters on nitrification process can be seen in Figure 2.4, Figure 2.5, and Figure 2.6.

In order to achieve complete removal of nitrogen in the system, a supplementary phase is needed. Denitrification process must be combined with nitrification to fulfill the objective.

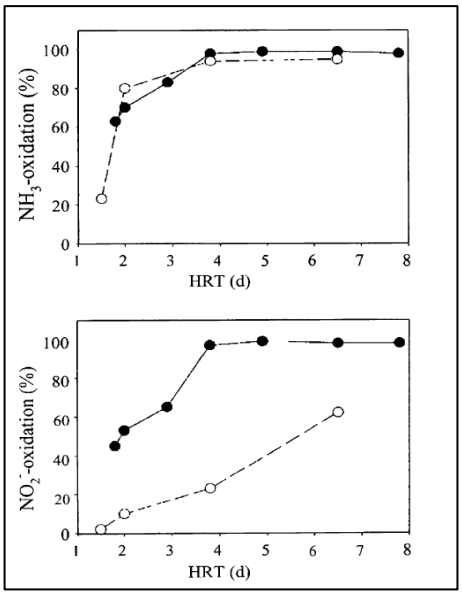

Figure 2.4 : O_2 concentration effect, sufficient O_2 (•) and0.5 mg O_2 l^{-1} (o), on oxidation processes for different HRTs (Sinha & Annachhatre, 2006).

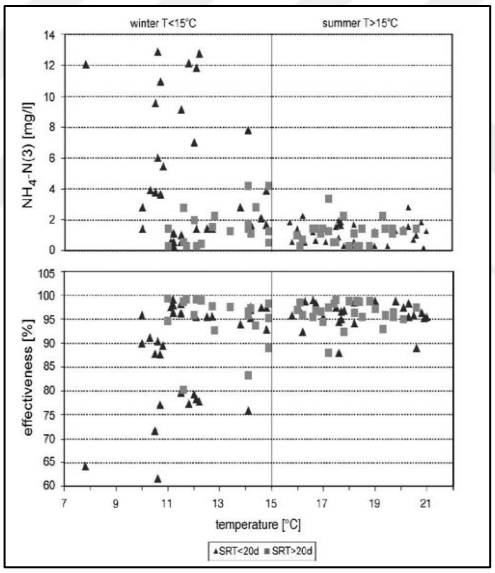

Figure 2.5 : Effect of Temperature on NH_4-N concentration and effectiveness of nitrification (Komorowska-Kaufman et al., 2006).

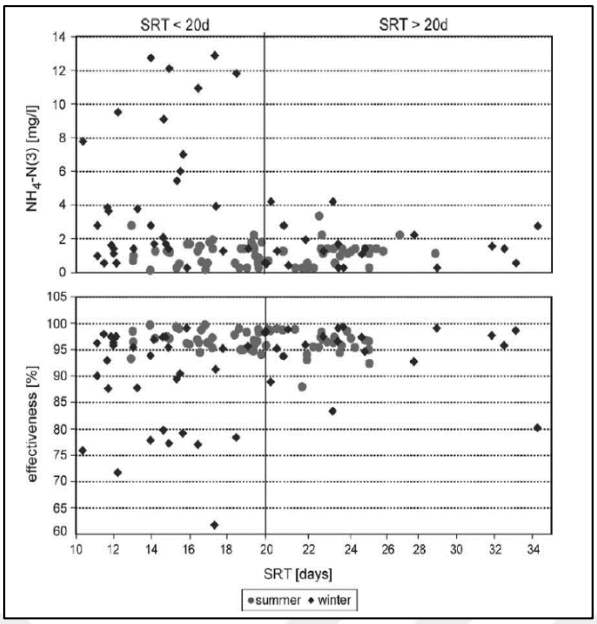

Figure 2.6 : Effect of SRT on NH_4-N concentration and effectiveness of nitrification (Komorowska-Kaufman et al, 2006).

2.2.1.2 Denitrification

Denitrification is the second step of biological nitrogen removal in activated sludge systems which achieves the conversion of nitrate nitrogen (NO3-) into nitrogen gas (N2). Conversion of nitrate nitrogen is accomplished by four sequential steps (Feleke, 2002) as it can be seen in Equation 2.3.

$$NO_3^- \rightarrow NO_2^- \rightarrow NO \rightarrow N_2O \rightarrow N_2 \quad (2.3)$$

Biological nitrogen removal in wastewater treatment systems is dominantly performed by facultative heterotrophic bacteria in anoxic conditions. Anoxic reactors do not contain dissolved oxygen, instead they contain oxygen in the form of nitrogen oxides.

Nitrate (NO3-) is the electron acceptor in this case whereas carbondioxide (CO2) is the electron donor. For the purpose of achieving complete biological nitrogen removal, nitrification and denitrification processes are coupled with the help of various configuration setups.

Among the single-sludge designed systems, most widely used ones are the pre-denitrification and the post-denitrification systems.

2.2.2 Biological nitrogen removal configurations

2.2.2.1 Pre-denitrification systems

Pre-denitrification systems are designed based on the fact that having sufficient amounts of substrate in anoxic reactors is vital for the facultative bacteria to maintain their metabolical activities. In pre-denitrification systems, anoxic reactors are placed ahead of aerobic reactors in order to fulfill this objective. Constant feed of substrate from the influent wastewater creates the optimum ambient for the facultative bacteria to prevail. The single sludge Ludzack-Ettinger model consisting of anoxic and aerobic reactors in series and a sludge recyle from the settling tank was designed for achieving nitrogen removal in wastewater. This predenitrification design was later on improved with Modified Ludzack-Ettinger configuration by addition of an internal recycle flow from aerobic reactor to the anoxic reactor as it can be seen in Figure 2.7.

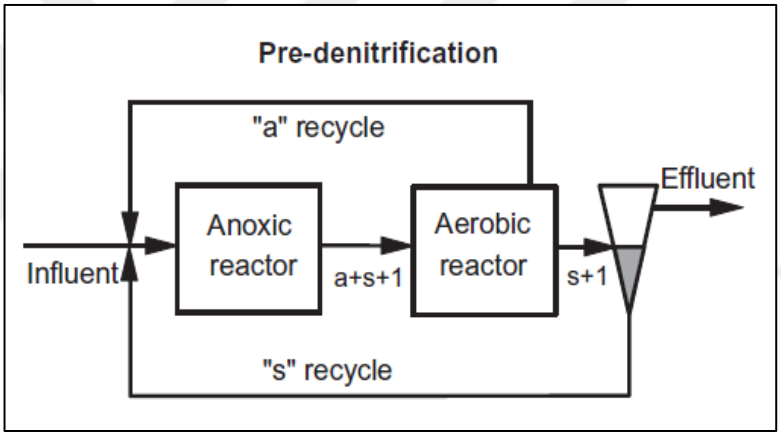

Figure 2.7 : Pre-denitrification system design (Haandel, 2012).

The difference between two configurations can also be seen in Figure 2.8. Under favour of this enhancement, constant feed of nitrate rich content to the anoxic tank was achieved while a reduction in effluent nitrate concentration was accomplished due to the internal recycle. Constant feeding of anoxic reactor with nitrate rich content also increased the growth rate of denitrifiers as nitrate nitrogen is the electron donor for their utilization reactions.Internal feed of nitrate effluent from the aerobic reactor is accomplished by an internal recycle flow to the anoxic reactor Particulate matter are also recycled after the settling tank for the aim of sustaining sufficient biomass concentrations in the anoxic reactor. Altering the effluent nitrate nitrogen which recycles to the anoxic reactor into nitrogen gas makes it possible to remove nitrogen in the system.

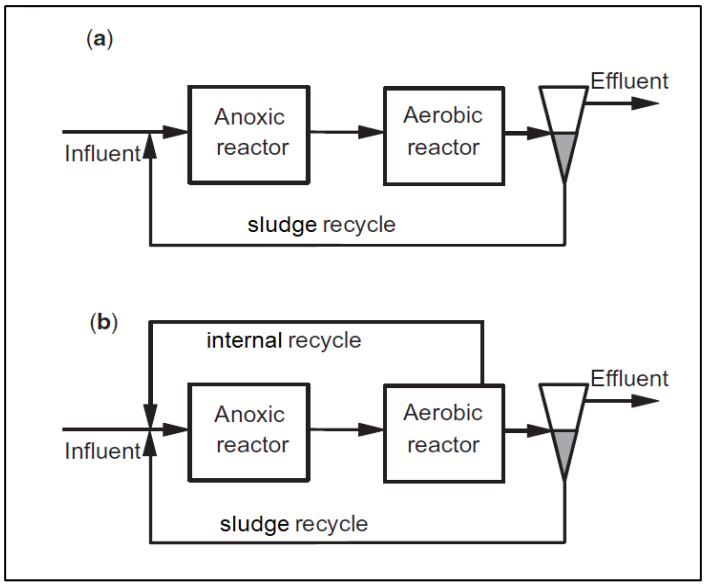

Figure 2.8 : Difference between (a) Ludzack-Ettinger and (b) Modified Ludzack-Ettinger Models (Haandel, 2012).

2.2.2.2 Post-denitrification systems

In contrast to pre-denitrification systems, aerobic reactors are placed ahead of anoxic reactors in post-denitrification systems as it can be seen below in Figure 2.9. The advantage of post-denitrification systems is the potential of complete removal of nitrogen in wastewater. Pre-denitrification systems discharge some of the nitrate nitrogen content as effluent from aerobic reactors. The disadvantage on the other hand is having lower denitrification rates compared to pre-denitrification system as most of the substrate concentrations are consumed in the aerobic reactor and in order to achieve higher denitrification rates substrate addition to the anoxic reactor is required.

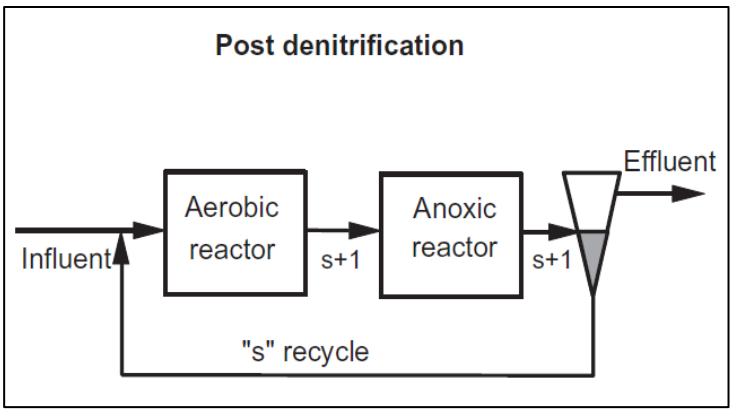

Figure 2.9 : Post-denitrification system design (Haandel, 2012).

2.3 Modelling of Activated Sludge Systems

2.3.1 Model development

Through the years, knowledge of environmental scientists/engineers on wastewater treatment has exponentially increased. This ended up uprising the need for creating and improving models in order to have a better understanding of the processes taking place in wastewater treatment and enabling more efficient plant designs.

Even though various mathematical models have been developed before, on the purpose of forming a framework introducing a globally accepted new model, Activated Sludge Model No.1 (ASM1) was developed by International Association on Water Quality (IAWQ) in 1987.

In 1999, IAWQ merged with the International Water Supply Association (IWSA) to form the International Water Association (IWA). Even now, models are being established inspired by the ASM1 and implementation of these models into simulation platforms are ongoing (Henze et al., 2015). Further studies on the model resulted in publications of new models as it is shown below in Table 2.1.

Table 2.1 : Publication years of activated sludge models by IWA.

Model	Year of Publication	Reference
ASM1	1987	(Henze et al., 1987)
ASM2	1995	(Henze et al., 1995)
ASM2d	1999	(Henze et al., 1999)
ASM3	1999	(Gujer et al., 1999)

Activated Sludge Model No.2 (ASM2) was developed in 1995, as the previous reference model is unable to define Enhanced biological phoshorus removal (EBPR) mechanism. Similar to ASM1, an expanded version of ASM2, Activated Sludge Model No.2d (ASM2d) was released in 1999. Following the publication of ASM2d, Activated Sludge Model No.3 (ASM3) was released in the same year.

2.3.2 Activated sludge model no. 1

In order to create a simple activated sludge model capable of computing precise predictions, a task group was formed by the International Association on Water Quality (IAWQ) in 1987 which initially focused on earlier model studies for creating a universal framework. Monod-like expressions for growth rates of autotrophic and heterotrophic bacteria and concepts like bisubstrate hypothesis that suggested the fragmentation of influent wastewater fractions as readily and slowly biodegradable COD were embraced from the University of Cape Town (UCT) model (Jeppsson, 1996).

Switching functions that enabled limiting the process rates gradually in the absence of components required for the processes to take place, such as the dissolved oxygen, were introduced (Jeppsson, 1996). Also, the task group determined using a matrix format for the demonstration of the interactions of model processes, components and process rates. The flow of chemical oxygen demand (COD) in ASM1 can be seen below in Figure 2.10.

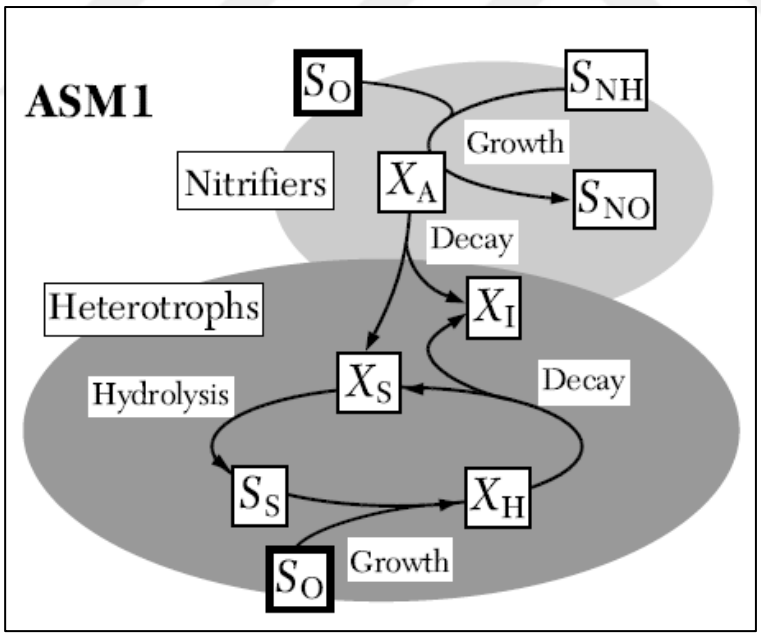

Figure 2.10 : Flow of COD in ASM1 (Henze et al., 2015).

The structure of ASM1 involves a strong interralation between the decay regeneration cycle of the heterotrophs and the decay process of nitrifiers (Henze et al., 2015).

2.3.3 Activated sludge model no. 3

The task group of International Water Association (IWA) published Activated Sludge Model No.3 (ASM3) in 1999 due to the requirement of a renovated model that could take advantage of the developments occurred in computation methods.

In ASM3, endogenous respiration was introduced instead of the decay process (lysis) used in the ASM1 (Henze et al., 2015). The profound effect of hydrolysis that was defined as a combined process of hydrolysis, lysis of organisms and storage of substrates is prevented in ASM3 with the introduction of cell internal storage mechanism (Henze et al., 2015). The flow of chemical oxygen demand (COD) in ASM3 can be seen below in Figure 2.11.

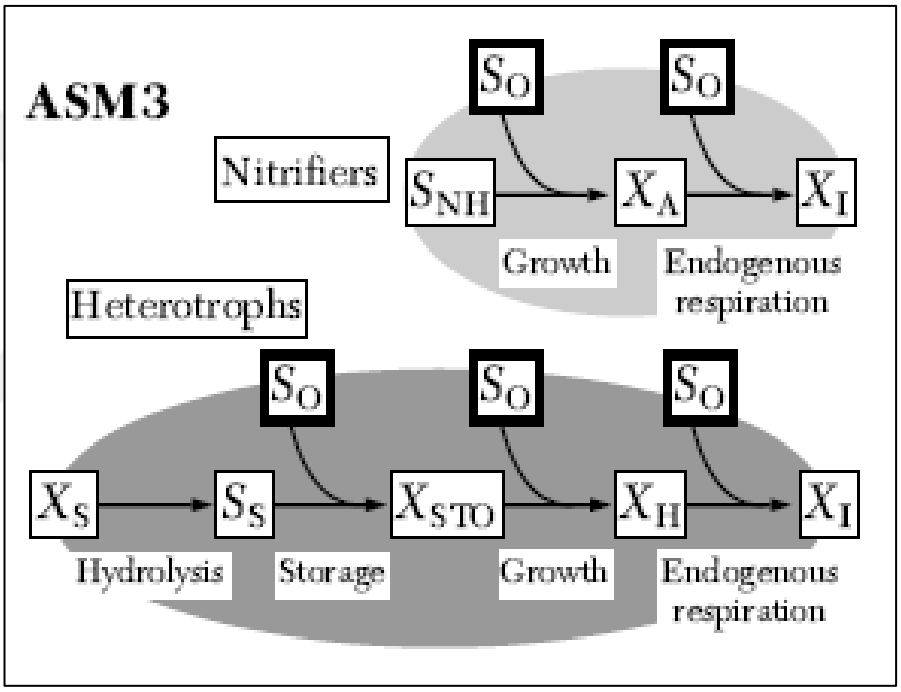

Figure 2.11 : Flow of COD in ASM3 (Henze et al., 2015).

As it can be seen in Figure 2.11, all the processes related with both of the heterotrophic and the autotrophic organisms are defined separately in contrast to ASM1 and decay processes are identically defined (Henze et al., 2015).

2.4 Software Platforms for Activated Sludge Simulation

2.4.1 AQUASIM

AQUASIM simulation program was developed for providing environmental scientists a platform able to define their processes and variables and perform simulations according to the model they have defined. It was developed by Swiss Federal Institute for Environmental Science and Technology (EAWAG) not only for the purpose of designing a program with a user friendly graphical user interface but also for creating a simulation platform uncomplicatedly comprehended by environmental scientists due to its familiar language (Reichert, 1998). Aquasim system consists of four subsystems that the user has to adjust for the intended model amplification as it can be seen in Figure 2.12.

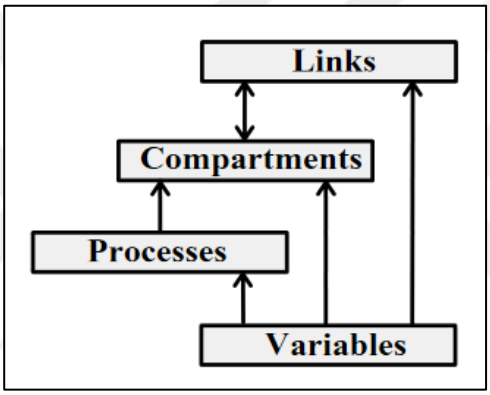

Figure 2.12 : Main elements of model structure (Reichert, 1998**)**.

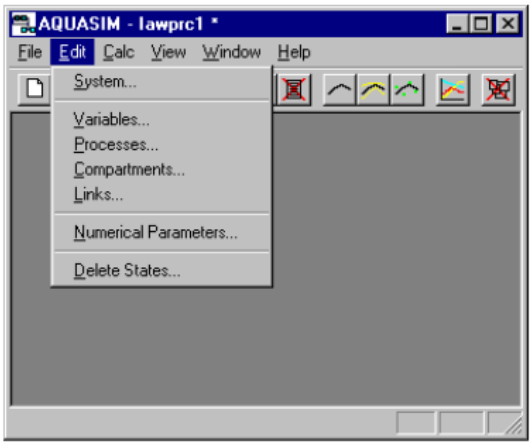

Figure 2.13 : Edit menu (Reichert, 1998**)**.

These four subsystems are variables, processes, compartments and links. Aquasim users have to define all the subsystem parameters and specify the types of variables, processes and links.

System inputs can either be defined inside the program as constant inputs or loaded to the software by a time series real list from a text file. Defining a real list variable inside the program is also possible.

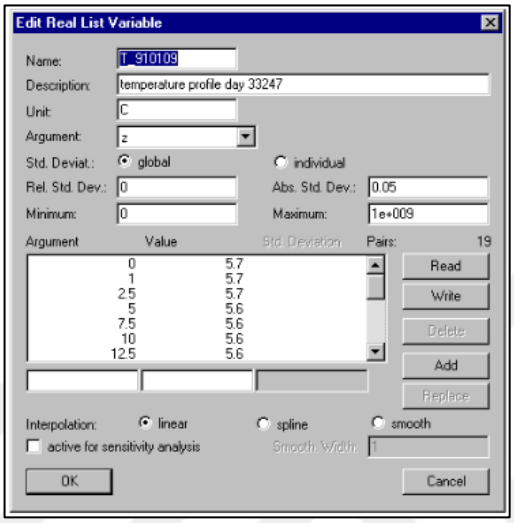

Figure 2.14 : Dialog box for editing a real list variable (Reichert, 1998**)**.

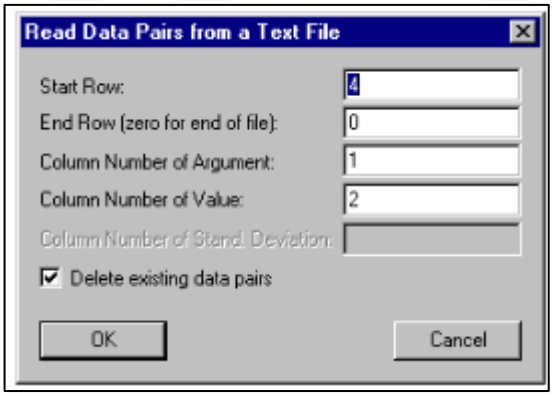

Figure 2.15 : Dialog box for reading data pairs from a text (Reichert, 1998**)**.

There are six types of variables, two types of processes and three types of compartments in the program as shown in Table 2.2 and setting a recycle flow between compartments are achieved by the links subsystem with the bifurcation option (Reichert, 1995**)**.

Setting the predefined initial values for state variables, adjusting reactor dimension and input flows, activating the intended processes and choosing the reactor type can be done through compartment editing section.

Table 2.2 : Types of subsystem elements in AQUASIM (Reichert, 1995**)**.

Subsystem	Type
Variables	State Variables
	Program Variables
	Constant Variables
	Real List Variables
	Variable List Variables
	Formula Variables
Processes	Dynamic Processes
	Equilibrium Processes
Compartments	Mixed Reactor Compartments
	Biofilm Reactor Compartments
	River Section Reactor Compartments

Besides simulation, AQUASIM provides identifiability analysis, parameter estimation and uncertainty analysis funcitonalities to the users (Reichert, 1995).

In this thesis study, validation of the created simulation program has been achieved by comparing output data with the output data obtained from simulating the same model in AQUASIM.

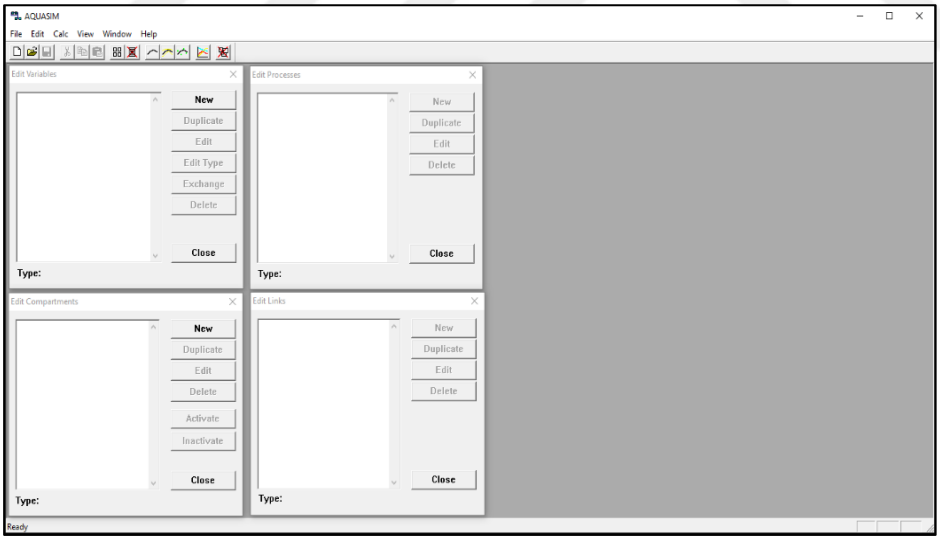

Figure 2.16 : Graphical user interface of AQUASIM (Reichert, 1998**)**.

2.4.2 SUMO

The Super Model (SUMO) wastewater simulation software is among the best-known softwares in the field of environmental engineering. It was developed by Dynamita software and process modelling company and contains open-source model and process unit libraries (SUMO | dynamita, 2021). These libraries were coded in a unique language called SumoLang which was designed for the software itself. In order to build advanced level models and perform modifications on existing models, users have to master the SumoLang through the user manual Dynamita company provides them with. The simulation software also provides the users with the opportunity of performing steady-state and dynamic simulations.

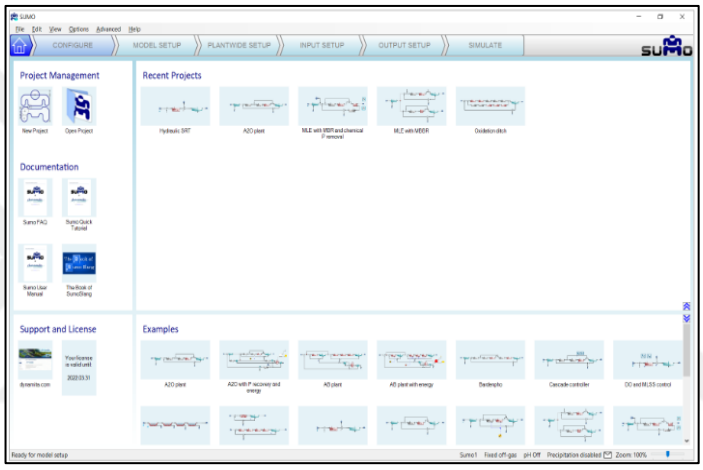

Figure 2.17 : Graphical user interface of SUMO (SUMO | dynamita, 2021).

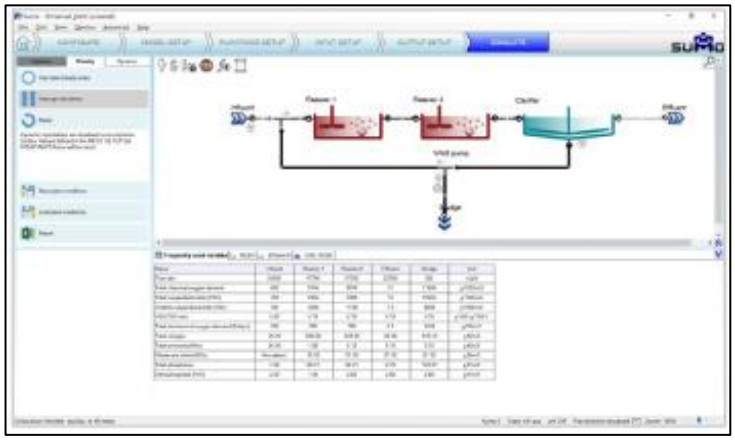

Figure 2.18 : Steady-state calculation results in SUMO (SUMO | dynamita, 2021).

2.4.3 BioWin

BioWin is a wastewater treatment plant simulation software and it was developed by EnviroSim company which was established in 1990. It is a globally known software used for optimizing, designing and upgrading any type of wastewater treatment plant (EnviroSim, 2021). BioWin software provides models that integrates biological, chemical, and physical processes and it is capable of performing simulations of water chemistry models for calculation of pH and precipitation reactions, mass transfer models for oxygen modeling and other gas-liquid interactions with the help of supplementary packages (EnviroSim, 2021). BioWin has a user friendly graphical user interface as it can be seen in Figure 2.19. It also provides report generation function in the format of Excel and Word.

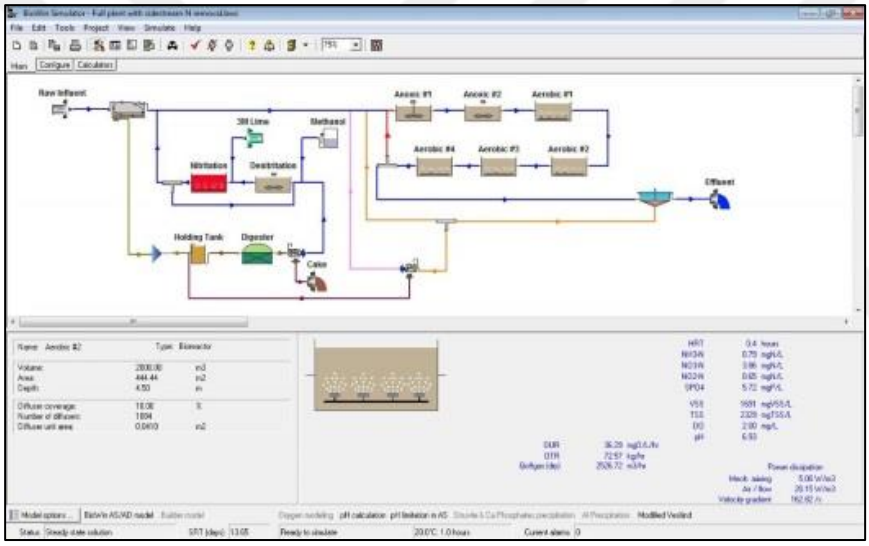

Figure 2.19 : Graphical user interface of BioWin (EnviroSim, 2021).

Figure 2.20 : Result graphs from BioWin (EnviroSim, 2021).

2.4.4 GPS-X^{TM}

GPS-XTM was developed by Hydromantis, an environmental engineering company based in Canada which was founded in 1985. Hydromantis focuses on software development comprising plant optimization, collection and distribution systems and water resource management (Hydromantis, 2021). Their dynamic wastewater treatment simulation software GPS-XTM contains powerful tools providing options to the users such as model development, dynamic parameter estimation and python integration. GPS-XTM also contains a wide range of unit processes and enables running simulations by getting input data from the user.

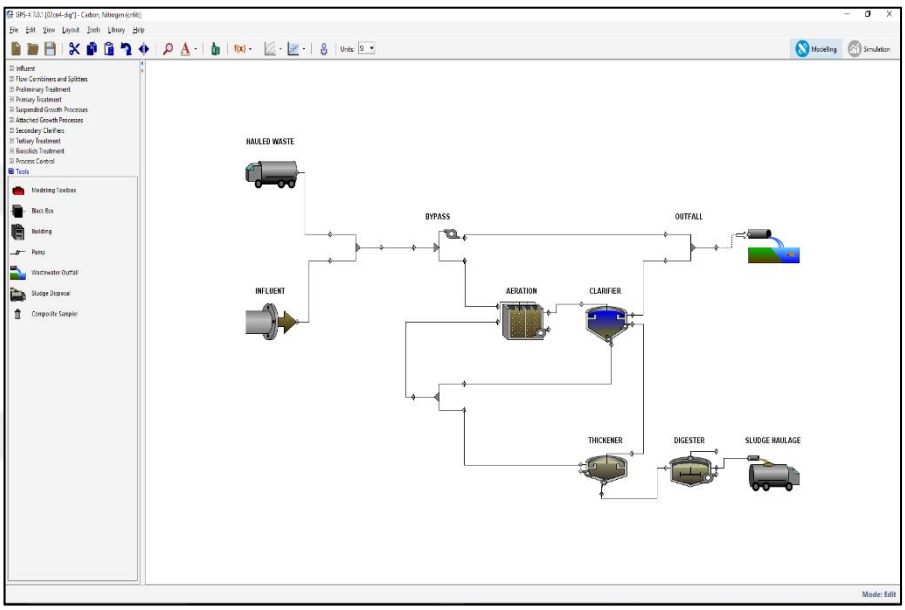

Figure 2.21 : Graphical user interface of GPS-X^{TM} (Hydromantis, 2021).

Interface of the software is designed user friendly with its drag-n-drop function. Each unit process can be linked by the user with connection paths. It is possible to plot energy usage and operating cost values in the program. Through mass balances diagram option, users are enabled to visualize the system layout with additional information tables in which they can adjust the parameters of selected unit processes. Performing statistical comparison of measured and simulated datasets can be plotted with the statistical analysis tool.

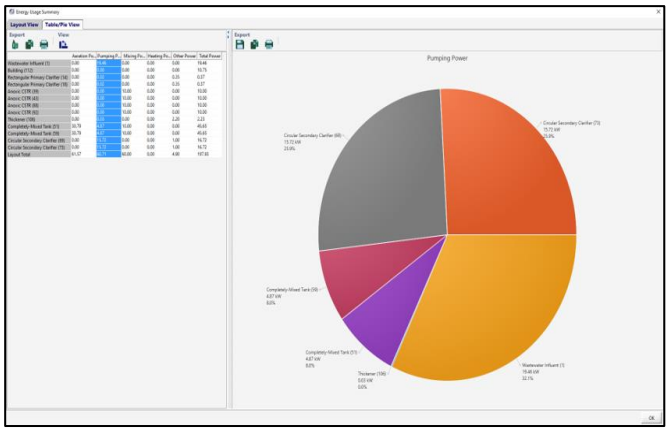

Figure 2.22 : Visualization of energy usage and operation costs on GPS-X^{TM} (Hydromantis, 2021).

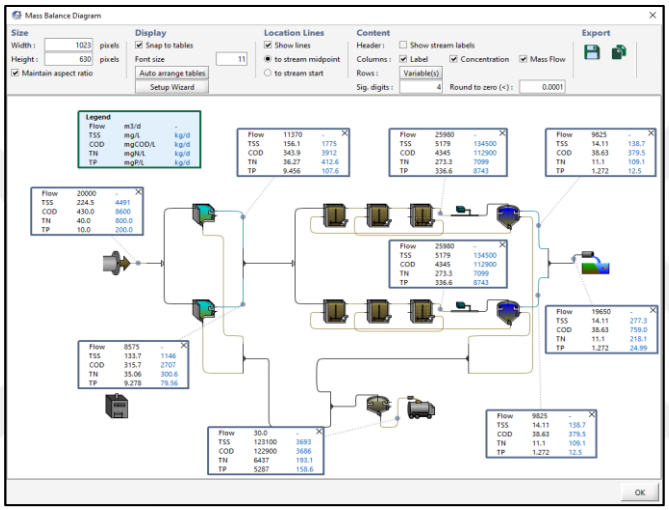

Figure 2.23 : Mass balance diagram of GPS-X^{TM} (Hydromantis, 2021).

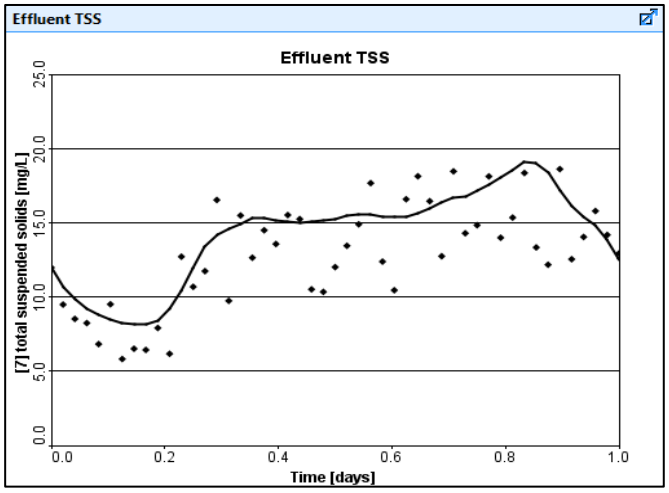

Figure 2.24 : Model predicted and measured effluent TSS concentration vs. Time graph from GPS-X^{TM} (Hydromantis, 2021).

2.4.5 SIMBA

Simba was first developed by the Water & Energy department at ifak e.V. in 1994. It has then been modified and the latest member of the Simba™ simulator family is SIMBA# (SIMBA#, 2021). SIMBA#water is used for the simulations, mathematical modellings and optimizations of wastewater treatment systems with its wide unit process library that enables dynamic simulations.

The software has a modern GUI that provides visualization of the simulation results and a model editor that enables biological and unit process models implementation (SIMBA#, 2021).

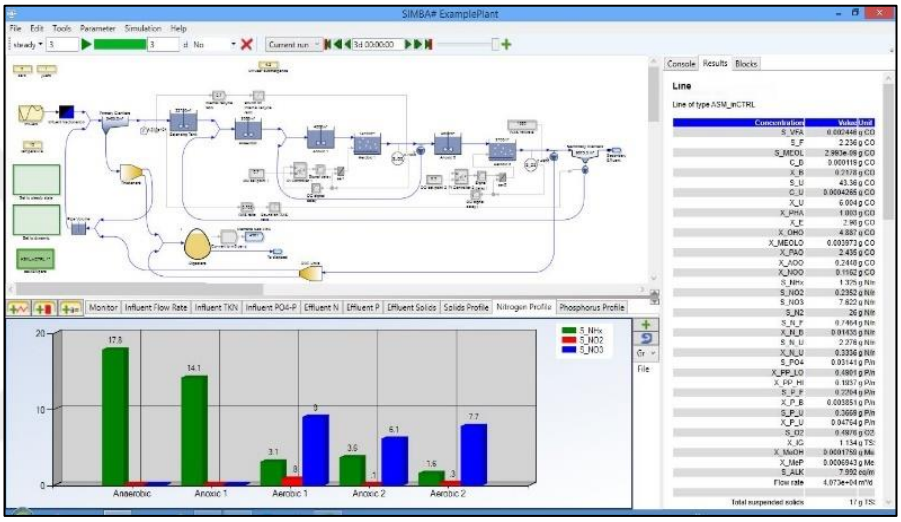

Figure 2.25 : Complete plant model in SIMBA# (SIMBA#, 2021).

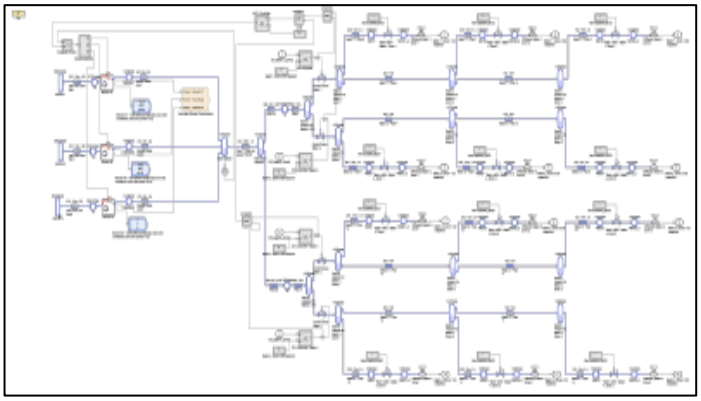

Figure 2.26 : Aeration system model in SIMBA# (SIMBA#, 2021).

2.4.6 WEST

WEST simulation platform has been developed by DHI company in order to provide optimization of treatment plants, comparison of treatment system scenarios, development of custom process models and simulation of integrated models (WEST, 2021). WEST software is also capable of performing carboon footprint calculations and implementation of control strategies.

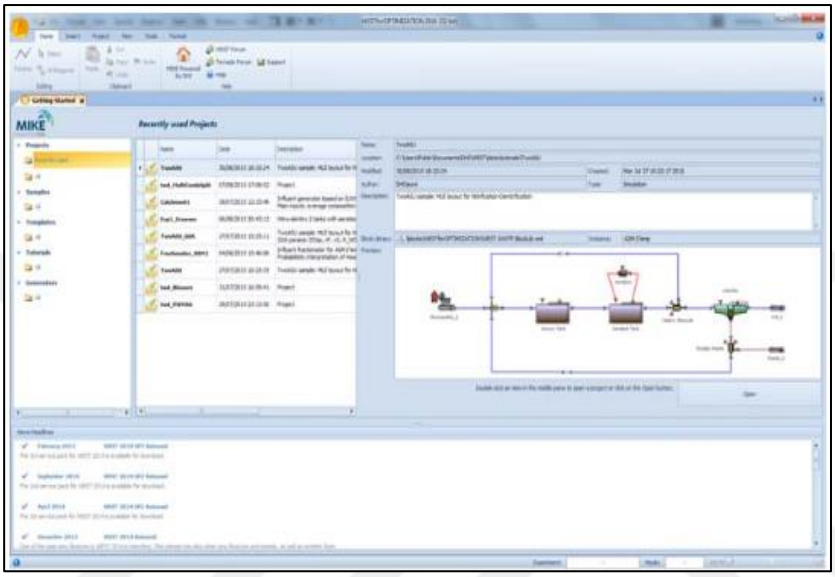

Figure 2.27 : The start-up view of WEST (WEST, 2021).

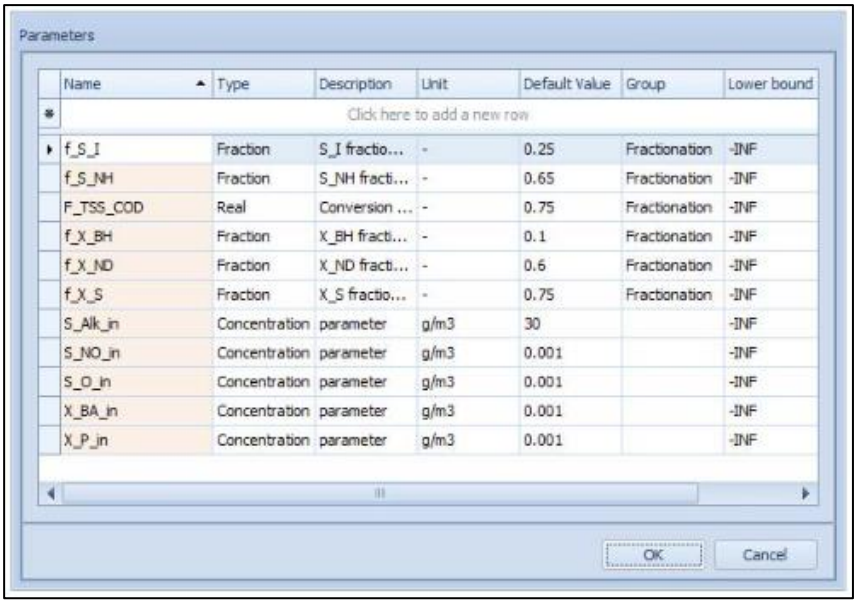

Figure 2.28 : Parameters of the fractionation model (WEST, 2021).

3. SOFTWARE DEVELOPMENT

3.1 Selection of Programming Language

Throughout the process of software development, Python programming language was chosen due to its comprehensive open-source libraries. Recently, Python language is one of the most known and widely used programming languages in data science under favour of these open-source libraries which provides the user with various useful packages and modules. As part of this thesis study, packages that contain practical tools for performing complicated mathematical calculations, storing the data in multi-dimensional arrays, plotting the results of each state variable and creating a friendly graphical user interface were used. In addition to the benefits they provide in regard to data science, most of the packages constituted for python are written in different programming languages that are quicker in the compiling process such as C and C++. Programming languages like C and C++ are considered to be low-level programming languages meaning that their syntax are closer to the machine language and compiling source codes of low-level programming languages to machine language is faster when compared to high-level programming languages like Python.

On the other hand, high-level programming languages are similar to modern day languages in terms of their syntax structures and therefore easier to learn and master in a shorter period of time.

Machine language, also known as machine code, is the language that operates computers and provides users with the opportunity to get their commands done by computers. Machine language is made up of binary numbers which are comprised of ones and zeros and in order for a computer to run a program written by the user in any of the existing programming languages, first it should be compiled into machine language. However, converting a source code writtten in Python language into machine code is performed by interpreters instead of compilers.

One of the most important differences between interpreters and compilers is the need for compilers to create an object code in the compiling process, ending up using more memory but at the same time considerably decreasing execution time. On the contrary, interpreters execute the source code line by line without creating an object code and saving memory in the process.

3.2 Biochemical Process Model

The biochemical reactions demonstrated in the model matrix of simulation software as shown in Table 3.1, are integrated into the mass balance equations of Modified Ludzack-Ettinger (pre-denitrification) configuration. The biochemical process model consists of hydrolization processes of rapidly hydrolyzable COD, slowly hydrolyzable COD, soluble organic nitrogen and particulate organic nitrogen as well as growth and decay processes of heterotrophic and autotrophic biomasses maintaining in the aerobic and anoxic tanks. In total, process model consists of 10 processes and 2 operational parameters defined for 15 state variables. Reactions occuring in both tanks are included into the mass balance equations of each state variable. In order to accomplish this, cofefficients and stoichiometric parameters defined on process lines of a single component's column are multiplied by the process rates of the corresponding processes. The same principle is applied to the operational processes in order to incorporate aeration process for the aerobic biomass by considering a constant feed of dissolved oxygen and sludge disposal process for the particulate matter that are going to be wasted. Users are enabled to adjust the dissolved oxygen saturation concentration prior to running the simulation through the graphical interface. Sludge disposal is also achieved by the sludge retention time input that the users provide the software with and total volume of the reactors are considered in the computation process of sludge disposal. Correction factors for the process rates of heteroptrophic biomass maintaining under anoxic conditions are included to kinetic parameters along with the heterotrophic and autotrophic growth and decay coefficients. Hydrolysis rates and coefficients are also included in the related process rates.

Table 3.1 : Model matrix of the simulation software.

Components→ *i*		1	2	3	4	5	6	7	8	9	10	11	12	13	14	15	Process Rate, ϱ_j [$ML^{-3}T^{-1}$]
j	**Process**↓	S_I	S_S	X_I	X_S	$X_{B,H}$	$X_{B,A}$	S_P	X_P	S_O	S_{NO}	S_{NH}	S_H	S_{ND}	X_{ND}	S_{ALK}	
1	Aerobic growth of heterotrophs		$\frac{-1}{Y_H}$			1				$-\frac{1-Y_H}{Y_H}$		- i_{XB}				$\frac{-i_{XB}}{14}$	$\mu_{H,max}\frac{S_S}{K_S+S_S}\frac{S_O}{K_{O,H}+S_O}\frac{K_{NO}}{K_{NO}+S_{NO}}\frac{S_{NH}}{K_{NH}+S_{NH}}X_{B,H}$
2	Anoxic growth of heterotrophs		$\frac{-1}{Y_{HD}}$			1					$-\frac{(1-Y_{HD})}{2{,}86Y_{HD}}$	- i_{XB}				$\frac{(1-Y_{HD})}{14\times 2.86Y_{HD}}$ $-\frac{i_{XB}}{14}$	$\eta_g\mu_{maxH}\frac{S_S}{K_S+S_S}\frac{K_{O,H}}{K_{O,H}+S_O}\frac{S_{NO}}{K_{NO}+S_{NO}}\frac{S_{NH}}{K_{NH}+S_{NH}}X_{B,H}$
3	Aerobic growth of autotrophs						1			$-\frac{4{,}57-Y_A}{Y_A}$	$\frac{1}{Y_A}$	$\frac{-1}{Y_A}$ $-i_{XB}$				$-\frac{i_{XB}}{14}-\frac{1}{7Y_A}$	$\mu_{A,max}\frac{S_{NH}}{K_{NH}+S_{NH}}\frac{S_O}{K_{O,A}+S_O}X_{B,A}$
Observed Conversion Rates [$ML^{-3}T^{-1}$]			$r_i=\sum_j v_{ij}\varrho_j$														
Stoichiometric Parameters: Heterotophic yield: Y_H, Y_{HD} Autotrophic yield: Y_A Fraction of biomass yielding products: f_{EX}, f_{ES} Mass N/Mass COD in biomass: i_{XB} Mass N/Mass COD in products from biomass: i_{XP}		Soluble inert organic matter [M(COD)L^{-3}]	Readily biodegradable substrate [M(COD)L^{-3}]	Particulate inert organic matter [M(COD)L^{-3}]	Slowly biodegradable substrate [M(COD)L^{-3}]	Active heterotrophic biomass [M(COD)L^{-3}]	Active autotrophic biomass [M(COD)L^{-3}]	Soluble products arising from biomass decay [M(COD)L^{-3}]	Particulate products arising from biomass decay [M(COD)L^{-3}]	Oxygen (negative COD) [M(-COD)L^{-3}]	Nitrate and nitrite nitrogen [M(N)L^{-3}]	$NH_4^+ + NH_3$ nitrogen [M(N)L^{-3}]	Rapidly biodegradable substrate [M(COD)L^{-3}]	Soluble biodegradable organic nitrogen [M(COD)L^{-3}]	Particulate biodegradable organic nitrogen [M(COD)L^{-3}]	Alkalinity – Molar units	Kinetic Parameters: Heterotophic growth and decay: μ_H, K_S, $K_{O,H}$, K_{NO}, b_H Autotrophic growth and decay: μ_A, K_{NH}, $K_{O,A}$, b_A Correction factor for anoxic growth of heterotrophs : η_g Correction factor for anoxic decay of heterotrophs : η_d Hydrolysis: K_{hS}, K_{hX}, K_{XS}, K_{XX}

Table 3.1 (continued): Model matrix of the simulation software.

Components→ i		1	2	3	4	5	6	7	8	9	10	11	12	13	14	15	Process Rate, ϱ_j [$ML^{-3}T^{-1}$]
j	Process↓	S_I	S_S	X_I	X_S	$X_{B,H}$	$X_{B,A}$	S_P	X_P	S_O	S_{NO}	S_{NH}	S_H	S_{ND}	X_{ND}	S_{ALK}	
4	Endogeneous decay of heterotrophs under aerobic conditions					-1		f_{ES}	f_{EX}	- (1 - f_{EX} - f_{ES})					$i_{XB} - (f_{EX} + f_{ES})i_{XP}$		$b_H \frac{S_O}{K_{O,H}+S_O}\frac{S_{NO}}{K_{NO}+S_{NO}}X_{B,H}$
5	Endogeneous decay of heterotrophs under anoxic conditions					-1		f_{ES}	f_{EX}		$-\frac{(1-f_{EX}-f_{ES})}{2{,}86}$				$i_{XB} - (f_{EX} + f_{ES})i_{XP}$		$\eta_d b_H \frac{K_{O,H}}{K_{O,H}+S_O}\frac{S_{NO}}{K_{NO}+S_{NO}}X_{B,H}$
6	Endogeneous decay of autotrophs						-1	f_{ES}	f_{EX}	- (1 - f_{EX} - f_{ES})					$i_{XB} - (f_{EX} + f_{ES})i_{XP}$		$b_A \frac{S_O}{K_{O,A}+S_O}X_{B,A}$
Observed Conversion Rates [$ML^{-3}T^{-1}$]		$r_i = \sum_j v_{ij}\varrho_j$															
Stoichiometric Parameters: Heterotophic yield: Y_H, Y_{HD} Autotrophic yield: Y_A Fraction of biomass yielding products: f_{EX}, f_{ES} Mass N/Mass COD in biomass: i_{XB} Mass N/Mass COD in products from biomass: i_{XP}		Soluble inert organic matter [M(COD)L^{-3}]	Readily biodegradable substrate [M(COD)L^{-3}]	Particulate inert organic matter [M(COD)L^{-3}]	Slowly biodegradable substrate [M(COD)L^{-3}]	Active heterotrophic biomass [M(COD)L^{-3}]	Active autotrophic biomass [M(COD)L^{-3}]	Soluble products arising from biomass decay [M(COD)L^{-3}]	Particulate products arising from biomass decay [M(COD)L^{-3}]	Oxygen (negative COD) [M(-COD)L^{-3}]	Nitrate and nitrite nitrogen [M(N)L^{-3}]	$NH_4^+ + NH_3$ nitrogen [M(N)L^{-3}]	Rapidly biodegradable substrate [M(COD)L^{-3}]	Soluble biodegradable organic nitrogen [M(COD)L^{-3}]	Particulate biodegradable organic nitrogen [M(COD)L^{-3}]	Alkalinity – Molar units	Kinetic Parameters: Heterotophic growth and decay: μ_H, K_S, $K_{O,H}$, K_{NO}, b_H Autotrophic growth and decay: μ_A, K_{NH}, $K_{O,A}$, b_A Correction factor for anoxic growth of heterotrophs : η_g Correction factor for anoxic decay of heterotrophs : η_d Hydrolysis: K_{hS}, K_{hX}, K_{XS}, K_{XX}

Table 3.1 (continued): Model matrix of the simulation software.

Components→ *i*		1	2	3	4	5	6	7	8	9	10	11	12	13	14	15	Process Rate, ϱ_j [$ML^{-3}T^{-1}$]
j	**Process↓**	S_I	S_S	X_I	X_S	$X_{B,H}$	$X_{B,A}$	S_P	X_P	S_O	S_{NO}	S_{NH}	S_H	S_{ND}	X_{ND}	S_{ALK}	
7	Hydrolysis of Rapidly Hydrolyzable COD		1										-1				$K_{hS}\frac{S_H / X_{B,H}}{K_{XS} + (S_H / X_{B,H})}X_{B,H}$
8	Hydrolysis of soluble organic nitrogen											1		-1		$\frac{1}{14}$	$K_{hS}\frac{S_H / X_{B,H}}{K_{XS} + (S_H / X_{B,H})}X_{B,H}\frac{S_{ND}}{S_H}$
9	Hydrolysis of Slowly Hydrolyzable COD		1		-1												$K_{hX}\frac{X_S / X_{B,H}}{K_{XX} + (X_S / X_{B,H})}X_{B,H}$
10	Hydrolysis of particulate organic nitrogen											1			-1	$\frac{1}{14}$	$K_{hX}\frac{X_S / X_{B,H}}{K_{XX} + (X_S / X_{B,H})}X_{B,H}\frac{X_{ND}}{X_S}$
Operations																	
1	Aeration									1							kLa ($S_{Osat} - S_O$)
2	Sludge Disposal			-X_I	-X_S	-$X_{B,H}$	-$X_{B,A}$		-X_P						-X_{ND}		1 / θ_X
Observed Conversion Rates [$ML^{-3}T^{-1}$]		$r_i = \sum_j v_{ij}\varrho_j$															
Stoichiometric Parameters: Heterotrophic yield: Y_H, Y_{HD} Autotrophic yield: Y_A Fraction of biomass yielding products: f_{EX}, f_{ES} Mass N/Mass COD in biomass: i_{XB} Mass N/Mass COD in products from biomass: i_{XP}		Soluble inert organic matter [M(COD)L^{-3}]	Readily biodegradable substrate [M(COD)L^{-3}]	Particulate inert organic matter [M(COD)L^{-3}]	Slowly biodegradable substrate [M(COD)L^{-3}]	Active heterotrophic biomass [M(COD)L^{-3}]	Active autotrophic biomass [M(COD)L^{-3}]	Soluble products arising from biomass decay [M(COD)L^{-3}]	Particulate products arising from biomass decay [M(COD)L^{-3}]	Oxygen (negative COD) [M(-COD)L^{-3}]	Nitrate and nitrite nitrogen [M(N)L^{-3}]	$NH_4^+ + NH_3$ nitrogen [M(N)L^{-3}]	Rapidly biodegradable substrate [M(COD)L^{-3}]	Soluble biodegradable organic nitrogen [M(COD)L^{-3}]	Particulate biodegradable organic nitrogen [M(COD)L^{-3}]	Alkalinity – Molar units	Kinetic Parameters: Heterotrophic growth and decay: μ_H, K_S, $K_{O,H}$, K_{NO}, b_H Autotrophic growth and decay: μ_A, K_{NH}, $K_{O,A}$, b_A Correction factor for anoxic growth of heterotrophs : η_g Correction factor for anoxic decay of heterotrophs : η_d Hydrolysis: K_{hS}, K_{hX}, K_{XS}, K_{XX}

3.3 Mass Balances and Settling Model

For this thesis study, reactors in the Modified Ludzack-Ettinger configuration are considered to be Continuous Stirred Tank Reactors (CSTR) and the hydraulics of these reactors are assumed to be identical with ideal reactor features. The reactant concentrations in the system are therefore reckon as distributed homogenously through the reactor volume and the effluent concentrations of the reactants are equal to the reactant concentrations within the reactor. In order to define the mass balances of the system, rate of accumulation in the reactor was computed for each state variable according to the Equation 3.1 as it can be seen below:

Rate of accumulation in the reactor = *Rate of mass flow into the reactor* - *Rate of mass flow out of the reactor* + *Rate of conversion of mass by reaction in the reactor* (3.1)

$$\frac{dVC}{dt} = QC_0 - QC - rV \tag{3.2}$$

3.3.1 Mass balance equations of anoxic tank variables

Mass balance equations of the state variables in the anoxic tank are shown below:

$$\frac{dS_S}{dt} = \frac{Q}{V_{Anoxic}}\left(S_{S_{influent}} - S_{S_{Anoxic}}\right) + rS_{S_{anoxic}} \tag{3.3}$$

$$\frac{dX_S}{dt} = \frac{Q}{V_{Anoxic}}\left(X_{S_{influent}} - X_{S_{Anoxic}}\right) + rX_{S_{anoxic}} \tag{3.4}$$

$$\frac{dX_H}{dt} = \frac{Q}{V_{Anoxic}}\left(X_{H_{influent}} - X_{H_{Anoxic}}\right) + rX_{H_{anoxic}} \tag{3.5}$$

$$\frac{dX_A}{dt} = \frac{Q}{V_{Anoxic}}\left(X_{A_{influent}} - X_{A_{Anoxic}}\right) + rX_{A_{anoxic}} \tag{3.6}$$

$$\frac{dS_P}{dt} = \frac{Q}{V_{Anoxic}}\left(S_{P_{influent}} - S_{P_{Anoxic}}\right) + rS_{P_{anoxic}} \tag{3.7}$$

$$\frac{dX_P}{dt} = \frac{Q}{V_{Anoxic}}\left(X_{P_{influent}} - X_{P_{Anoxic}}\right) + rX_{P_{anoxic}} \tag{3.8}$$

$$\frac{dS_O}{dt} = \frac{Q}{V_{Anoxic}}\left(S_{O_{influent}} - S_{O_{Anoxic}}\right) + rS_{O_{anoxic}} \quad (3.9)$$

$$\frac{dS_{NH}}{dt} = \frac{Q}{V_{Anoxic}}\left(S_{NH_{influent}} - S_{NH_{Anoxic}}\right) + rS_{NH_{anoxic}} \quad (3.10)$$

$$\frac{dS_{NO}}{dt} = \frac{Q}{V_{Anoxic}}\left(S_{NO_{influent}} - S_{NO_{Anoxic}}\right) + rS_{NO_{anoxic}} \quad (3.11)$$

$$\frac{dS_{ND}}{dt} = \frac{Q}{V_{Anoxic}}\left(S_{ND_{influent}} - S_{ND_{Anoxic}}\right) + rS_{ND_{anoxic}} \quad (3.12)$$

$$\frac{dX_{ND}}{dt} = \frac{Q}{V_{Anoxic}}\left(X_{ND_{influent}} - X_{ND_{Anoxic}}\right) + rX_{ND_{anoxic}} \quad (3.13)$$

$$\frac{dS_{ALK}}{dt} = \frac{Q}{V_{Anoxic}}\left(S_{ALK_{influent}} - S_{ALK_{Anoxic}}\right) + rS_{ALK_{anoxic}} \quad (3.14)$$

$$\frac{dS_H}{dt} = \frac{Q}{V_{Anoxic}}\left(S_{H_{influent}} - S_{H_{Anoxic}}\right) + rS_{H_{anoxic}} \quad (3.15)$$

$$\frac{dS_I}{dt} = \frac{Q}{V_{Anoxic}}\left(S_{I_{influent}} - S_{I_{Anoxic}}\right) \quad (3.16)$$

$$\frac{dX_I}{dt} = \frac{Q}{V_{Anoxic}}\left(X_{I_{influent}} - X_{I_{Anoxic}}\right) \quad (3.17)$$

3.3.2 Mass balance equations of aerobic tank variables

Mass balance equations of the state variables in the aerobic tank are shown below:

$$\frac{dS_S}{dt} = \frac{Q}{V_{Aerobic}}\left(S_{S_{Anoxic\ Effluent}} - S_{S_{Aerobic}}\right) + rS_{S_{Aerobic}} \quad (3.18)$$

$$\frac{dX_S}{dt} = \frac{Q}{V_{Aerobic}}\left(X_{S_{Anoxic\ Effluent}} - X_{S_{Aerobic}}\right) + rX_{S_{Aerobic}} - X_{S_{Aerobic}}\left(\frac{1}{\theta}\right)\left(\frac{V_{Total}}{V_{Aerobic}}\right) \quad (3.19)$$

$$\frac{dX_H}{dt} = \frac{Q}{V_{Aerobic}}\left(X_{H_{Anoxic\ Effluent}} - X_{H_{Aerobic}}\right) + rX_{H_{Aerobic}} - X_{H_{Aerobic}}\left(\frac{1}{\theta}\right)\left(\frac{V_{Total}}{V_{Aerobic}}\right) \quad (3.20)$$

$$\frac{dX_A}{dt} = \frac{Q}{V_{Aerobic}}\left(X_{A_{Anoxic\ Effluent}} - X_{A_{Aerobic}}\right) + rX_{A_{Aerobic}} - X_{A_{Aerobic}}\left(\frac{1}{\theta}\right)\left(\frac{V_{Total}}{V_{Aerobic}}\right) \quad (3.21)$$

$$\frac{dS_P}{dt} = \frac{Q}{V_{Aerobic}}\left(S_{P_{Anoxic\ Effluent}} - S_{P_{Aerobic}}\right) + rS_{P_{Aerobic}} \quad (3.22)$$

$$\frac{dX_P}{dt} = \frac{Q}{V_{Aerobic}}\left(X_{P_{Anoxic\ Effluent}} - X_{P_{Aerobic}}\right) + rX_{P_{Aerobic}} - X_{P_{Aerobic}}\left(\frac{1}{\theta}\right)\left(\frac{V_{Total}}{V_{Aerobic}}\right) \quad (3.23)$$

$$\frac{dS_O}{dt} = \frac{Q}{V_{Aerobic}}\left(S_{O_{Anoxic\ Effluent}} - S_{O_{Aerobic}}\right) + rS_{O_{Aerobic}} + kLa(S_{O_{Sat}} - S_O) \quad (3.24)$$

$$\frac{dS_{NH}}{dt} = \frac{Q}{V_{Aerobic}}\left(S_{NH_{Anoxic\ Effluent}} - S_{NH_{Aerobic}}\right) + rS_{NH_{Aerobic}} \quad (3.25)$$

$$\frac{dS_{NO}}{dt} = \frac{Q}{V_{Aerobic}}\left(S_{NO_{Anoxic\ Effluent}} - S_{NO_{Aerobic}}\right) + rS_{NO_{Aerobic}} \quad (3.26)$$

$$\frac{dS_{ND}}{dt} = \frac{Q}{V_{Aerobic}}\left(S_{ND_{Anoxic\ Effluent}} - S_{ND_{Aerobic}}\right) + rS_{ND_{Aerobic}} \quad (3.27)$$

$$\frac{dX_{ND}}{dt} = \frac{Q}{V_{Aerobic}}\left(X_{ND_{Anoxic\ Effluent}} - X_{ND_{Aerobic}}\right) + rX_{ND_{Aerobic}} - X_{ND_{Aerobic}}\left(\frac{1}{\theta}\right)\left(\frac{V_{Total}}{V_{Aerobic}}\right) \quad (3.28)$$

$$\frac{dS_{ALK}}{dt} = \frac{Q}{V_{Aerobic}}\left(S_{ALK_{Anoxic\ Effluent}} - S_{ALK_{Aerobic}}\right) + rS_{ALK_{Aerobic}} \quad (3.29)$$

$$\frac{dS_H}{dt} = \frac{Q}{V_{Aerobic}}\left(S_{H_{Anoxic\ Effluent}} - S_{H_{Aerobic}}\right) + rS_{H_{Aerobic}} \quad (3.30)$$

$$\frac{dS_I}{dt} = \frac{Q}{V_{Aerobic}}\left(S_{I_{Anoxic\ Effluent}} - S_{I_{Aerobic}}\right) \quad (3.31)$$

$$\frac{dX_I}{dt} = \frac{Q}{V_{Aerobic}}\left(X_{I_{Anoxic\ Effluent}} - X_{I_{Aerobic}}\right) - X_{I_{Aerobic}}\left(\frac{1}{\theta}\right)\left(\frac{V_{Total}}{V_{Aerobic}}\right) \quad (3.32)$$

3.4 Internal and Sludge Recycle Flows and Settling Model

The influent flow of the system is mixed with the internal and sludge recycle flows in each iteration step. The new flowrate entering the anoxic tank is defined as the reactor flowrate and is equal to the sum of internal, sludge and influent flowrates as it can be seen in Equation 3.33. Calculating the concentrations of state variables in the reactor flow is achieved by separately computing the total mass of each concentration coming from the internal recycle, flow recycle and influent pipelines and dividing them by the reactor flowrate.

The total mass flowrate coming from different pipelines is acquired by firstly achieving separate mass calculations.

$$Q_{reactor} = Q_{influent} + Q_{internal} + Q_{sludge} \tag{3.33}$$

The soluble and particulate parameter concentrations in the internal recycle line are equal to the concentrations of aerobic reactor effluents. On the other hand, particulate matter concentrations in the sludge recycle line are found by seperately multiplying particulate component concentrations maintaining in the pipeline with a flowrate equal to the sum of sludge and influent flowrates by a settling constant in order to apply settling tank mechanics in the configuration. Soluble parameter concentrations in the sludge recycle line are also equal to the concentrations of aerobic reactor effluents.

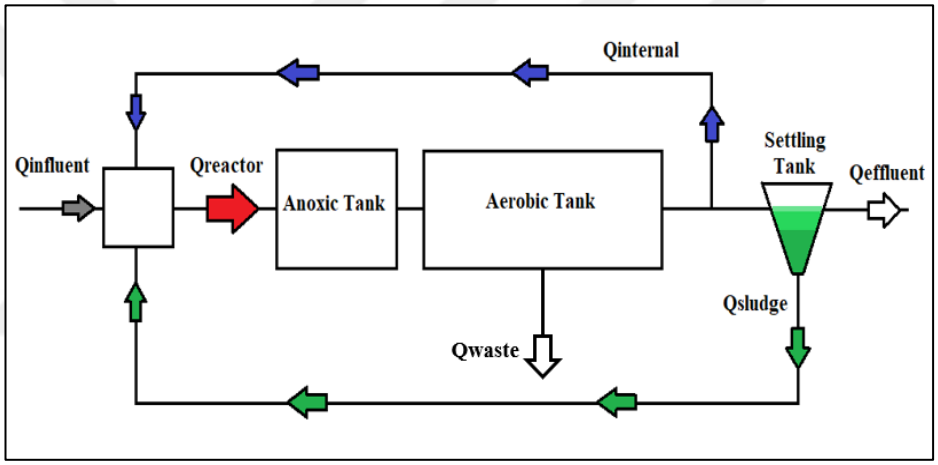

Figure 3.1 : Flow diagram of the MLE configuration.

The residual particulate concentrations that bypass the settling process are assumed to proceed to the effluent pipeline and considered as the effluent particulate concentrations. Similarly, soluble effluent concentrations are assumed to be equal to the aerobic reactor effluent concentrations. The mass flowrate calculations of internal recycle, sludge recycle and effluent flows are given below:

$$X_{\text{Internal Mass}} = Q_{\text{Internal}} \cdot X_{\text{Aerobic Effluent}} \tag{3.34}$$

$$S_{\text{Sludge Mass}} = Q_{\text{Sludge}} \cdot S_{\text{Aerobic Effluent}} \tag{3.35}$$

$$X_{\text{Sludge Mass}} = (Q_{\text{Influent}} + Q_{\text{Sludge}}) \cdot X_{\text{Aerobic Effluent}} \cdot \text{Settling Efficiency} \tag{3.36}$$

$$S_{\text{Effluent Mass}} = Q_{\text{Influent}} \cdot S_{\text{Aerobic Effluent}} \tag{3.37}$$

$$X_{\text{Effluent Mass}} = (Q_{\text{Influent}} + Q_{\text{Sludge}}) \cdot X_{\text{Aerobic Effluent}} \cdot (1 - \text{Settling Efficiency}) \tag{3.38}$$

$$S_{\text{Influent Mass}} = Q_{\text{Influent}} \cdot S_{\text{Influent}} \tag{3.39}$$

$$X_{\text{Influent Mass}} = Q_{\text{Influent}} \cdot X_{\text{Influent}} \tag{3.40}$$

Influent soluble and particulate concentrations are calculated at the end of each iteration step after all the mass flowrate calculations are completed. The concentration values found by these calculations are then used as the new influent concentrations at the next iteration step. The equations used for computing the concentration values can be seen below:

$$S_{\text{Influent}} = \frac{(S_{\text{Internal Mass}} + S_{\text{Sludge Mass}} + S_{\text{Influent Mass}})}{Q_{\text{Reactor}}} \tag{3.41}$$

$$X_{\text{Influent}} = \frac{(X_{\text{Internal Mass}} + X_{\text{Sludge Mass}} + X_{\text{Influent Mass}})}{Q_{\text{Reactor}}} \tag{3.42}$$

3.5 Simulation Algorithm

The algorithm of the simulation platform is based on the input type choice of users. Software contains two main function pathways to choose depending on this choice. If the user prefers a simulation with constant inputs, software first checks the compatibility and correctness of input data entered by the user from the user interface.

Fraction ratios are being checked just before software controls the input lineedit boxes from the GUI in order to ensure that all data entered by the user are numerical and there are no empty input space left behind. A warning dialog pops up if any of the possibilities stated occurs and asks for the user to correct the input data according to the type of error. After ensuring all the constant input data is appropriate for the simulation, simulate function initiates in which long lists containing input data and lists that are going to store the output data are being created.

Iteration initiates by providing the input data as arguements necessary for the functions that virtually imitates denitrification and nitrification processes.

During the iteration, the lists that contain output data are constantly being updated at the end of each step. Software opens the visualized output data in the results section of interface when the simulation is completed and concurrently writes the output data in a default excel file having a CSV format. On the other hand, while users are running a simulation with time series input data another path of algorithms are chosen by the program.

For the dynamic simulation function to initiate, an input file containing the data should be uploaded to the program via the load input file dialog existing on the interface. The system again checks for possible errors of kinetic, stoichiometric, reactor design and iteration parameter values entered by the user and proceeds with the real time simulation function. This function has the same algorithm with the simulate function of constant input method. The only difference is the variation in values of the input parameters and the creation of interval data by using linear interpolation according to the step size chosen by the user. After the input and output storage lists are created, simulation starts running with the iteration of denitrification and nitrification process functions. The output data is written into the same output excel file as the constant input method and software opens the results section to visually demonstrate the output data. The flowchart of the software can be seen in Figure 3.2.

3.6 Python Packages

3.6.1 NumPy

NumPy is one of the most useful python packages alongside with SciPy when it comes to creating applications requiring data science. It enables the users to save and operate data as ndarrays (N-dimensional arrays) instead of lists and dictionaries that are used for saving data in python. One of the distinguishing features of ndarrays is their duration time in operations on data elements which is way much shorter when compared to the duration of operation time in python lists. On the other hand, ndarrays are capable of storing only one type of data in each column such as integers, strings and floats while lists can store different types of elements at the same time (Bressert, 2013).

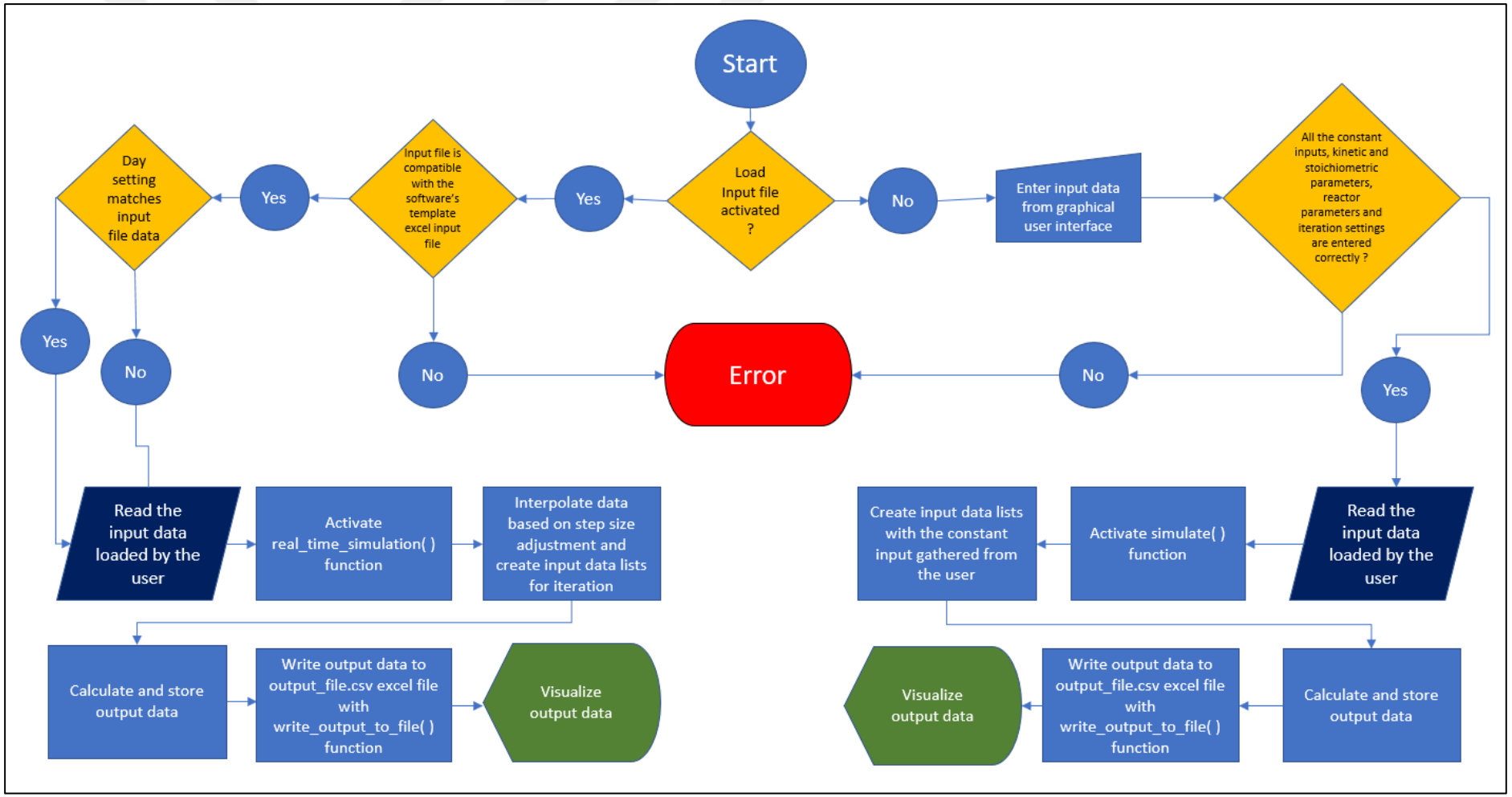

Figure 3.2 : Software flowchart.

NumPy also provides functions that help us read, save and write data from excel files in CSV format that leads to the opportunity of integrating data input and output handling in the software. The python libraries used in data science can be seen below in Figure 3.3.

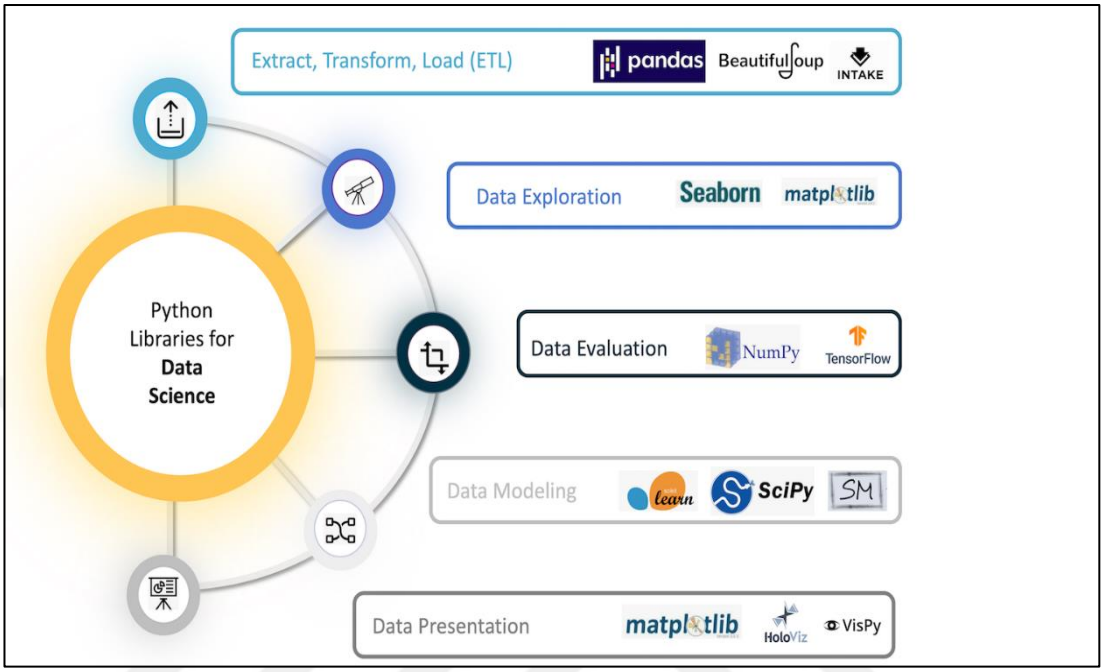

Figure 3.3 : Python libraries for data science (NumPy, 2021).

3.6.2 SciPy

SciPy is another powerful python package containing tools to utilize the data we have stored and indexed with the help of NumPy objects and functions. It is an essential package to use while conducting scientific studies due to its useful functions enabling the users to solve ordinary differential equations (ODE), apply optimization and interpolation to the existing data (Bressert, 2013).

Solving equations on the default python setup with existing mathematical operators and iteration algorithms is less efficient when we have the SciPy and NumPy packages as an option.

3.6.3 PySide2

In the graphical user interface (GUI) development phase of software, advanced and flexible designing tools of PySide2 have been used. PySide2 module was developed by The Qt Company in order to integrate Qt framework into python programming language.

After creating user friendly interface drafts from the Qt Designer application existing in the module itself, it is possible to convert the source code of designed configuration written in extensible markup language (XML) format into a python file. Files that contain the configuration of designed drafts written in XML format are created with the ui extension.

Once the python file containing all the class, subclass, object and many other relevant object oriented programming (OOP) elements is converted from the ui file, it is not possible to change the existing design from inside the Qt Designer application anymore.

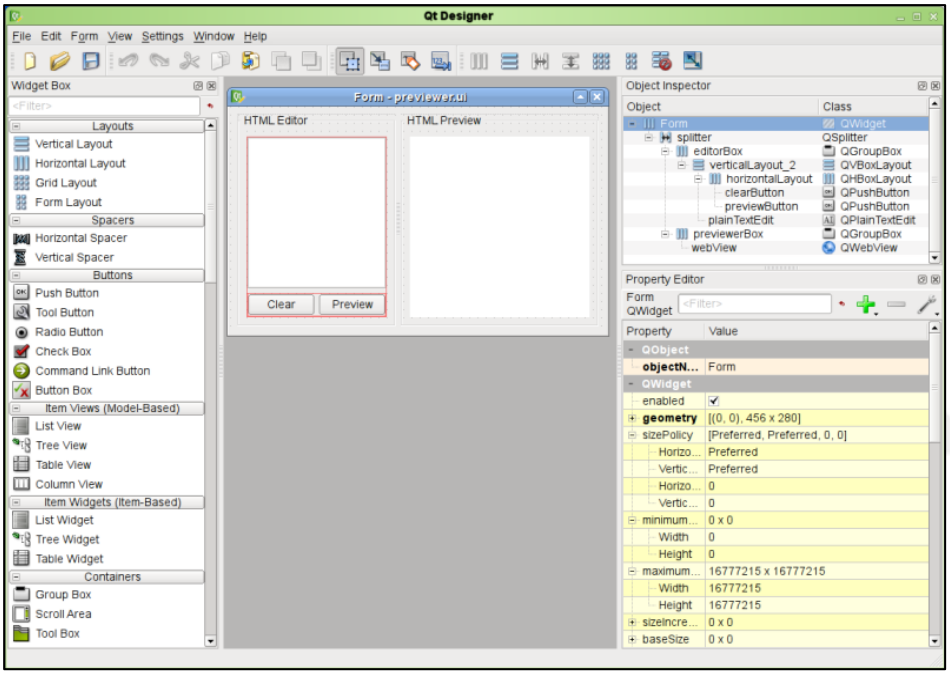

Figure 3.4 : Interface of Qt Designer **(**Qt 5.15, 2021).

Modifications from the python file itself can be achieved despite the fact that sufficient knowledge in Qt elements such as widgets, layouts, signals and slots mechanism and etc. is required.

Anyone with a fundamental knowledge in PySide2 can acquire this knowledge by reading the existing Qt documents that contain every vital information about the Qt elements. Other than that, the only option of modifying the interface features is to redesign the draft in Qt Designer and convert the ui file into a python file again.

3.6.4 MatPlotlib

MatPlotlib is another essential library for the data scientists on demonstrating and analyzing their findings in a visualized way. It is a plotting library mostly used along with Numpy library and it is used for creating a figure canvas that is able to plot the results data of the scientific study in this case. In MatPlotlib means of editing the figure is practical and easy to learn while at the same time it offers quite unique and divergent visualization options to the user. In this thesis study, FigureCanvasTkAgg and NavigationToolbar2QT classes existing in the MatPlotlib library are imported and embedded in the results section of the software which was created by PySide2. Entegration of figure canvas and navigation toolbar into the interface provides convenience while comparing different parameters in the model and comparing same parameters in different reactors and effluent values. Therefore, visualization of the results data is a component of the software development process as crucial as the model implementation phase. Some of the divergent figure styles can be seen in Figure 3.5, Figure 3.6 and Figure 3.7.

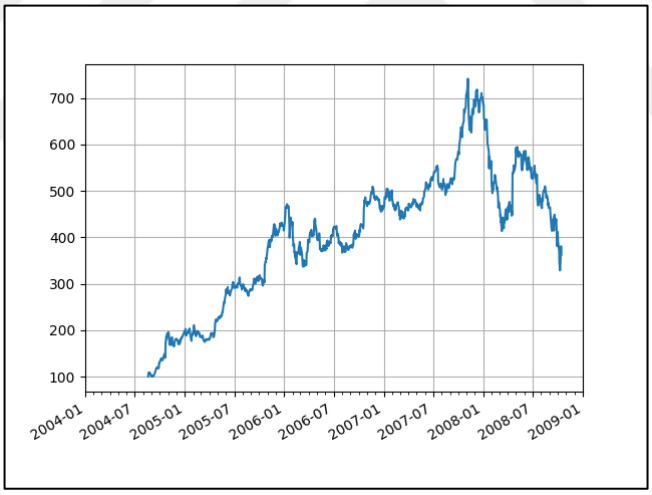

Figure 3.5 : Date tick feature of MatPlotlib canvas (Matplotlib — Visualization with Python, 2021).

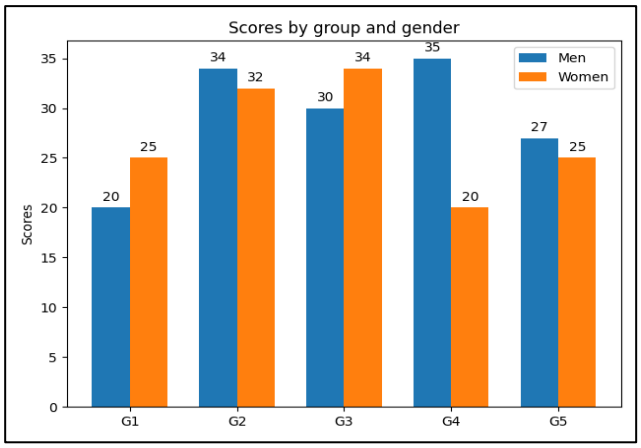

Figure 3.6 : Grouped bar chart with labels (Matplotlib — Visualization with Python, 2021).

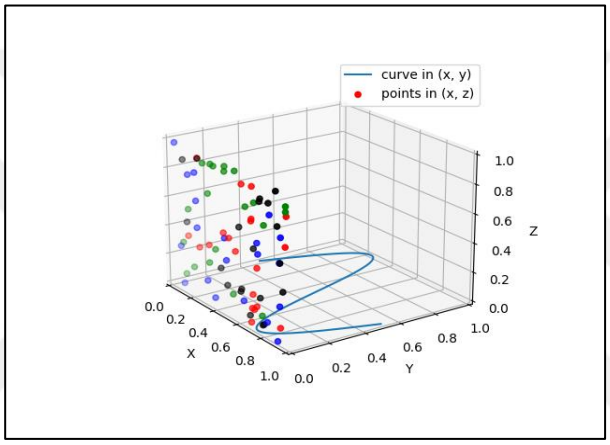

Figure 3.7 : Plotting 2D data on 3D plot (Matplotlib — Visualization with Python, 2021).

3.6.5 Pandas

Lastly another important open source data analysis and data manipulation package, Pandas, has been used in the software for reading the input file data and storing them in fast and efficient dataframe objects (Pandas - Python Data Analysis Library, 2022). Pandas has been integrated with NumPy's functions for a more efficient data handling.

3.7 Software Features

3.7.1 Input data handling

There are two methods for input handling in the simulation software and it is up to the user to choose which method to use according to the existing data. These methods can be defined as constant input and time series input methods. Default simulation algorithm is compatible with the constant input algorithm once we run the simulation.

As it can be seen in Figure 3.8, input values section contains two sub-divisions; influent values and COD and organic nitrogen fractions. Data entry of constant influent values for Influent Flowrate ($Q_{influent}$), Total Influent COD ($CT_{influent}$), Total Kjeldahl Nitrogen (TKN), Influent Ammonia Nitrogen Concentration (NH_4-N), Influent Nitrate Nitrogen Concentration (NO_3-N), Influent Dissolved Oxygen Concentration (S_O) and Influent Alkalinity Concentration (S_{ALK}) can be achieved from the influent values division.

During the simulation process, fragmentation of Total Influent COD concentration into influent values of various variables in each iteration step is accomplished by the fraction values entered by user from the fractions for influent conversions division.

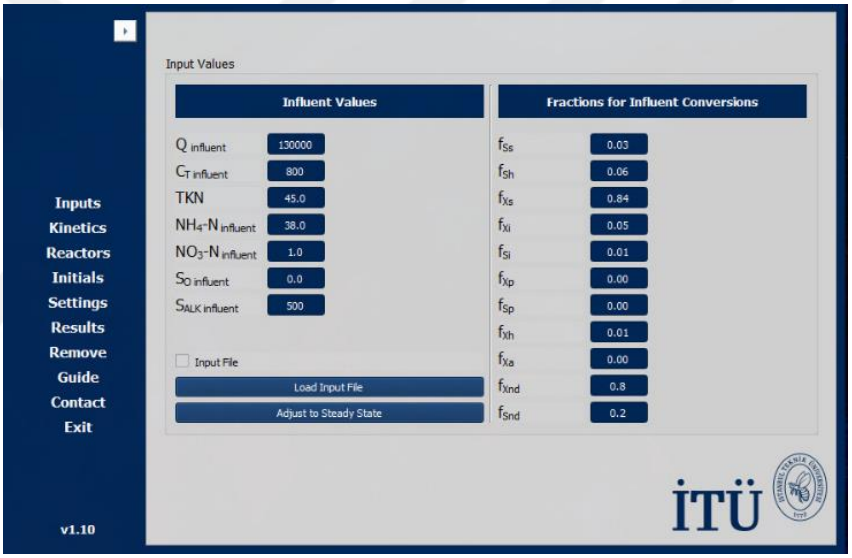

Figure 3.8 : Default Input Values Section of the Software.

While entering the fraction input values, users should be cautious about the total sum of COD fraction percentages. The sum of COD fraction percentages till f_{XND} and f_{SND} must be equal to one in order for the simulation to run. The sum of f_{XND} and f_{SND} percentages must be equal to one either. Otherwise, users will encounter an error dialog warning them about the inaccurate input values as it can be seen in Figure 3.9.

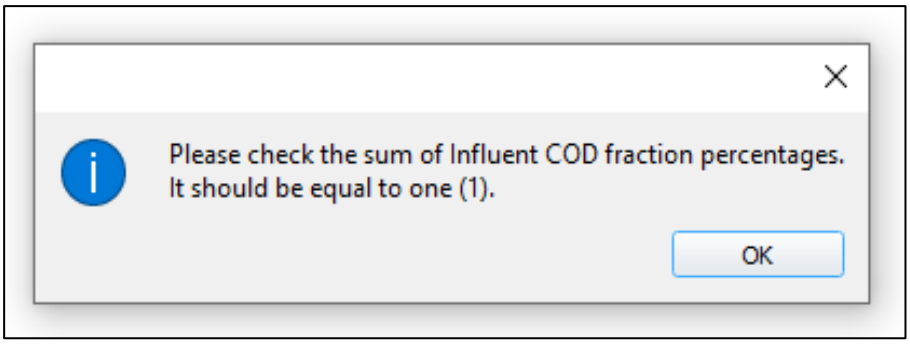

Figure 3.9 : Inaccurate COD fraction percentage error.

Similarly, users must avoid leaving empty input boxes or entering invalid input values such as nonnumeric characters. In that case, another error dialog warning the user about the invalid input will be encountered as seen in Figure 3.10.

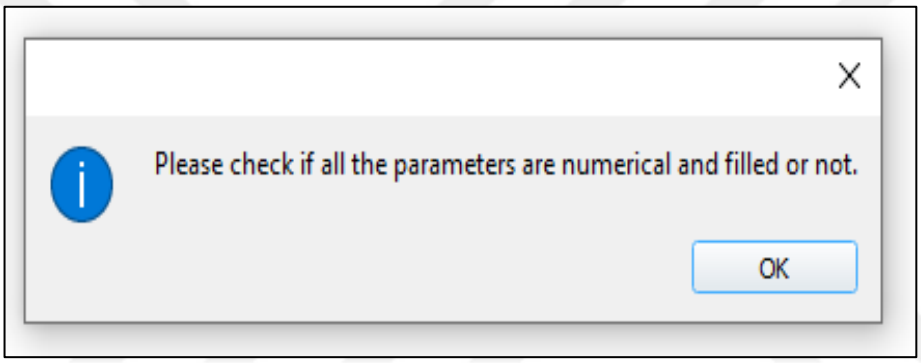

Figure 3.10 : Invalid input error.

Another point to take into account is entering the inputs with correct units. Users can easily prevent this situation by getting explanation texts from the interface. Parameter and unit information can be seen by simply holding the cursor on each parameter or unit input box as shown in Figure 3.11, Figure 3.12 and Figure 3.13.

Data entry for time series influent values is achieved by enabling the Load Input File button from checkbox and loading the input file from the directory.

Software automatically detects loaded input file and changes its simulation structure by using time series simulation function.

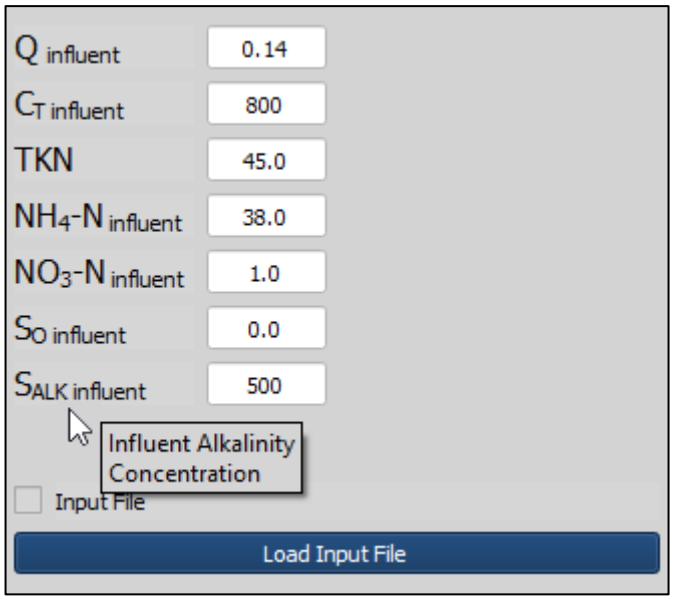

Figure 3.11 : Information text for influent parameters.

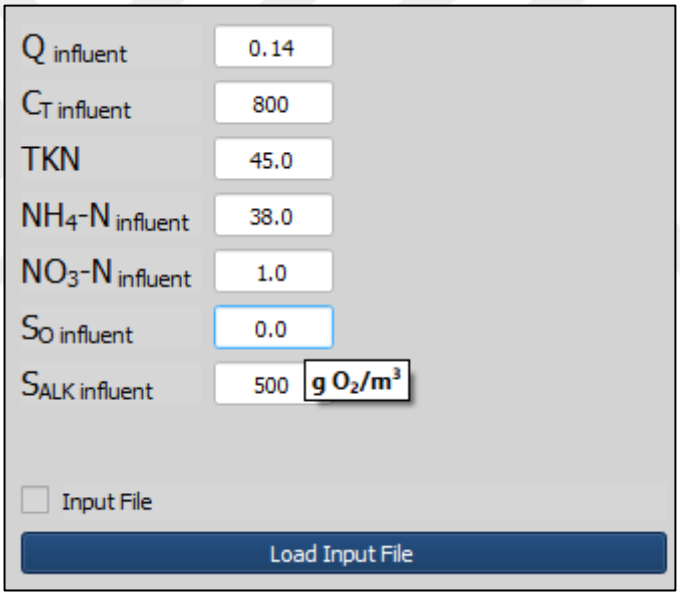

Figure 3.12 : Information text for influent units.

In the software directory, a sample input file in the format of comma-separated values (CSV) file exists by default. First row of the input file contains the input parameters. The order of input parameter values are important and should be adjusted to the sample CSV file as it can be seen from Figure 3.14. In each calculation step, influent values are fragmentated into different fractions same as the constant input algorithm. According to the time series data, Day and Steps values should be adjusted from the settings section. Step size adjustments are achieved by interpolation in order to assign new intermediate data values between the data values users have entered. Increasing the step size will extend simulation duration substantially.

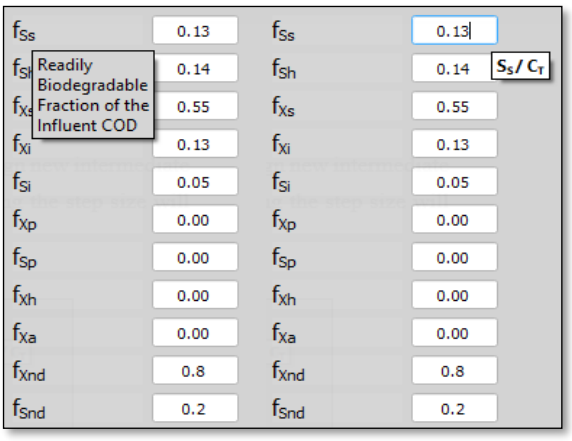

Figure 3.13 : Information text for COD fractions.

	A	B	C	D	E	F	G
1	t,Q,CT,TKN,NH4,NO3,So,Salk						
2	d,m^3/d,g/m^3,gTKN/m^3,gNH4-N/m^3,gNO3-N/m^3,gSo/m^3,molar						
3	1,0.126,1515,35,28,1.0,0.0,100						
4	11,0.125,1330,35,28,1.0,0.0,100						
5	21,0.190,1545,35,28,1.0,0.0,100						
6	31,0.116,1325,35,28,1.0,0.0,100						
7	41,0.199,2395,35,28,1.0,0.0,100						
8	51,0.180,2485,35,28,1.0,0.0,100						
9	62,0.120,2000,35,28,1.0,0.0,100						
10	72,0.151,1390,35,28,1.0,0.0,100						

Figure 3.14 : Sample input file in CSV format.

Interpolation is a numerical analysis method used for estimating unknown data values between certain data values.

Currently, linear interpolation is applied to the data set given by users. Structure of interpolation function written for estimating new values can be seen below:

$$\text{Delta} = \text{Next Value} - \text{Value} \tag{2.4}$$

$$\text{Value} = \text{Value} + \frac{\text{Delta}}{\text{Total Steps x (Current Step} - 1)} \tag{2.5}$$

The new value is appended to the existing data list after calculation of the new value is completed. In both constant input and time series input methods, influent input parameters are the same and they are shown in Table 3.2.

Table 3.2 : Units and definitions of input parameters.

Input Parameter	Unit	Definition
t	day	Time
Q	m^3/d	Influent Flowrate
C_T	g/m^3	Total Influent COD
TKN	g TKN/m^3	Influent Total Kjeldahl Nitrogen
NH_4-N	g NH_4-N/m^3	Influent Ammonia Nitrogen Concentration
NO_3-N	g NO_3-N/m^3	Influent Nitrate Nitrogen Concentration
S_O	g O_2/m^3	Influent Dissolved Oxygen Concentration
S_{ALK}	molar	Influent Alkalinity Concentration

It should also be taken into account that Total Biodegradable Organic Nitrogen Concentration (CND) is not entered as an influent input from the interface. It is calculated by subtracting influent Ammonia Nitrogen (NH_4-N) concentration from influent Total Kjeldahl Nitrogen (TKN) concentration as it can be seen in Equation 3.43.

$$C_{ND} = TKN - (NH_4 - N) \tag{3.43}$$

The fractions used for influent parameter conversions and their definitions are given in Table 3.3. Units and definitions of state variables are given in Table 3.4.

Table 3.3 : Fraction conversions of input parameters.

Influent Parameter (mg/l)	Fraction Constant	Definition	Converted Parameter (mg/l)	Definition
C_T (Total Influent COD)	f_{SS} (S_S / C_T)	Readily Biodegradable Fraction of the Influent COD	S_S	Readily Biodegradable COD
	f_{SH} (S_H / C_T)	Rapidly Hydrolyzable Fraction of the Influent COD	S_H	Rapidly Hydrolyzable COD
	f_{XS} (X_S / C_T)	Slowly Biodegradable Fraction of the Influent COD	X_S	Slowly Biodegradable COD
	f_{XI} (X_I / C_T)	Particulate Inert Fraction of the Influent COD	X_I	Particulate Inert COD
	f_{SI} (S_I / C_T)	Soluble Inert Fraction of the Influent COD	S_I	Soluble Inert COD
	f_{XP} (X_P / C_T)	Particulate Inert Organic Product Fraction of the COD	X_P	Particulate Inert Organic Product Concentration
	f_{SP} (S_P / C_T)	Soluble Inert Organic Product Fraction of the COD	S_P	Soluble Inert Organic Product Concentration
	f_{XH} (X_H / C_T)	Heterotrophic Biomass Fraction of the Influent COD	X_H	Heterotrophic Biomass Concentration
	f_{XA} (X_A / C_T)	Autotrophic Biomass Fraction of the Influent COD	X_A	Autotrophic Biomass Concentration
C_{ND} (Total Biodegradable Organic Nitrogen)	f_{XND} (X_{ND} / C_{ND})	Particulate Biodegradable Organic Nitrogen Fraction of the Total Biodegradable Organic Nitrogen	X_{ND}	Particulate Biodegradable Organic Nitrogen Concentration
	f_{SND} (S_{ND} / C_{ND})	Soluble Biodegradable Organic Nitrogen Fraction of the Total Biodegradable Organic Nitrogen	S_{ND}	Soluble Biodegradable Organic Nitrogen Concentration

Table 3.4 : State variables.

State Variable	Unit	Definition
S_S	mg/l	Readily Biodegradable COD
X_S	mg/l	Slowly Biodegradable COD
X_H	mg/l	Heterotrophic Biomass Concentration
X_A	mg/l	Autotrophic Biomass Concentration
X_P	mg/l	Particulate Inert Organic Product Concentration
S_P	mg/l	Soluble Inert Organic Product Concentration
S_O	mg/l	Dissolved Oxygen Concentration
S_{NH}	mg/l	Ammonia Nitrogen Concentration
S_{NO}	mg/l	Nitrate Nitrogen Concentration
S_{ND}	mg/l	Soluble Biodegradable Organic Nitrogen Concentration
X_{ND}	mg/l	Particulate Biodegradable Organic Nitrogen Concentration
S_{ALK}	molar	Alkalinity Concentration
S_H	mg/l	Rapidly Hydrolyzable COD
S_I	mg/l	Soluble Inert COD
X_I	mg/l	Particulate Inert COD

3.7.2 Kinetic and stoichiometric parameter inputs

Inputs of kinetic and stoichiometric parameters can be entered from the Kinetics section present on the left side of the user interface. Kinetics section can be seen in Figure 3.15. In addition to kinetic and stoichiometric parameters, temperature and pH adjustments can also be done by enabling the checkbox of desired parameter. It should be noted that changes in pH values only affect the growth rate of nitrifiers. A list of all kinetic and stoichiometric parameters including their units and definitions are given in Table 3.5.

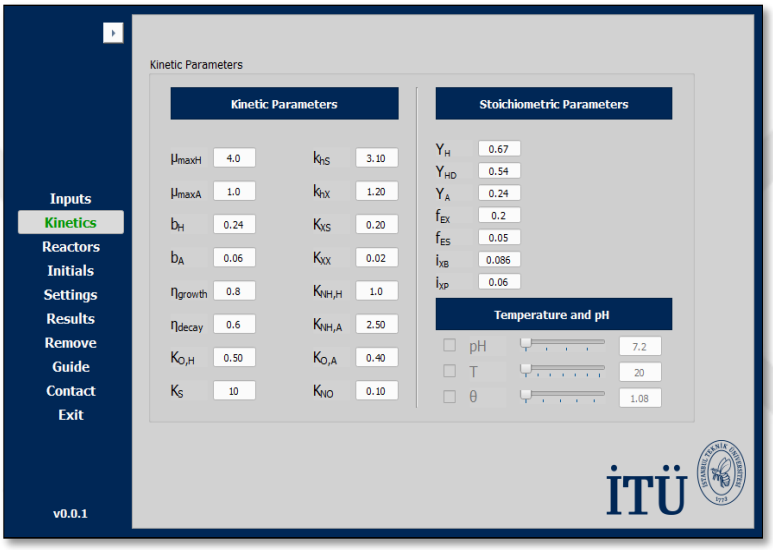

Figure 3.15 : Kinetics section in the software interface.

Adjustments of pH values are constricted due to the obscurities in the applied formula. Values between 7.2 and 8.5 are considered constant, therefore the pH adjustment range was arranged between 0 to 7.2 on the software. Equation 3.44 (Downing et al., 1967) was applied for the adjustment of pH values.

$$\mu_A = \mu_{Amax}[1 - 0.833(7.2 - pH)] \tag{3.44}$$

For the temperature corrections in the range of 7 to 30°C, an Arrhenius-type equation was implemented as shown below.

$$\mu = \mu_{20}(\theta^{T-20}) \tag{3.45}$$

Equation 3.45 is applied to the growth rates and decay rates of autotoprohic and heterotrophic biomass. Default growth rate of heterotrophic and autotrophic organisms are considered to be the value they possess at 20°C. Another input parameter related with the temperature impact is the θ constant used in the Equation 3.44. According to (Sözen, Orhon & San, 1996), θ constant has a value between 1.08 to 1.123. Users are free to choose any value between the given range with the help of sliders as it can be seen below in Figure 3.16.

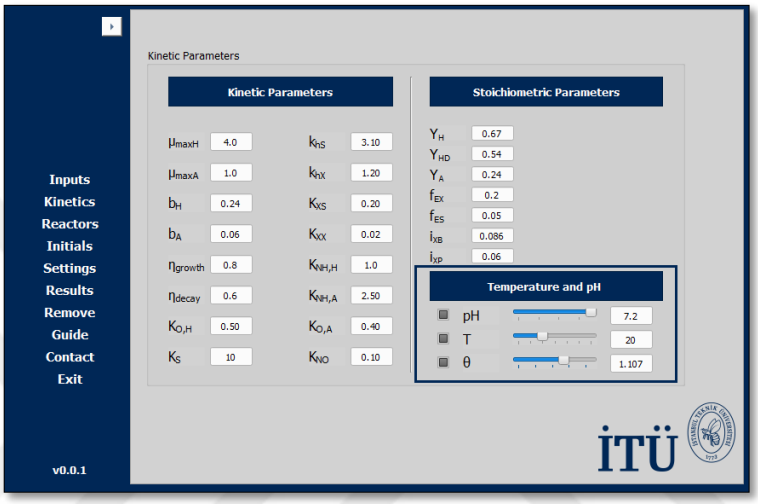

Figure 3.16 : Enabling temperature and pH set values.

The total number of iterations and the number of steps for each day can be entered from the settings section as it is demonstrated in Figure 3.17.

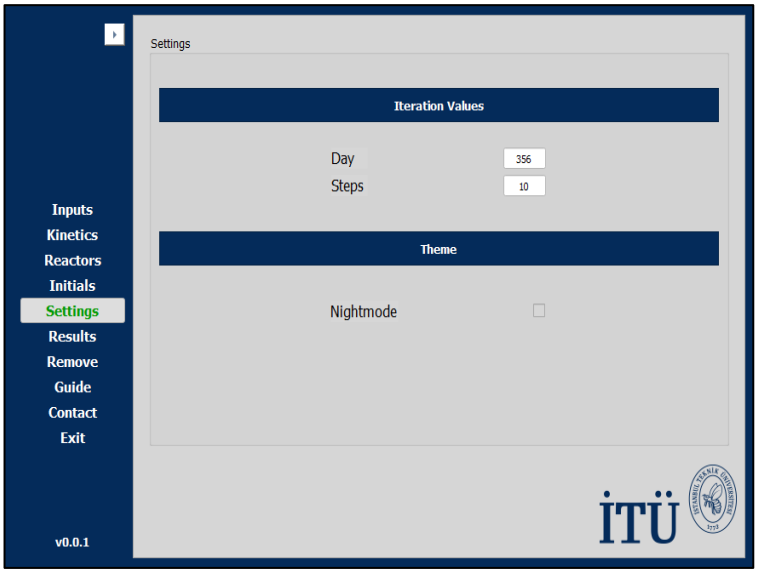

Figure 3.17 : Day and step size value adjustments.

Table 3.5 : Kinetic and stoichiometric parameters.

Parameter	Unit	Definition
μ_{maxH}	d^{-1}	Maximum Specific Growth Rate of Heterotrophic Biomass
μ_{maxA}	d^{-1}	Maximum Specific Growth Rate of Autotrophic Biomass
b_H	d^{-1}	Endogenous Decay Coefficient for Heterotrophic Biomass
b_A	d^{-1}	Endogenous Decay Coefficient for Autotrophic Biomass
η_{growth}	-	Correction Factor for μ_{maxH} under Anoxic Conditions
η_{decay}	-	Correction Factor for b_H under Anoxic Conditions
$K_{O,H}$	g O_2/m^3	Oxygen Half-Saturation Coefficient for Heterotrophic Biomass
$K_{O,A}$	g O_2/m^3	Oxygen Half-Saturation Coefficient for Autotrophic Biomass
kLa	d^{-1}	Overall Oxygen Transfer Coefficient
K_S	g COD/m^3	Oxygen Half-Saturation Coefficient for the Carbon Source
k_{hS}	d^{-1}	Maximum Specific Hydrolysis Rate of S_H
k_{hX}	d^{-1}	Maximum Specific Hydrolysis Rate of Xs
K_{XS}	g S_H /g cell COD	Hydrolysis Half-Saturation Constant for S_H
K_{XX}	g X_S /g cell COD	Hydrolysis Half-Saturation Constant for Xs
K_{NO}	g NO_3-N/m^3	Half-Saturation Constant for NO_3-N
$K_{NH,H}$	g NH_4-N/m^3	NH_4-N Half-Saturation Constant for Heterotrophic Biomass
$K_{NH,A}$	g NH_4-N/m^3	NH_4-N Half-Saturation Constant for Autotrophic Biomass
Y_H	cell COD/COD	Heterotrophic Growth Yield Coefficient
Y_{HD}	cell COD/COD	Growth Yield Coefficient of the Denitrifiers
Y_A	cell COD/g NH_4-N COD	Autotrophic Growth Yield Coefficient
f_{EX}	-	Particulate Inert COD Fraction of Biomass
f_{ES}	-	Soluble Inert COD Fraction of Biomass
i_{XB}	g N /g cell COD	Nitrogen Content of the Active Sludge Fraction
i_{XP}	g N /g COD	Nitrogen Content of the Endogenous Sludge Fraction

3.7.3 Reactor parameter inputs

Parameters related to reactors in the wastewater treatment system can be changed within the Reactors section. Reactor parameters are given in Table 3.6 with their units and definitions.

Table 3.6 : Reactor parameters.

Parameters	Units	Definitions
V_{Anoxic}	m^3	Volume of the Anoxic Reactor
$V_{Aerobic}$	m^3	Volume of the Aerobic Reactor
SRT	day	Sludge Retention Time
S_{Osat}	g/m^3	Dissolved Oxygen Saturation Concentration
S_{Oset}	g/m^3	Control Set Dissolved Oxygen Concentration
kLa	day^{-1}	Overall Oxygen Transfer Coefficient
$R_{Internal}$	-	Internal Recycle Ratio
R_{Sludge}	-	Sludge Recycle Ratio

3.7.4 Intermittent aeration feature

The software provides the users with the intermittent aeration feature which can be enabled by checking the Intermittent checkbox located on the reactor parameters section, as it can be seen in Fig. 3.18. Once it is enabled, users are able to change the intermittent aeration values located on the bottom side of the checkbox.

The first intermittent aeration parameter, Taeration , defines the period of aeration time per cycle with the unit of hour. The second parameter , Caeration , is the number of cycles per day. Units and definitions of intermittent aeration parameters can be seen in Table 3.7.

Table 3.7 : Units and definitions of intermittent aeration parameters.

Parameters	Units	Definitions
$T_{aeration}$	hour	Aeration period per cycle
$C_{aeration}$	-	Number of cycles for aeration per day

Figure 3.18 : Reactor parameter inputs.

3.7.5 Plug flow reactor feature for aeration tank

The last parameter located on reactor parameters section, Naeration , is the number of identical aeration units the aeration reactor volume is going to be divided into. The sole purpose of this division process is to achieve performing simulations with a treatment efficiency closer to that of a plug flow reactor's (PFR).

According to (Sperling, 2007), a plug flow reactor is created when the treatment configuration contains infinite number of reactors in series, and a complete-mix reactor is created when a single reactor is consisted in the series. As it can be seen above in Fig. 3.19, the treatment efficiency of a system with CSTR cells in series increases as the number of CSTR units increases.

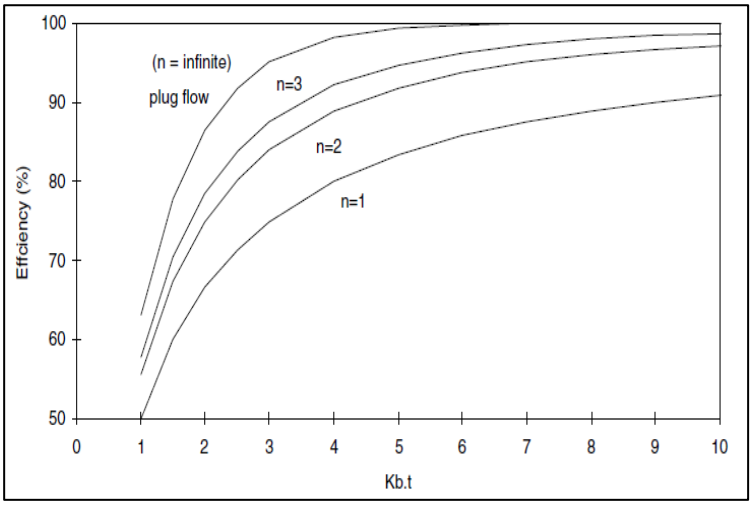

Figure 3.19 : Removal efficiencies for first-order kinetics in a system composed of CSTR cells in series, as a function of the dimensionless product K.t (Sperling, 2007).

3.7.6 Dissolved oxygen control feature

Another important feature of the software is the control set option which can be enabled by simply checking the Soset checkbox and entering the desired dissolved oxygen concentration as an input. At the end of each iteration, the simulation is programmed to calculate the overall oxygen transfer coefficient needed in the next iteration for maintaining the desired dissolved oxygen concentration level in the aerobic tank.

The overall oxygen transfer coefficient is calculated with the equation 3.46 seen below:

$$kLa = \frac{(So_{set} - So)}{(So_{sat} - So)} dt \tag{3.46}$$

where, kLa = Overall oxygen transfer coefficient

So_{set} = Control set value for dissolved oxygen concentration

So_{sat} = Saturation concentration of dissolved oxygen

dt = Iteration time step interval

It should be noted that if both of intermittent aeration and dissolved oxygen control functions are enabled during the simulation, the pausing period of intermittent aeration will surpass the dissolved oxygen control feature.

As the overall oxygen transfer coefficient is taken as zero, new values for achieving the desired dissolved oxygen concentration in the aerobic reactor will not be calculated until the pausing period finalizes.

3.7.7 Gradual dissolved oxygen saturation feature

Gradual Dissolved Oxygen Saturation feature was implemented to the software for enabling the users with the opportunity of running simulations with divergent dissolved oxygen saturation concentrations that can be specified from the input dialog for this feature. As it can be seen in Figure 3.20, this dialog can be reached by clicking on the So_{sat} label located in the reactor parameters section. It should be noted that this feature can only be used with time series input function and therefore, the software will not allow the users to change dissolved oxygen saturation concentrations for specific time intervals with constant input simulation mode.

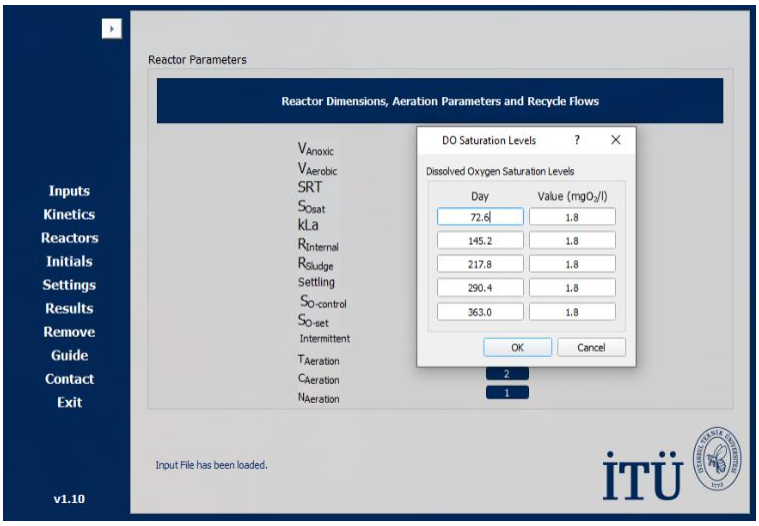

Figure 3.20 : Gradual dissolved oxygen saturation feature.

3.7.8 Steady state adjustment feature

Steady State Adjustment feature is another function created for simulations with time series inputs and can be performed through the Inputs section simply by clicking the Adjust to Steady State pushbutton once the time series input is loaded to the software.

The purpose of this feature is to adjust the initial state variable values for the time series input simulation and it is achieved by calculating the mean influent values of the time series input and running a constant simulation with the entered time and step size inputs.

Once the adjustment simulation is completed, the initial values of state variables are changed and the software is ready to perform a time series simulation.

3.7.9 Settling efficiency

The settling efficiency is taken as an input from users for calculating the percentage of particulate component concentrations that are going to be recycled to the anoxic reactor from the sludge recycle pipeline.

The sum of influent flowrate and sludge recycle flowrate is multplied by the settling efficiency for calculating the mass load recycling to the anoxic reactor. Mass loadings from the influent, internal and sludge recycle pipelines are then used for calculating parameter concentrations entering the anoxic reactor with reactor flowrate.

3.7.10 Setting initial values for state variables

Initial Values for state variables in anoxic and aerobic reactors are entered from the Initials section. Initial values section can be seen in Figure 3.21.

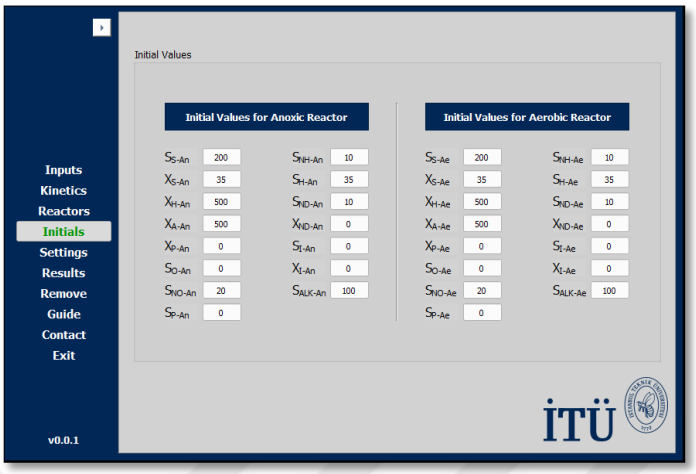

Figure 3.21 : Setting initial values for state variables.

3.7.11 Results visualization and data handling

After the simulation is completed, interface automatically switches to the results section. In the results section, users are able to plot the results of state variables for the anoxic reactor, aerobic reactor and their effluent concentrations. Plotting of the results are achieved by changing the combobox located at the top of the figure canvas as it can be seen in Figure 3.22.

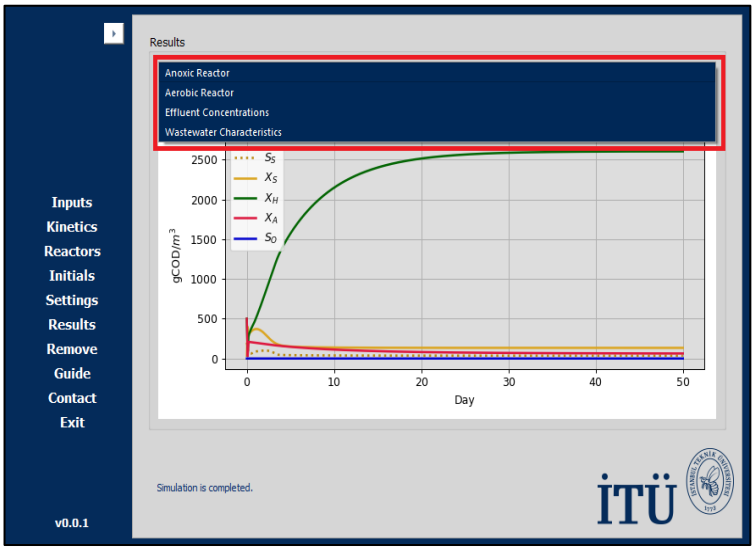

Figure 3.22 : Results section combobox.

Additionally, wastewater characteristics including the influent concentrations, effluent concentrations and removal efficiencies of Total Soluble COD, Total Particulate COD, Total Nitrogen COD, Total Kjeldahl Nitrogen and Total COD can be displayed from this section.

Displaying influent and effluent concentrations and the removal efficiency in the wastewater characteristics section while running the simulation with constant inputs is achieved by plotting the last effluent concentration values of the simulation.

As input values do not change with time, entered input values are used for the calculation of influent concentrations.

On the other hand, average values of influent and effluent concentrations during the simulation are taken into consideration while running the simulation with time series inputs. Wastewater Characteristics section can be seen in Figure 3.23.

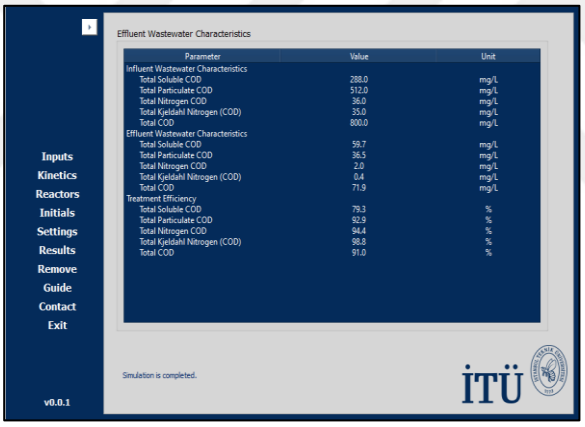

Figure 3.23 : Wastewater characteristics.

Default state variables plotted in the figure are Readily Biodegradable COD (S_S), Slowly Biodegradable COD (X_S), Heterotrophic Biomass Concentration (X_H), Autotrophic Biomass Concentration (X_A) and Dissolved Oxygen Concentration (S_O). In order to display different state variables or remove the existing variables from the figure, Navigation Toolbar feature of Matplotlib should be used.

As it can be seen in Figure 3.24, Navigation Toolbar is located on top of the figure canvas. Through the edit axis section, users can add and remove parameters by simply choosing the particular variable and make changes in the line style option in curves tab. Users can also change the style of each parameter line including color, width and draw style.

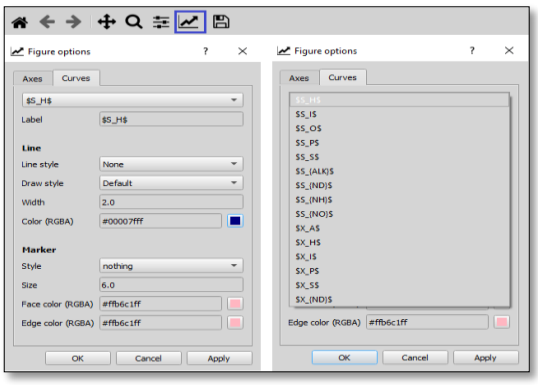

Figure 3.24 : Figure options.

Another feature of figure options is the opportunity to use markers for results plotting instead of lines. Apart from the stated features, result graphics can also be saved from Navigation Toolbar. Sample graph from the simulation can be seen in Figure 3.25.

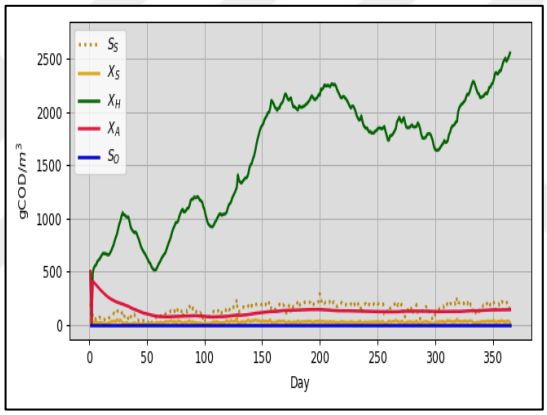

Figure 3.25 : Anoxic reactor results graph.

3.7.12 Output data handling

Following the completion of simulation, the default output file in the format of comma-separated values (CSV) located in the software directory is updated with the calculated effluent concentrations of all state variables.

3.7.13 Remove function

Remove function of the software instantly clears the result section graphs while at the same time setting default parameter values to all the input fields. Entered input values and adjustments of users will be removed once the remove button is clicked.

4. RESULTS AND DISCUSSION

4.1 Calibration of the Simulation Model

Calibration of the process model is of prime importance in terms of applicability of simulation outputs to possible real life problems. The purpose of calibration is to find the most optimized process model version that is capable of generating output data which fits the real data obtained from an actual resource recovery facility by adjusting each model parameter step by step. In this thesis study, calibration of the simulation model has been accomplished manually by changing one model parameter at a time. Studies were performed with the data obtained from an existing water resource recovery facility with Johannesburg configuration and the data has been given in appendix-A2. In order to alter the Johannesburg configuration of the facility into an MLE configuration, the volume of anaerobic reactor structured ahead of the anoxic tank has been neglected. Another vital assumption made for converting the existing configuration into an MLE configuration was to merge the volume of anoxic tank with another anoxic tank stationed at the sludge recycle line to the anaerobic tank that was designed for decreasing the nitrate concentration of sludge recycle in order to prevent possible phosphorus removal process interruptions. Design parameters of studied water resource recovery facility can be seen below in Table 4.1.

Table 4.1 : Design parameters of the WWTP.

Parameter	Value	Unit
Total volume of the anoxic tank	35.597	m^3
Total volume of the aerobic tank	92.112	m^3
Sludge retention time	25 - 30	day
Internal recycle ratio	0.8 – 1.1	-

Calibration of the model has been achieved by first assigning reference parameter values acquired from the literature as the model parameter values.

These reference parameter values are then changed step by step until the modeller ensures the output data of the simulation fits the real data. This stage of the calibration process depends on the modeller's subjective opinion on the data comparison visuals.

The data list acquired from the RRF contains daily influent and effluent values of COD, BOD, TKN, TN, ammonia nitrogen, nitrate nitrogen, total suspended solids (TSS) and pH concentrations along with the measurements of influent flowrate.

In this study calibration phase focusses on total COD, total BOD, TKN, TN, ammonia nitrogen, nitrate nitrogen, TSS and particulate COD (pCOD) parameters. Equations used for the estimation of stated parameters can be seen below:

$$\text{Total COD} = S_S + S_H + X_S + X_I + S_I + X_H + X_A + X_P \quad (4.1)$$

$$\text{Total BOD} = S_S + S_H + X_S + X_H + X_A \quad (4.2)$$

$$\text{TN} = S_{NH} + S_{ND} + X_{ND} + S_{NO} \quad (4.3)$$

$$\text{TKN} = S_{NH} + S_{ND} + X_{ND} \quad (4.4)$$

$$\text{pCOD} = X_S + X_I + X_H + X_A + X_P \quad (4.5)$$

Two third of the data set acquired from the WRRF was used for calibrating the and one third of the data was used for the validation. In this thesis study, first 220 days of the data set were used for calibration while last 143 days were used for the validation. It can be seen from Figure 4.1 that overall simulation outputs match the analysis results for the total COD parameter.

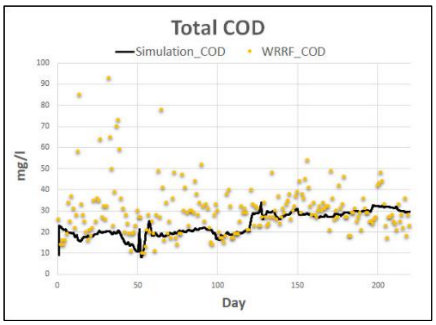

Figure 4.1 : Effluent total COD results of resource recovery data and calibrated simulation results.

The results comparison of simulation outputs and resource recovery data for total nitrogen is shown in Figure 4.2. It can be seen that simulation outputs match the analysis results during the first 220 days of the analysis results data set.

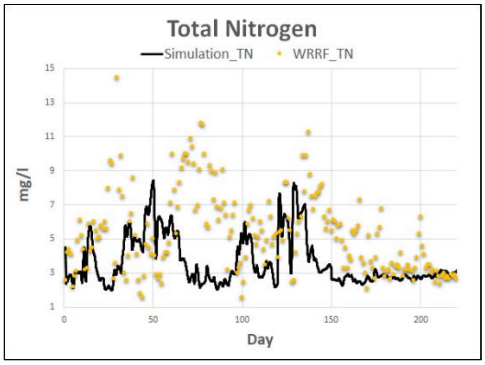

Figure 4.2 : Effluent TN results of resource recovery data and calibrated simulation results.

The results comparison of simulation outputs and analysis values for total kjeldahl nitrogen is shown below in Figure 4.3. It can be seen that by majority, simulation outputs cover the lower boundary of analysis results.

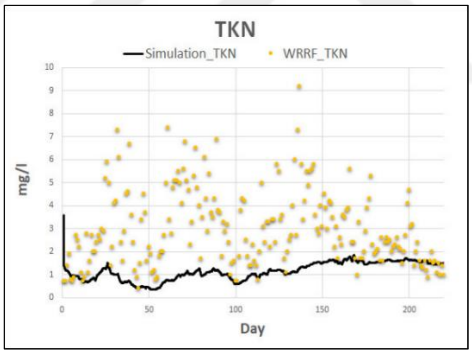

Figure 4.3 : Effluent TKN results of resource recovery data and calibrated simulation results.

It can be seen from Figure 4.4 that between days 150 and 220, model outputs cover the upper boundary of the analysis results in regard to total BOD. On contrary, simulation outputs of first 150 days cover the lower boundary of resource recovery data.

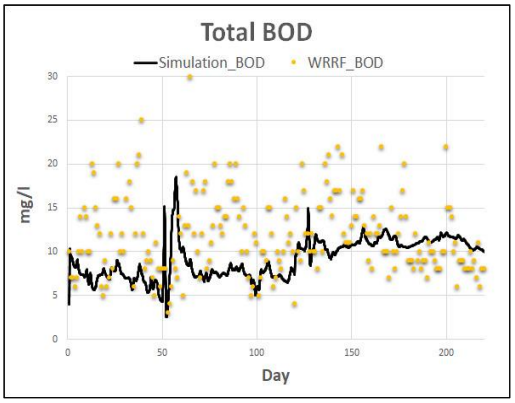

Figure 4.4 : Effluent total BOD results of resource recovery data and calibrated simulation results.

The nitrate nitrogen results comparison is given below in Figure 4.5. It can be seen from the graph that the simulation results are dominantly above the resource recovery data between days 25 to 75. Until day 150, simulation outputs match the upper boundary of resource recovery data. After day 150, an opposite pattern can be observed in the simulation outputs.

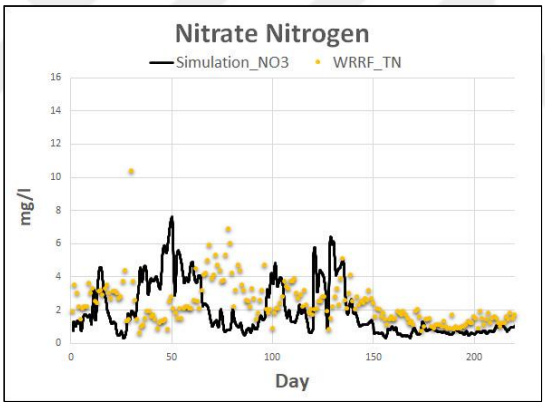

Figure 4.5 : Effluent nitrate nitrogen results of resource recovery data and calibrated simulation results.

The results comparison of simulation outputs and analysis values for ammonia nitrogen is shown below in Figure 4.6, where it can be seen that simulation outputs match the lower boundary of resource recovery data.

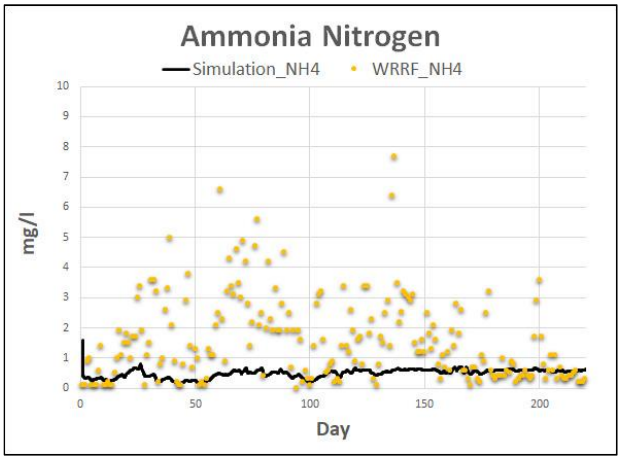

Figure 4.6 : Effluent ammonia nitrogen results of resource recovery data and calibrated simulation results.

The simulation outputs are below the threshold of particulate COD concentrations of analysis results till day 100 as it can be seen in Figure 4.7.

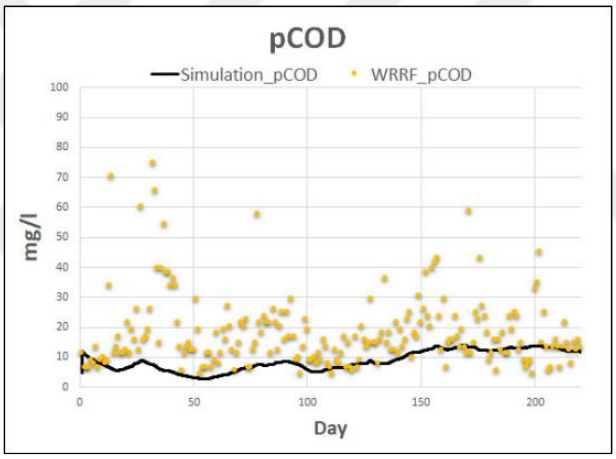

Figure 4.7 : Effluent total particulate COD (pCOD) results of resource recovery data and calibrated simulation results.

A list of reference parameters used in the initial calibration simulations are given in Table 4.2. The maximum specific growth rate of heterotrophic and autotrophic biomasses have been increased during the calibration process in order to adjust the removal rates of influent substrate and to accelerate the nitrification process in the aeration tank. Values of model coefficients that are defined after the calibration and values of fraction coefficients after the calibration can be seen in Table 4.3 and Table 4.4, respectively.

Table 4.2 : Reference coefficients of calibration.

Parameter	Unit	Definition	This Study	Type	Reference
μ_{maxH}	d^{-1}	Maximum Specific Growth Rate of Heterotrophic Biomass	3.5	Kinetic	ASM1-(Henze et al., 1987)
μ_{maxA}	d^{-1}	Maximum Specific Growth Rate of Autotrophic Biomass	0.6	Kinetic	ASM1-(Henze et al., 1987)
b_H	d^{-1}	Endogenous Decay Coefficient for Heterotrophic Biomass	0.24	Kinetic	ASM1-(Henze et al., 1987)
b_A	d^{-1}	Endogenous Decay Coefficient for Autotrophic Biomass	0.06	Kinetic	ASM1-(Henze et al., 1987)
η_{growth}	-	Correction Factor for μ_{maxH} under Anoxic Conditions	0.8	Kinetic	ASM1-(Henze et al., 1987)
η_{decay}	-	Correction Factor for b_H under Anoxic Conditions	1.0	Kinetic	-
$K_{O,H}$	g O_2/m^3	Oxygen Half-Saturation Coefficient for Heterotrophic Biomass	0.5	Kinetic	ASM1-(Henze et al., 1987)
$K_{O,A}$	g O_2/m^3	Oxygen Half-Saturation Coefficient for Autotrophic Biomass	0.5	Kinetic	ASM1-(Henze et al., 1987)
K_S	g COD/m^3	Oxygen Half-Saturation Coefficient for the Carbon Source	20	Kinetic	ASM1-(Henze et al., 1987)
k_{hS}	d^{-1}	Maximum Specific Hydrolyze Rate of S_H	3.0	Kinetic	(Orhon et al., 1998)
k_{hX}	d^{-1}	Maximum Specific Hydrolyze Rate of Xs	1.20	Kinetic	(Orhon et al., 1998)
K_{XS}	g S_H /g cell COD	Hydrolyze Half-Saturation Constant for S_H	0.20	Kinetic	(Orhon et al., 1998)
K_{XX}	g X_S /g cell COD	Hydrolyze Half-Saturation Constant for Xs	0.55	Kinetic	(Orhon et al., 1998)
K_{NO}	g NO_3-N/m^3	Half-Saturation Constant for NO_3-N	0.50	Kinetic	ASM1-(Henze et al., 1987)
$K_{NH,H}$	g NH_4-N/m^3	NH_4-N Half-Saturation Constant for Heterotrophic Biomass	0.1	Kinetic	ASM3-(Gujer *et* al., 1999)
$K_{NH,A}$	g NH_4-N/m^3	NH_4-N Half-Saturation Constant for Autotrophic Biomass	0.1	Kinetic	ASM1-(Henze et al., 1987)
Y_H	cell COD/COD	Heterotrophic Yield Coefficient	0.67	Stoichiometric	ASM1-(Henze et al., 1987)
Y_{HD}	cell COD/COD	Yield Coefficient of the Denitrifiers	0.54	Stoichiometric	ASM3-(Gujer et al., 1999)
Y_A	cell COD/g NH_4-N COD	Autotrophic Yield Coefficient	0.24	Stoichiometric	ASM1-(Henze et al., 1987)

Table 4.2 (continued): Reference coefficients of calibration.

Parameter	Unit	Definition	This Study	Type	Reference
f_{EX}	-	Particulate Inert Matter Fraction of Biomass	0.2	Stoichiometric	(Orhon et al., 1998)
f_{ES}	-	Soluble Inert Matter Fraction of Biomass	0.05	Stoichiometric	(Orhon et al., 1998)
i_{XB}	g N /g cell COD	Nitrogen Content of the Active Sludge Fraction	0.086	Stoichiometric	ASM1-(Henze et al., 1987)
i_{XP}	g N /g COD	Nitrogen Content of the Endogenous Sludge Fraction	0.06	Stoichiometric	ASM1-(Henze et al., 1987)

Table 4.3 : Calibrated coefficients.

Parameter	Unit	Predefined Value	This Study	Type	Reference
μ_{maxH}	d^{-1}	3.5	4.0	Kinetic	ASM1-(Henze et al., 1987)
μ_{maxA}	d^{-1}	0.6	1.0	Kinetic	ASM1-(Henze et al., 1987)
k_{hX}	d^{-1}	1.2	2.0	Kinetic	ASM1-(Henze et al., 1987)
b_A	d^{-1}	0.06	0.06	Kinetic	ASM1-(Henze et al., 1987)
η_{decay}	-	1.0	0.9	Kinetic	-
$K_{O,H}$	g O_2/m^3	0.5	0.1	Kinetic	ASM1-(Henze et al., 1987)
$K_{O,A}$	g O_2/m^3	0.5	0.05	Kinetic	ASM1-(Henze et al., 1987)
K_S	g COD/m^3	20	10	Kinetic	ASM1-(Henze et al., 1987)
K_{NO}	g COD/m^3	0.50	1. 0	Kinetic	ASM1-(Henze et al., 1987)
k_{hS}	d^{-1}	3.0	3.1	Kinetic	(Orhon et al., 1998)
K_{XX}	g X_S /g cell COD	0.55	0.02	Kinetic	(Orhon et al,. 1998)
k_{hX}	d^{-1}	1.2	2.0	Kinetic	(Orhon et al,. 1998)
$K_{NH,A}$	g NH_4-N/m^3	0.1	1.0	Kinetic	ASM3-(Gujer et al., 1999)

Correction Factor for Endogenous Decay Coefficient for Heterotrophic Biomass under Anoxic Conditions have been decreased from 1.0 to 0.9 for the same purpose. It was observed that the hydrolization rates were not high enough, specifically for the biomasses to utilize the slowly biodegradable COD and therefore Maximum Specific Hydrolyze Rate of the slowly biodegradable COD was increased from 1.2 to 2.0 in the calibration process.

Table 4.4 : Calibrated fraction coefficients.

Fraction	Definition	Predefined Value	This Study	(Orhon et al., 1998)	(Jarvis et al., 2014)
f_{SS}	S_S / C_T	0.13	0.03	0.09	0.13
f_{SH}	S_H / C_T	0.14	0.06	0.215	0.14
f_{XS}	X_S / C_T	0.55	0.84	0.555	0.55
f_{XI}	X_I / C_T	0.10	0.05	0.10	0.13
f_{SI}	S_I / C_T	0.4	0.01	0.04	0.05
f_{XP}	X_P / C_T	0.04	0	-	-
f_{XH}	X_H / C_T	0.10	0.01	-	-
f_{XA}	X_A / C_T	0	0	-	-
f_{XND}	X_{ND} / C_{ND}	0.8	0.8	-	-
f_{SND}	S_{ND} / C_{ND}	0.2	0.2	-	-

4.2 Validation of the Simulation Model

Validation of the software has been achieved by comparing the simulation outputs with analysis results corresponding to the last 143 days of data set acquired from the WRRF. It can be seen from Figure 4.8 that simulation matches the water resource recovery facility data in regard to total COD concentrations.

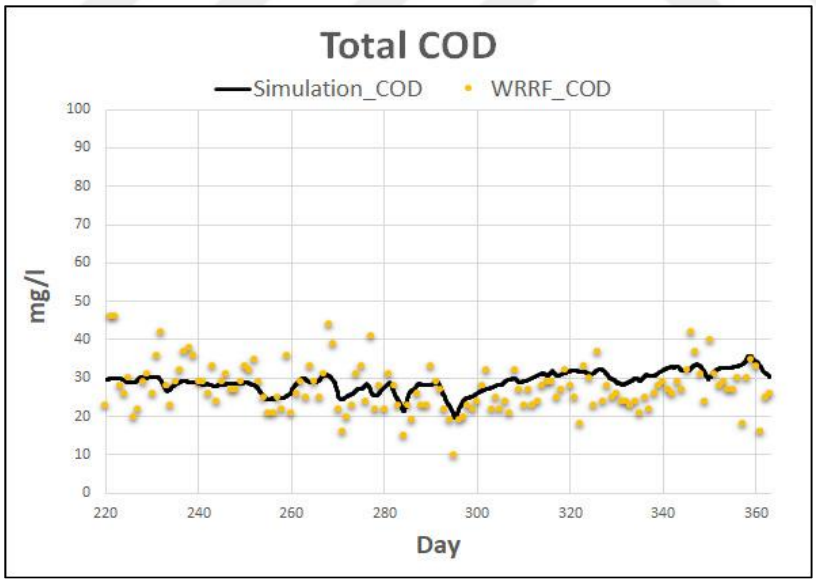

Figure 4.8 : Comparison of total COD results from analysis and simulation for validation.

The results comparison of simulation outputs and analysis values for nitrate nitrogen concentrations in the effluent wastewater is shown in Figure 4.9. It can be seen that overall, simulation outputs do not match the analysis results.

The nitrate nitrogen concentrations differ depending on the dissolved oxygen concentration maintaining in the aerobic reactor and the utilization rate of the dissolved oxygen concentration by the autotrophic biomass concentration. Therefore, the decrease in the nitrate nitrogen concentration after day 300 can be considered as a result of the autotrophic biomass concentration decline.

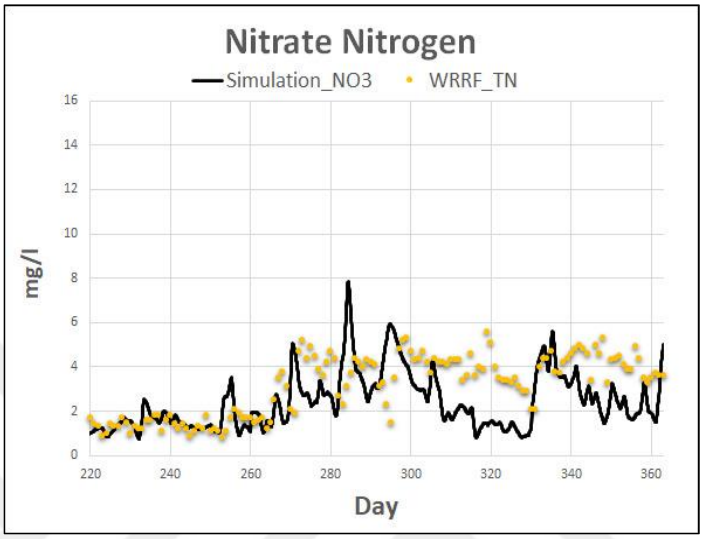

Figure 4.9 : Comparison of nitrate nitrogen results from analysis and simulation for validation.

It can be seen from Figure 4.10 that in overall simulation effluent wastewater outputs match with the analysis results in regard to TKN concentrations. In Figure 4.11 on the other hand, it can be observed that the precision of total nitrogen concentrations of simulation decreases drastically after day 300, as a result of the difference occured in the nitrate nitrogen concentrations.

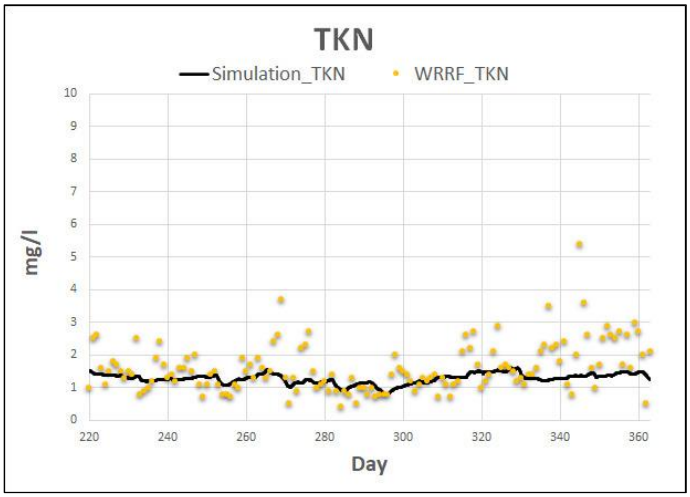

Figure 4.10 : Comparison of TKN results from analysis and simulation for validation.

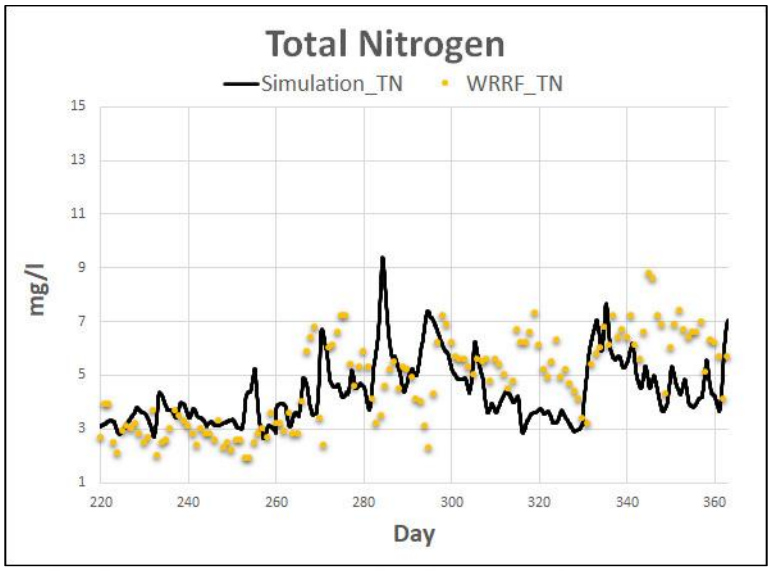

Figure 4.11 : Comparison of TN results from analysis and simulation for validation.

The results comparison of simulation outputs and analysis values for total BOD concentrations in the effluent wastewater is shown below in Figure 4.12 where it can be seen that overall simulation outputs match the analysis results.

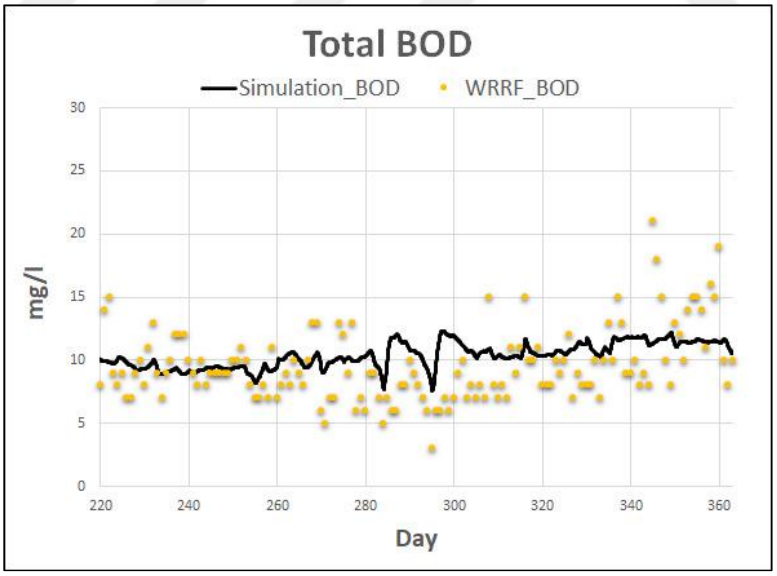

Figure 4.12 : Comparison of total BOD results from analysis and simulation for validation.

The comparison of ammonia nitrogen concentration outputs from the simulation and the analysis can be seen above in Figure 4.13. Simulation outputs for ammonia nitrogen are above the analysis results until day 340 where possibly due to a marginal increase in the influent of WWTP, analysis results surpass the simulation outputs.

Particulate COD concentrations are depicted in Figure 4.14. It can be observed that simulation outputs are mostly below the analysis results.

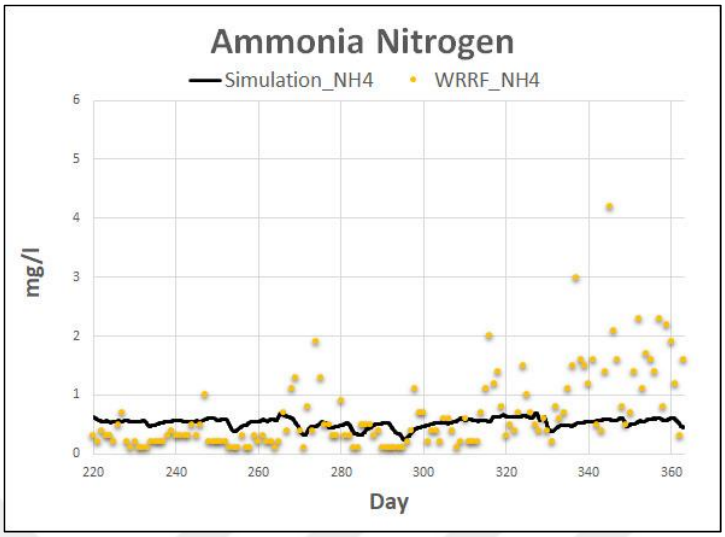

Figure 4.13 : Comparison of ammonia nitrogen results from analysis and simulation for validation.

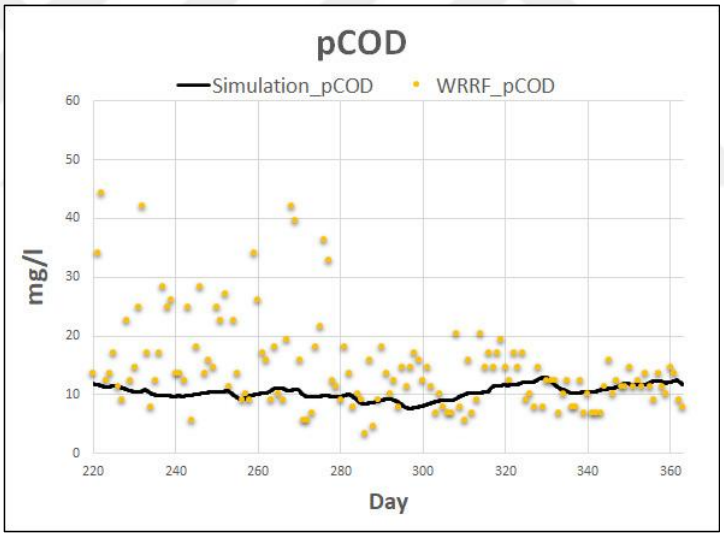

Figure 4.14 : Comparison of pCOD results from analysis and simulation for validation.

4.3 Statistical Evaluation of Simulation Outputs

In order to evaluate the precision of model outputs statistically, Root Mean Square Error (RMSE) and Janus coefficient methods have been selected. Calculation of Root Mean Square Error (RMSE) value and Janus coefficient can be seen below in Equation 4.6 and 4.7. The RMSE values and Janus coefficients found can be seen in Table 4.5.

It should be noted that the precision of the model increases as the RMSE value of a particular parameter decreases. Janus coefficient on the other hand, demonstrates the validity of process model. The more the Janus coefficient of a parameter approaches to 1, the more closer the error ranges of validation and calibration for the parameter are.

$$RMSE = \sqrt{\frac{1}{n}\sum_{i=1}^{n}\left(y_{m_{eas,i}-y(t_i)}\right)^2} \tag{4.6}$$

$$J^2 = \frac{\frac{1}{n_{val}}\sum_{i=1}^{n_{val}}\left(y_{meas,i} - y(t_i)\right)^2}{\frac{1}{n_{cal}}\sum_{i=1}^{n_{cal}}\left(y_{meas,i} - y(t_i)\right)^2} \tag{4.7}$$

As it can be seen in Table 4.5, each Root Mean Square Error (RMSE) value computed with the calibrated coefficients of parameters decrease in the validation process. The most precise predictions in the calibration were achieved for the NH4-N and the NO3-N parameters with Root Mean Square Error values of 1,73 and 2,01, respectively. In the validation phase on the other hand, the most precise predictions were achieved for the NH4-N and the TKN parameters with Root Mean Square Error values of 0,65 and 0,78, respectively.

It was observed that the least precise predictions were achieved for the COD and pCOD parameters on both of the calibration and validation processes with Root Mean Square Error values of 14,41 and 14,14, respectively for the calibration and 5,82 and 7,93, respectively for the validation processes. The parameters possesing the Janus Coefficient values closest to 1, were calculated as NO3-N and TN with Janus Coefficient values of 0,75 and 0,73, respectively. On the other hand, parameters having the most distant values to 1, were computed as NH4-N and COD with Janus Coefficient values of 0,38 and 0,40, respectively.

Table 4.5 : RMSE and Janus coefficients of model parameters.

Parameter	RMSE (Calibration)	RMSE (Validation)	Janus Coefficient
COD	14,41	5,82	0,40
TN	3,16	1,59	0,73
TKN	2,52	0,78	0,50
NH_4	1,73	0,65	0,38
NO_3	2,01	1,51	0,75
pCOD	14,14	7,93	0,56
BOD	5,72	2,76	0,48

4.4 Comparison of Simulation Outputs with AQUASIM

The output data of aerobic and anoxic compartment parameters are taken from the software for a comparison with the results of same model configuration created in the AQUASIM software. Each mass balance equation, biochemical and operational process as well as the kinetic, stoichiometric and operational parameter are identical with the software created for this thesis study. Simulations were run with the input data of an existing WRRF. Graphical visualizations for comparison of some of the crucial parameters can be seen in the following pages. The comparison of heterotrophic biomass concentrations in the aerobic reactor of the configuration from thesis and AQUASIM are shown above in Figure 4.15 where the heterotrophic biomass concentrations computed with thesis model match with AQUASIM results.

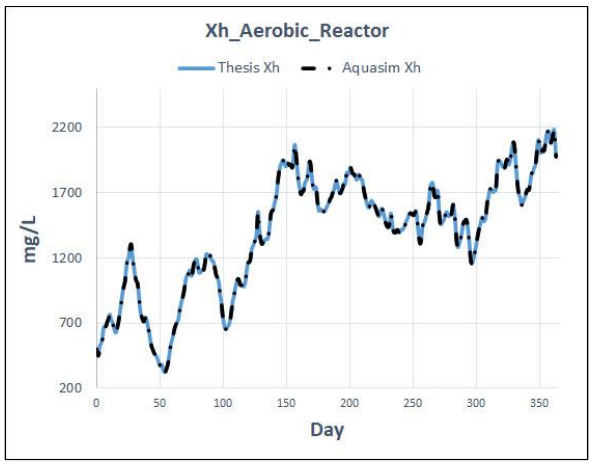

Figure 4.15 : Comparison of heterotrophic biomass concentration results in the aerobic reactor of Aquasim and the developed software in this study.

The outputs of autotrophic biomass concentrations from AQUASIM and thesis model match each other as it can be seen in Figure 4.16.

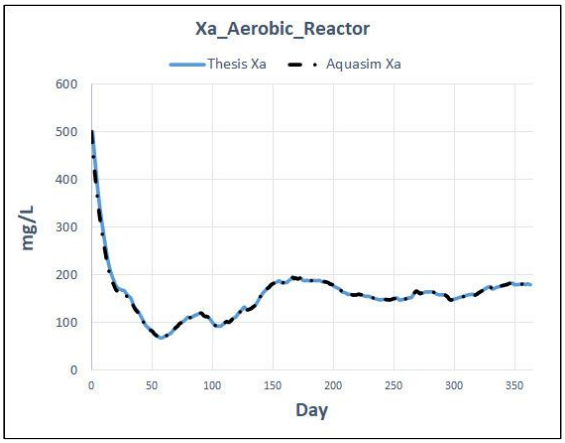

Figure 4.16 : Comparison of autotrophic biomass concentration results in the aerobic reactor of Aquasim and the developed software in this study.

The results comparison of thesis simulation outputs and AQUASIM outputs for dissolved oxygen concentration is shown below in Figure 4.17 where it can be seen that thesis dissolved oxygen concentration outputs match with AQUASIM outputs.

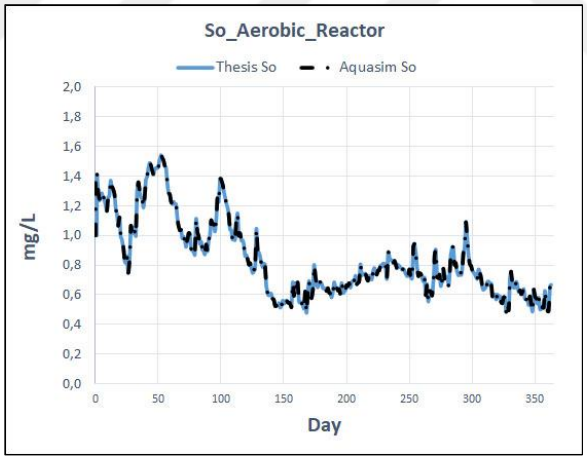

Figure 4.17 : Comparison of dissolved oxygen concentration results in the aerobic reactor of Aquasim and the developed software in this study.

It can be seen below from Figure 4.18 that in overall, simulation aerobic reactor parameter outputs match with the AQUASIM simulation results in regard to nitrate nitrogen concentrations.

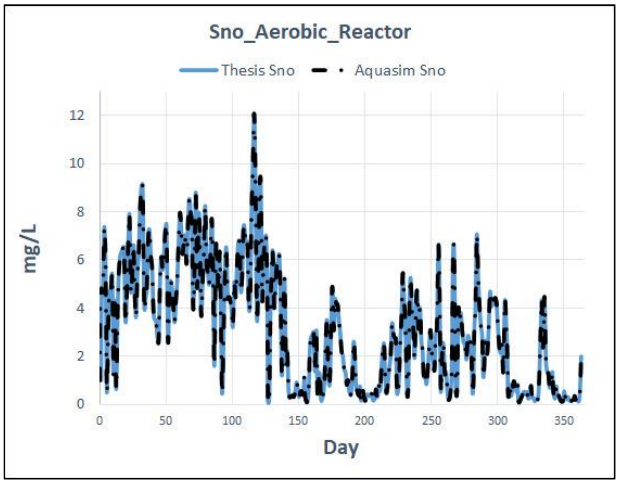

Figure 4.18 : Comparison of nitrate nitrogen concentration results in the aerobic reactor of Aquasim and the developed software in this study.

The results comparison of thesis simulation outputs and AQUASIM output values for rapidly hydrolyzable COD concentrations in the aerobic reactor is shown in Figure 4.19 where it can be seen that overall thesis simulation outputs match the AQUASIM results.

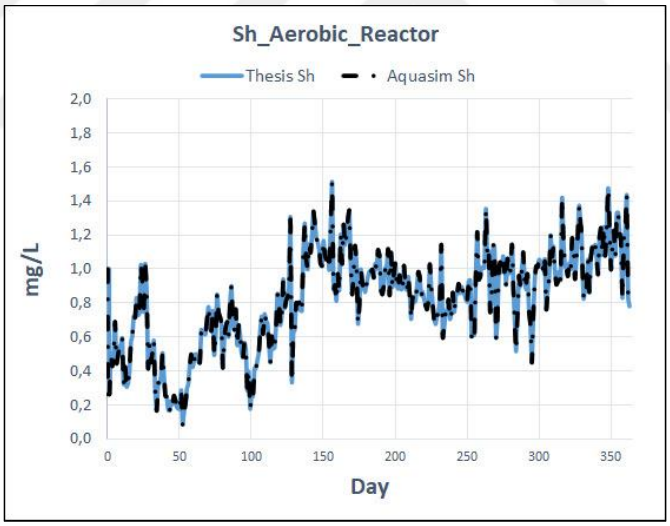

Figure 4.19 : Comparison of rapidly hydrolyzable COD concentration results in the aerobic reactor of Aquasim and the developed software in this study.

It can be seen from Figure 4.20 that in overall thesis simulation ammonia nitrogen concentrations match with the AQUASIM ammonia nitrogen concentration results.

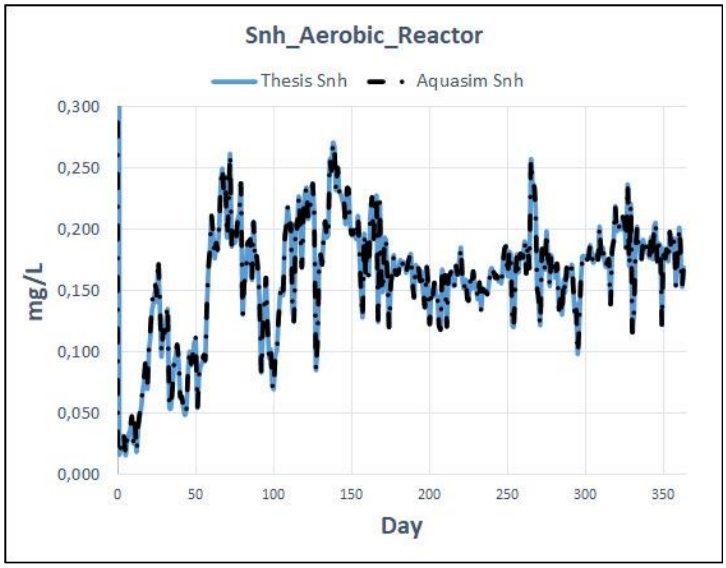

Figure 4.20 : Comparison of ammonia nitrogen concentration results in the aerobic reactor of Aquasim and the developed software in this study.

The comparison of heterotrophic biomass concentrations in the anoxic reactor of the configuration from thesis and AQUASIM are shown below in Figure 4.21 where the heterotrophic biomass concentrations computed within the thesis model demonstrate similar characteristics with AQUASIM results.

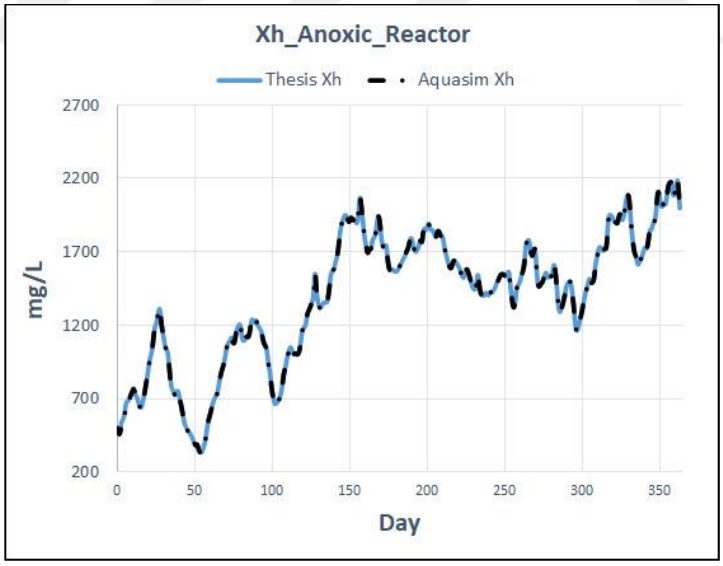

Figure 4.21 : Comparison of heterotrophic biomass concentration results in the anoxic reactor of Aquasim and the developed software in this study.

The comparison of autotrophic biomass concentrations in the anoxic reactor of the configuration from thesis and AQUASIM are shown below in Figure 4.22.

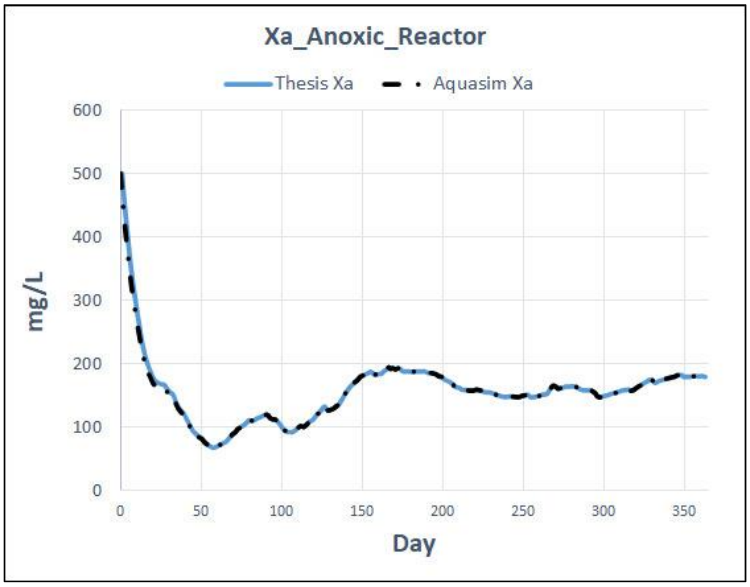

Figure 4.22 : Comparison of autotrophic biomass concentration results in anoxic reactor of Aquasim and the developed software in this study.

The results of dissolved oxygen concentrations in the anoxic reactor from the thesis simulation and AQUASIM can be seen below in Figure 4.23. Dissolved oxygen concentrations of thesis model show similar characteristics with AQUASIM results.

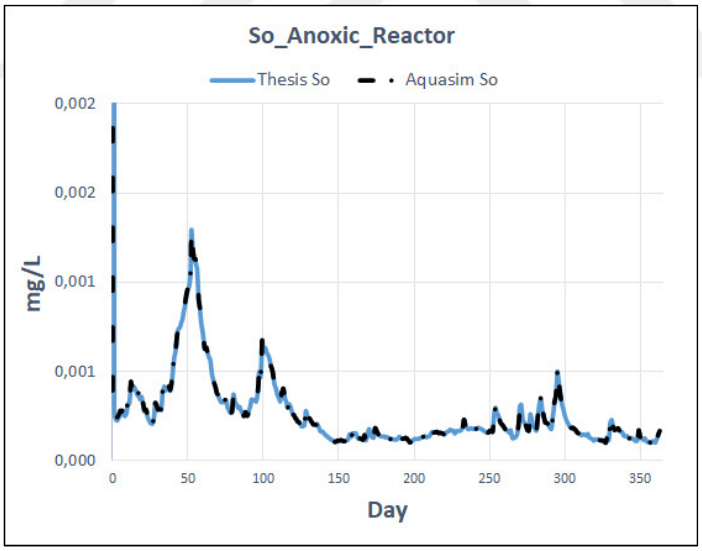

Figure 4.23 : Comparison of dissolved oxygen concentration results in the anoxic reactor of Aquasim and the developed software in this study.

Similar to the dissolved oxygen concentrations nitrate nitrogen concentration results taken from the thesis simulation and AQUASIM perform similar characteristics as it can be seen in Figure 4.24.

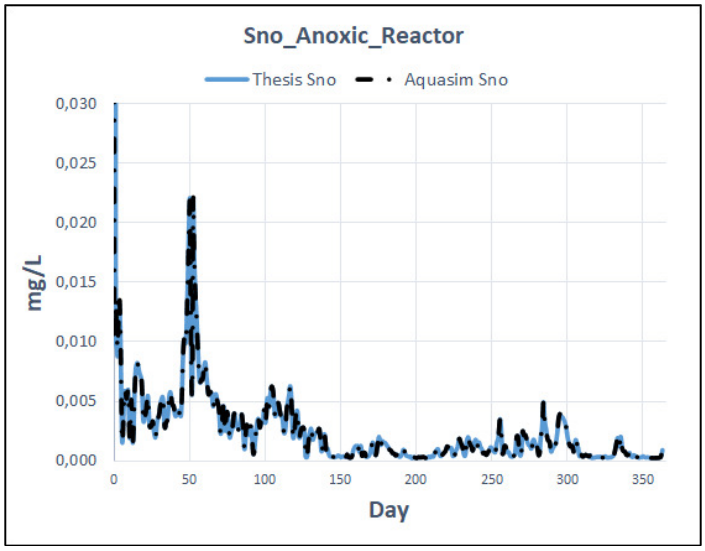

Figure 4.24 : Comparison of nitrate nitrogen concentration results in the anoxic reactor of Aquasim and the developed software in this study.

The results of rapidly hydrolyzable COD concentrations in the anoxic reactor from the thesis simulation and AQUASIM can be seen below in Figure 4.25. Rapidly hydrolyzable COD concentrations of thesis model show similar characteristics with AQUASIM results.

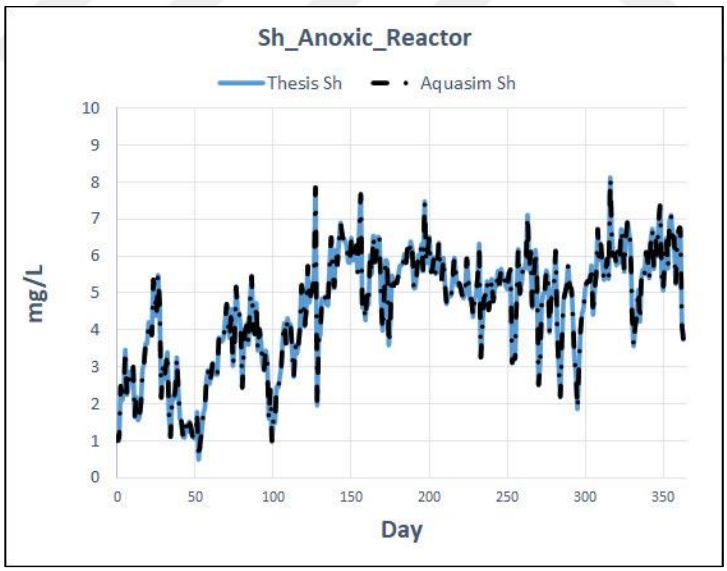

Figure 4.25 : Comparison of rapidly hydrolyzable COD concentration results in the anoxic reactor of Aquasim and the developed software in this study.

Lastly, the ammonia nitrogen concentrations from the anoxic reactor of thesis and AQUASIM simulations are shown above in Figure 4.26. It can be seen from the figure that ammonia nitrogen concentrations of AQUASIM simulation matches the results acquired from the developed software in this study.

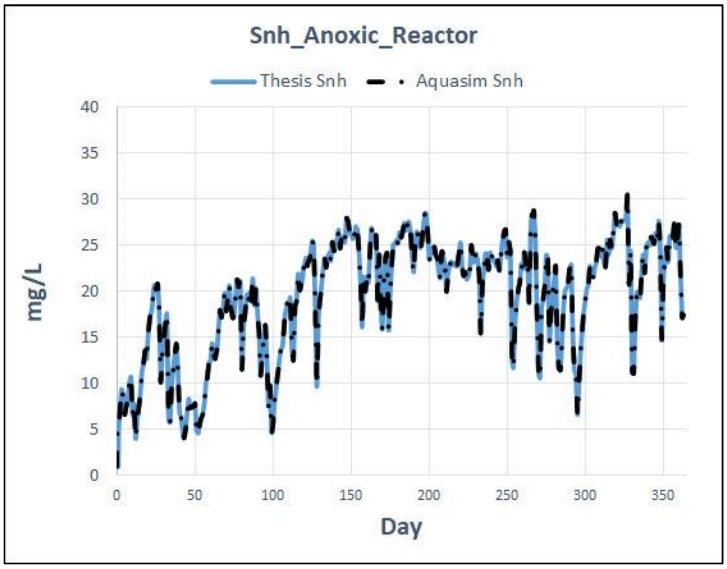

Figure 4.26 : Comparison of ammonia nitrogen concentration results in the anoxic reactor of Aquasim and the developed software in this study.

5. CONCLUSIONS AND RECOMMENDATIONS

An open-source software able to perform simulations of water resource recovery facilities with Modified Ludzack-Ettinger configuration has been developed within the scope of this study. Python programming language has been chosen for the development of the software due to its easy to learn syntax and its open-source libraries that contain powerful packages such as NumPy, SciPy, PySide2, Matplotlib and Pandas.

The data handling of inputs and outputs have been achieved with the help of useful built-in functions of NumPy and Pandas, whereas the graphical user interface of the software have been created with PySide2. SciPy.integrate's solve_ivp function has been used for performing computations of ordinary differential equations with the backward differentiation formula (BDF) method which is a multi-step variable-order implicit method used in solving stiff problems ("Scipy.integrate.solve_ivp — SciPy v1.7.1 Manual", 2021). Lastly for the development phase, figure canvas class of Matplotlib package has been integrated to the interface for visualizing the results of performed simulations.

A biochemical process model, consisting of 10 processes and 2 operational parameters defined for 15 state variables, have been created for the specific configuration that includes hydrolization processes of rapidly hydrolyzable COD, slowly hydrolyzable COD, soluble organic nitrogen and particulate organic nitrogen along with the growth and decay processes of heterotrophic and autotrophic biomasses.

Activated Sludge Model No. 1 (ASM1) has been taken as a base model for the creation of software model meanwhile endogenous respiration process definitions for two different heterotrophic organism species were adopted from the Activated Sludge Model No. 3 (ASM3).

Modifications have been made to the hybrid process model as the ammonification of soluble organic nitrogen process from Activated Sludge Model No. 1 and the storage mechanism of Activated Sludge Model No. 3 were removed from the process model in this thesis study. Once the process model was created, mass balance equations of each state variable were implemented in the software.

Configuration reactors were considered as Continuously Stirred Tank Reactors (CSTR) and therefore were assumed as ideal reactors. The reactant concentrations were considered to be distributed homogenously through the reactors meaning that the reactant concentrations within the reactor are assumed to be equal to the effluent concentrations of the reactors.

Rate of accumulation in the reactors were computed for each state variable for defining the mass balance equations of the specific configuration. Coefficients and stoichiometric parameters defined on process model matrix were multiplied by the process rates of each component for calculating the rate of accumulation in the reactors. Operational processes like constant feed of dissolved oxygen and sludge disposal process for the particulate matter that are going to be wasted were included in the matrix. Computation of sludge disposal was achieved by a sludge retention time input parameter and correction factors for the process rates of denitrifiers were also included to kinetic parameters alongside the coefficients of heterotrophic and autotrophic growth and decay processes. Lastly, hydrolysis rates and coefficients were appended to the model.

Calibration and validation of the process model have been achieved by using the data set of an existing WRRF. First 220 days of the data set of 363 days were used for the calibration and last 143 days were used for the validation of the parameter coefficients. Calibration has been achieved by performing simulations with one parameter value changed each step. Overall, it was observed that first 150 days of the data set possessed a more scattered data pattern when compared to the data intensity after day 150. The hydrolization rate of the slowly biodegradable COD was observed unsufficient and therefore the hydrolization coefficient was increased.

Another change was the increase in maximum specific growth rates for heterotrophic and autotrophic biomasses due to the unsufficient substrate removal and nitrification rates observed during the simulations.

Root Mean Square Error (RMSE) and Janus Coefficient methods have been selected for evaluating the precision of model simulation outputs. The most precise predictions in the calibration were achieved for the NH4-N and the NO3-N parameters with Root Mean Square Error values of 1,73 and 2,01, respectively while in the validation phase, the most precise predictions were achieved for the NH4-N and the TKN parameters with Root Mean Square Error values of 0,65 and 0,78, respectively.

The least precise predictions were computed for the COD and pCOD parameters on both of the calibration and validation processes with Root Mean Square Error values of 14,41 and 14,14, respectively for the calibration and 5,82 and 7,93, respectively for the validation processes.

The parameters possesing the Janus Coefficient values closest to 1, were calculated as NO3-N and TN with Janus Coefficient values of 0,75 and 0,73, respectively while parameters having the most distant values to 1, were computed as NH4-N and COD with Janus Coefficient values of 0,38 and 0,40, respectively.

The verification of the developed software was achieved by implementing the Modified-Ludzack Ettinger model in AQUASIM, an acknowledged simulation software used in environmental science, and comparing the results obtained from AQUASIM and the developed software created in this thesis study. Several simulations were done using the same operational parameters, kinetic and stoichiometric coefficients in each software while changing the parameters and coefficients each time a simulation was performed.

Similarly, simulation outputs of each software were compared with simulations having different step sizes like 10^{-1}, 10^{-2} and 10^{-3}. On all of the simulations mentioned, it was seen that the outputs of the developed software matched the outputs of AQUASIM software.

For further development of the software, options for choosing different carbon and nitrogen removal configurations should be implemented.

A better but more complicated modification would be to enable the users to define their own configurations by defining reactor and pipeline classes possessing divergent features with the help object oriented programming. Implementation of Enhanced Biological Phosphorus Removal (EBPR) configurations with effluent wastewater characteristics fit for reuse should be accomplished.

Another important modification would be to update the software with a proper settling model rather than using a settling efficiency coefficient for sludge recycle and effluent wastewater calculations. Additional tools for model calibration, energy consumption and cost efficiency calculations and CO_2 generation calculations for sustainability assesment can be integrated into the software.

Lastly, functions that enable the users to save the existing options and adjustments must be implemented into the software and different scenarios for real case optimization studies should be applied.

In conclusion, the developed software within the scope of this thesis study will be a useful tool to predict the performances of nitrogen removal process schemes for different water quality and treatment requirements.

Considering a decent automation integration is achieved to the software, simpler softwares created with more user friendly graphical user interfaces will end up increasing the control of facility operators over the operation of the systems. The need for specific case studies on the modeled configuration will reduce with the efficient use of the software and younger generations of environmental engineers will be provided a better mean of comprehension for the operational, kinetic and stoichiometric parameters and their impacts on the processes.

REFERENCES

Ansari, A., Hai, F., Price, W., Drewes, J., & Nghiem, L. (2017). Forward osmosis as a platform for resource recovery from municipal wastewater - A critical assessment of the literature. *Journal Of Membrane Science*, *529*, 195-206. doi: 10.1016/j.memsci.2017.01.054.

Bozek F., Navratil J., Kellner J. (2005) Efficiency of Nitrification and Denitrification Processes in Waste Water Treatment Plants. In: Omelchenko A., Pivovarov A.A., Swindall W.J. (eds) Modern Tools and Methods of Water Treatment for Improving Living Standards. NATO Science Series (Series IV: Earth and Environmental Series), vol 48. Springer, Dordrecht. https://doi.org/10.1007/1-4020-3116-5_16.

Bressert, E. (2013). *SciPy and NumPy* (pp. 1 - 41). Beijing: O'Reilly.

Chrispim, M., Scholz, M., & Nolasco, M. (2020). A framework for resource recovery from wastewater treatment plants in megacities of developing countries. *Environmental Research*, *188*, 109745. doi: 10.1016/j.envres.2020.109745.

Coskuner, G., & Jassim, M. (2008). Development of a correlation to study parameters affecting nitrification in a domestic wastewater treatment plant. *Journal Of Chemical Technology & Biotechnology*, *83*(3), 299-308. doi: 10.1002/jctb.1808.

Downing, A. L., & G. Knowles. (1967). Population dynamics in Activated Sludge Plants. *Advances in Water Pollution Research, Vol. 2, S. H. Jenkins, L. Mendia, eds., Washington, DC: Water Pollution Control Federation.*

EnviroSim – Wastewater Modeling Software. (1990). Retrieved 20 January 2022, from https://envirosim.com/

Feleke, Z. (2002). A bio-electrochemical reactor coupled with adsorber for the removal of nitrate and inhibitory pesticide. *Water Research*, *36*(12), 3092-3102. doi: 10.1016/s0043-1354(01)00538-3.

Gujer, W., Henze, M., Mino, T., & Van Loosdrecht, M. (1999). Activated sludge model no. 3. *Water science and technology*, 39(1), 183-193.

Haandel, A. (2012). *Handbook of biological wastewater treatment* (2nd ed., p. 144). IWA Publishing.

Henze, M., Grady, C. P., W., G., Marais, G. V., & Matsuo, T. (1987). *Activated Sludge Model No.1*. London: International Association on Water Pollution Research and Control.

Henze, M., Gujer, W., Mino, T., & van Loosedrecht, M. (2015). Activated Sludge Models ASM1, ASM2, ASM2d and ASM3. *Water Intelligence Online*, *5*(0), 9781780402369-9781780402369. doi: 10.2166/9781780402369.

Jarvis, S., Burger, G., Du, W., Bye, C., & Dold, P. (2014). Crude COD Characteristics Significant for Biological P Removal: A U.K. Example. *8th European Waste Water Management Conference.*

Jeppsson, U. (1996). *Modelling Aspects of Wastewater Treatment Processes* (Ph.D). Lund Institute of Technology.

Komorowska-Kaufman, M., Majcherek, H., & Klaczyński, E. (2006). Factors affecting the biological nitrogen removal from wastewater. *Process Biochemistry*, *41*(5), 1015-1021. doi: 10.1016/j.procbio.2005.11.001.

Mansouri, S., Udugama, I., Cignitti, S., Mitic, A., Flores-Alsina, X., & Gernaey, K. (2017). Resource recovery from bio-based production processes: a future necessity?. *Current Opinion In Chemical Engineering*, *18*, 1-9. doi: 10.1016/j.coche.2017.06.002.

Matplotlib — Visualization with Python. (2021). Retrieved 18 November 2021, from https://matplotlib.org/.

Mo, W., & Zhang, Q. (2013). Energy–nutrients–water nexus: Integrated resource recovery in municipal wastewater treatment plants. *Journal Of Environmental Management*, *127*, 255-267.

NumPy. (2021). Retrieved 18 November 2021, from https://numpy.org/.

Orhon, D., & Artan, N. (1994). *Modelling of activated sludge systems* (pp. 453-458). Lancaster: Technomic Publishing Co.

Orhon, D., Çokgör, E. U., & Sözen, S. (1998). Dual hydrolysis model of the slowly biodegradable substrate in activated sludge systems. *Biotechnology techniques*, 12(10), 737-741.

Pandas - Python Data Analysis Library. (2021). Retrieved 18 November 2021, from https://pandas.pydata.org/

Puyol, D., & Batstone, D. (2017). Editorial: Resource Recovery from Wastewater by Biological Technologies. *Frontiers In Microbiology, 8*. doi: 10.3389/fmicb.2017.00998.

Qt 5.15. (2021). Retrieved 18 November 2021, from https://doc.qt.io/qt-5/index.html.

Reichert, P. (1995). Design techniques of a computer program for the identification of processes and the simulation of water quality in aquatic systems. *Environmental Software*, *10*(3), 199-210. doi: 10.1016/0266-9838(95)00010-i.

Reichert, P., AQUASIM 2.0 - User Manual, Swiss Federal Institute for Environmental Science and Technology (EAWAG), CH-8600 Dübendorf, Switzerland, 214 p., 1998.

SIMBA# - inCTRL Solutions. (2021). Retrieved 18 November 2021, from https://www.inctrl.com/software/simba/

Sinha, B., & Annachhatre, A. (2006). Partial nitrification—operational parameters and microorganisms involved. *Reviews In Environmental Science And Bio/Technology*, *6*(4), 285-313. doi: 10.1007/s11157-006-9116-x.

Scipy.integrate.solve_ivp — SciPy v1.7.1 Manual. (2021). Retrieved 18 November 2021, from https://docs.scipy.org/doc/scipy/reference/generated/scipy.integrate.solve_ivp.html#r179348322575-5

Sperling, M. (2007). *Basic principles of wastewater treatment* (pp. 36,48). London: IWA Publishing.

Sözen, S., Orhon, D., & San, H. (1996). A new approach for the evaluation of the maximum specific growth rate in nitrification. *Water Research*, *30*(7), 1661-1669. doi: 10.1016/0043-1354(96)00031-0.

SUMO | dynamita. (2021). Retrieved 18 Novembera2021, from http://www.dynamita.com/

Wastewater Modelling and Simulation Software | GPS-X - Hydromantis. (2021). Retrieved 18 November 2021, from https://www.hydromantis.com/GPSX.html

WEST. (2021). Retrieved 18 November 2021, from https://www.mikepoweredbydhi.com/products/west

Yang, H., Ye, S., Zeng, Z., Zeng, G., Tan, X., & Xiao, R. (2020). Utilization of biochar for resource recovery from water: A review. *Chemical Engineering Journal*, *397*, 125502. doi: 10.1016/j.cej.2020.125502.

APPENDIX

APPENDIX A1 : Software executive file named Simulator.exe

APPENDIX A2 : Influent and effluent data of WRRF

APPENDIX A1

This appendix has been supplied electronically.

APPENDIX A2

This appendix has been supplied electronically.

6. CURRICULUM VITAE

Name Surname **: Doğa Binay**

EDUCATION **:**

- **B.Sc.** **:** 2018, Yıldız Technical University, Faculty of Civil Engineering, Department of Environmental Engineering